

## ABSTRACT

Title of Dissertation: CATANIONIC SURFACTANT VESICLES:  
TECHNOLOGY FOR VACCINE  
DEVELOPMENT AND TARGETED DRUG  
DELIVERY APPLICATIONS

Lenea H. Stocker, Doctor of Philosophy, 2013

Dissertation Directed By: Professor Philip DeShong  
Department of Chemistry and Biochemistry

Catanionic surfactant vesicles have gained attention due to their structural similarities to liposomes and their robust properties in biological media. Catanionic vesicles are formed from oppositely charged surfactants and can be exploited for applications in vaccine production and drug delivery. The focus of my research has been on the preparation, characterization, and application of functionalized catanionic surfactant vesicles.

Chapter 2 describes the preparation and characterization of catanionic vesicles containing sodium dodecylbenzenesulfonate (SDBS) and cetyltrimethylammonium tosylate (CTAT). Vesicle solutions were determined to be stable for greater than 6 months, formed vesicles with two populations of 80 and 160 nm, and had a membrane surface charge similar to human cells, -56 mV. Furthermore, vesicles

were stable between a pH of 2 and 12, in saline solutions up to 0.6 M NaCl, and after autoclaving. Next, I report the loading of various molecules into the vesicle leaflet and the characterization of the resulting functionalized systems. Hydrophobic molecules were readily incorporated into the hydrophobic region of the leaflet. Lipid conjugates of hydrophilic molecules were anchored in the vesicle bilayer.

Chapters 3 and 4 report the loading of biological materials (i.e. liposaccharides and proteins) into cationic vesicles for the development of bacterial vaccines. Initial studies, discussed in Chapter 3, pertain to the loading of the pure components lipooligosaccharide (LOS) and C<sub>12</sub>-Pan DR helper T cell epitope (PADRE) conjugate into cationic vesicles. A single dose of these vesicles generated a large IgG antibody titer in mice. Next, in Chapter 4, we focus on the extraction of cellular membrane components from cells for their direct incorporation into cationic vesicles. Vesicles were prepared by adding surfactants in the presence of *Neisseria gonorrhoeae* cells. Vesicle extracts contained pathogen-derived LOS F62ΔIgtD and a subset of proteins from the outer membrane of the bacterium, including porin and OPA.

Lastly, Chapter 5 describes cationic vesicles in drug delivery. Vesicles were loaded with 88 µg/mL of doxorubicin and shown to retain the drug over 15 days. Doxorubicin loaded into cationic vesicles were shown to be less toxic as compared to the free drug, IC<sub>50</sub> = 51 µg/mL and 0.16 µg/mL, respectively.

CATANIONIC SURFACTANT VESICLES: TECHNOLOGY FOR VACCINE  
DEVELOPMENT AND TARGETED DRUG DELIVERY APPLICATIONS

By

Lenea H. Stocker

Dissertation submitted to the Faculty of the Graduate School of the  
University of Maryland, College Park, in partial fulfillment  
of the requirements for the degree of  
Doctor of Philosophy  
2013

Advisory Committee:

Professor Philip DeShong, Chair

Professor Steven Rokita

Professor Herman Sintim

Professor YuHuang Wang

Professor John Fisher

© Copyright by

Lenea H. Stocker

2013

## DEDICATION

To my students and former chemistry teachers.

For they are the reason that I love teaching and pursued my Ph.D.

## ACKNOWLEDGMENTS

First and foremost, I thank God for granting me with the gift of teaching. I am grateful that He led me to the University of Maryland to complete my Ph.D., where along the way I met my husband and received a lecturing position. *“Each one should use whatever gift he has received to serve others, faithfully administering God’s grace in its various forms.” 1 Peter 4:10*

My sincere appreciation goes to my advisor and mentor, Dr. Philip DeShong. I truly believe that I could not have found a better advisor at the University of Maryland and I would not have made it through graduate school without his support and guidance. I especially thank him for always supporting me during my teaching endeavors. I am grateful that I can continue my career at the University of Maryland with him as my colleague.

I would like to thank all former and current members of the DeShong group, especially Juhee Park, Matthew Hurley, Frederick Nytko, III, Neeraja Dashaputre, Reyniak Richards, Abigail Horn, Anshu Manocha, Glen Thomas, and Kelly Brannock. We have shared many hours and memories together in the lab that I will cherish.

I am thankful to all of my committee members and for their advise and support. I would also like to thank Yiu-Fai Lam and Srinivasa Raghavan, Mikhail Anisimov, and Deepa Subramanian for their assistance with the NMR and DLS, respectively. I also thank our collaborators, specifically Douglas English, Daniel Stein, Stefanie Vogel, Catherine Fenselau, Martin Edelman, Rena Lapidus, and

Vincent Lee. I thank their students Lindsey Zimmerman, Amanda Mahle, Brittany Wheeler, Katharina Richard, Leah Cole, Avantika Dhabaria, and Rebecca Rose.

Personally, I thank my family and friends for their support and encouragement. I especially thank my parents and parents-in-law for their continuous prayers, love, and support over the course of graduate school. Last, but not least, I especially thank my husband Mike for his encouragement, constant support, and everlasting love. We have shared the ups and downs of graduate school together. I am grateful and blessed to have met him during orientation and to have had him by my side during this journey.

## TABLE OF CONTENTS

Dedication.....	ii
Acknowledgements.....	iii
List of Tables .....	x
List of Figures.....	xii
List of Schemes.....	xvii
List of Abbreviations .....	xix
Chapter 1: Comparison of Catanionic Surfactant Vesicles to Conventional Liposomes ....	1
1.1 Introduction.....	1
1.2 Physical Properties of Surfactants .....	4
1.3 Formation of Catanionic Surfactant Vesicles.....	8
1.4 Loading of Catanionic Surfactant Vesicles .....	11
1.5 Conclusions.....	15
1.6 Research Goals.....	15
References.....	17
Chapter 2: Loading and Characterization of Catanionic Surfactant Vesicles.....	24
2.1 Introduction.....	24
2.2 Specific Aims, Results, and Discussion.....	27
2.2.1 Synthesis and Characterization of Bare Catanionic Surfactant Vesicles.....	27
2.2.1.1 Stability of Bare Catanionic Surfactant Vesicles under Drug Formation Conditions.....	39

2.2.2 Surface Functionalization and Characterization of Catanionic Vesicles .....	43
2.2.2.1 Carbohydrate Functionalized Catanionic Vesicles .....	44
2.2.2.1.1 Stability of Carbohydrate Functionalized Catanionic Surfactant Vesicles .....	49
2.2.2.2 Loading of Peptides and Chromophores into Catanionic Vesicles.....	52
2.2.3 Dialysis .....	56
2.3 Conclusions.....	57
2.4 Experimental.....	57
2.4.1 General Experimental .....	57
2.4.2 Synthesis of Bare Surfactant Vesicles .....	58
2.4.3 Dynamic Light Scattering Techniques and Procedure.....	60
2.4.4 Sonication of Bare Vesicles .....	61
2.4.5 Zeta Potential Measurements.....	61
2.4.6 Preparation of Catanionic Vesicles in Buffered Solutions .....	61
2.4.7 Saline Studies.....	62
2.4.8 pH Studies.....	62
2.4.9 Freezing Studies on Bare Catanionic Vesicles .....	62
2.4.10 Sterilization of Vesicles .....	62
2.4.11 Measuring Disruption of Bare Vesicles with Ethanol .....	63
2.4.12 Surface Functionalization of Surfactant Vesicles .....	63
2.4.13 Size Exclusion Chromatography.....	64
2.4.14 Colorimetric Assay for Carbohydrate.....	65
2.4.15 Binding Studies.....	65
2.4.16 Transmission Electron Microscopy .....	66

2.4.17 Bicinchoninic Acid Assay for Protein .....	66
2.4.18 Quantifying Dye Incorporation into Catanionic Vesicles.....	67
2.4.19 Dialysis .....	67
References.....	68
Chapter 3: Loading Complex Carbohydrates and Peptides into Catanionic Surfactant Vesicles for Use in Vaccine Applications .....	71
3.1 Introduction.....	71
3.1.1 Vaccine Formulation.....	71
3.1.2 Bacterial Vaccines .....	72
3.1.3 Catanionic Surfactant Vesicle Vaccines .....	73
3.2 Results and Discussion .....	75
3.2.1 Catanionic Vaccines for <i>Neisseria gonorrhoeae</i> .....	75
3.2.1.1 Animal Studies with Vesicle Antigens .....	79
3.2.2 Catanionic Vaccines for <i>Francisella tularensis</i> .....	80
3.3 Conclusions.....	82
3.4 Future Work .....	82
3.5 Experimental .....	83
3.5.1 Materials .....	83
3.5.2 Synthesis of Conjugates.....	83
3.5.3 Isolation and characterization of LOS .....	85
3.5.4 Synthesis and Characterization of Surfactant Vesicles.....	85
3.5.5 Animal Trials .....	86
References.....	87

Chapter 4: Methodology for the Extraction of Membrane Components from <i>Neisseria gonorrhoeae</i> .....	89
4.1 Introduction.....	89
4.1.1 Reconstitution of Membrane Proteins into Liposomes.....	89
4.1.2 Liposomal Bacterial Vaccines .....	91
4.1.3 Outer Membrane Vesicles for Vaccines .....	92
4.1.4 Catanionic Vesicle Bacterial Vaccines .....	93
4.2 Results and Discussion .....	94
4.3 Conclusions.....	100
4.4 Experimental.....	101
4.4.1 General Experimental .....	101
4.4.2 Cell Cultures .....	101
4.4.3 Vesicle Preparation .....	102
4.4.4 Gel Electrophoresis.....	102
4.4.5 Silver Staining.....	103
4.4.6 Protection Experiments.....	104
4.4.7 Western Blotting .....	104
4.4.8 Proteomics Analysis.....	105
4.5 References.....	106
Chapter 5: Drug Delivery Applications for Catanionic Surfactant Vesicles .....	113
5.1 Introduction.....	113
5.1.1 Liposomes in Drug Formulation.....	113
5.2 Results and Discussion .....	116
5.2.1 Doxorubicin Loaded Catanionic Surfactant Vesicles .....	116

5.2.2 Targeted Doxorubicin Loaded Catanionic Surfactant Vesicles.....	122
5.2.3 Lutein Loaded Catanionic Surfactant Vesicles.....	125
5.2.4 Maytansine Loaded Catanionic Surfactant Vesicles.....	127
5.2.5 Paclitaxel Loaded Catanionic Surfactant Vesicles .....	129
5.3 Conclusions.....	130
5.4 Experimental.....	131
5.4.1 Doxorubicin .....	131
5.4.2 Lutein .....	132
5.4.3 Maytansine.....	132
5.4.4 Paclitaxel.....	133
5.4.5 Addendum.....	133
References.....	135
Appendix.....	137

## LIST OF TABLES

1.1	Comparison of cationic vesicles to liposomes. ....	4
1.2	Effect of amphiphile geometry on aggregate structure.....	7
2.1	Monitoring vesicle equilibrium by DLS over time.....	28
2.2	Monitoring temporal stability of vesicles by DLS.....	28
2.3	Confirmation of size distribution of bare vesicles studied by multi-angle DLS...30	
2.4	Various sizes of cationic vesicles prepared by various techniques.....	35
2.5	Average zeta potentials of bare cationic surfactant vesicles.....	38
2.6	Size distribution of vesicles studied by DLS.....	38
2.7	Purified vesicle-containing fractions by SEC before and after autoclaving.....	41
2.8	Glycoconjugate incorporation into cationic vesicles and DLS results.....	46
2.9	Initial rate of vesicle agglutination at RT using [Con A].....	48
2.10	Hydrodynamic radius (nm) of C <sub>12</sub> -glucose vesicles at increasing NaCl concentrations analyzed by DLS.....	50
2.11	Purified vesicle-containing fractions before and after autoclaving.....	51
3.1	Average amount of carbohydrate in TRIAD vaccine from two batches.....	79
3.2	Antibody titer results in mice inoculated with LOS and LOS/C <sub>12</sub> -PADRE functionalized surfactant vesicles.....	80
4.1	Total protein and carbohydrate concentrations in vesicle extract samples determined by colorimetric BCA and carbohydrate assays.....	95

5.1	Liposomal formulations of drug delivery vehicles .....	115
5.2	Amount of doxorubicin in vesicles from increasing concentrations .....	119

## LIST OF FIGURES

1.1	Chemical structures of a phospholipid and anionic and cationic surfactants and their aggregates .....	3
1.2	Critical micelle concentration in solution .....	5
1.3	Hydrophobic and hydrophilic moieties on amphiphiles .....	8
1.4	Association of cationic and anionic surfactants.....	9
1.5	Chemical structures of SDBS and CTAT .....	10
1.6	Phase diagram of CTAT/SDBS in water .....	11
1.7	Electrostatic adsorption of charged molecules into oppositely charged vesicles.....	13
1.8	Functionalizing cationic surfactant vesicles with molecules containing hydrophobic moieties.....	13
1.9	Cationic surfactant vesicles attached to a surface coated with HM chitosan....	15
2.1	Biotinylated cationic surfactant vesicle binding with streptavidin .....	24
2.2	Con A aggregation of carbohydrate-modified cationic surfactant vesicles .....	25
2.3	Poisson distribution and lipid rafts of glycoconjugates at the surface of cationic vesicles.. ..	26
2.4	Confirmation of size distribution of bare cationic vesicles studies by multi-angle DLS .....	31

2.5	Amplitude of small and large particle populations as the scattering angle increases .....	32
2.6	Cryo-TEM of bare cationic vesicles .....	33
2.7	Solutions of cationic bare vesicles formed from 1) solid surfactants and 2) blended surfactants.....	36
2.8	Cloudy vesicle suspensions compared to vesicles disrupted with ethanol .....	42
2.9	DLS intensity of a 1 mL colloidal solution of cationic vesicles disrupted with an increasing volume of ethanol .....	42
2.10	Vesicles modified with molecules that insert via different mechanisms .....	44
2.11	Glycoconjugates functionalized to vesicles C <sub>12</sub> -glucose, C <sub>8</sub> -glucose, C <sub>8</sub> -maltose, and C <sub>8</sub> -maltotriose .....	44
2.12	Results from SEC carbohydrate-functionalized cationic vesicles evaluated by DLS and colorimetric assay of carbohydrate-loaded vesicles .....	45
2.13	Effect of carbohydrate subunit length on Con A agglutination .....	48
2.14	Representative cryo-TEM micrographs of vesicles with C <sub>12</sub> -glucose .....	49
2.15	Comparison of sterile and non-sterile C <sub>12</sub> -glucose vesicles' second purification by SEC.....	51
2.16	Sequence of C <sub>12</sub> -PADRE peptide conjugate.....	52
2.17	Chemical structure of chromophores containing a hydrophobic linker .....	54

2.18	Chemical structure of dyes containing a charge .....	55
2.19	Chemical structure of hydrophobic molecules containing a chromophore .....	55
2.20	Absorption of lissamine rhodamine B-lipid vesicles after purification by SEC...	56
2.21	Determination of vesicle concentration in solution .....	59
2.22	Set-up used for dynamic light scattering .....	60
3.1	Chemical structure of lipooligosaccharide components from the Gram-negative bacteria <i>N. gonorrhoeae</i> .....	73
3.2	Chemical structure of lipid oligosaccharide (LOS) F62Δ lgtD purified from <i>N. gonorrhoeae</i> .....	78
3.3	Chemical structure of unconjugated PADRE peptide .....	78
3.4	Chemical structure of lipid polysaccharide (LPS) from <i>F. tularensis</i> .....	81
4.1	Vesicle-containing fractions purified by gel filtration followed by silver staining.....	96
4.2	Vesicle extract fractions from gel filtration analyzed by silver staining .....	97
4.3	Western blotting of vesicle-containing fractions, lysate, and supernatant.....	98
4.4	Proteinase K digestion .....	99
4.5	Protection from trypsin digestion.....	100
5.1	Chemical structure of doxorubicin and PEGylated liposomes provide a lipophilic barrier on the exterior of liposomes.....	114

5.2	Targeting of cationic surfactant vesicles to cells .....	116
5.3	Retention of doxorubicin over fifteen days in cationic surfactant vesicles ....	117
5.4	WST-1 cell proliferation assay on HepG2 cells treated with bare vesicles and doxorubicin loaded vesicles.....	121
5.5	WST-1 cell proliferation assay on HepG2 cells treated with doxorubicin .....	121
5.6	Free doxorubicin compared to doxorubicin loaded cationic vesicles incubated with normal cells. ....	122
5.7	Doxorubicin loaded untargeted and targeted cationic vesicles incubated with normal cells vs. cells that over express a receptor. ....	122
5.8	Chemical structure of C <sub>12</sub> -folate conjugate.....	123
5.9	WST-1 cell proliferation assay on A549 cells treated with folate targeted cationic vesicles .....	123
5.10	WST-1 cell proliferation assay on ovarian IGROV-1 cells, which over express folate, treated with folate targeted cationic vesicles .....	124
5.11	Fluorescently-labeled vesicles binding with cells.....	125
5.12	Chemical structure of lutein.....	126
5.13	Lutein spanning the bilayer of cationic surfactant vesicles .....	126
5.14	Chemical structure of maytansine.....	128
5.15	Absorbance of a maytansine analogue and maytansine loaded vesicle fraction from SEC .....	128

5.16	Chemical structure of paclitaxel fluorescein derivative.....	129
5.17	Absorbance of paclitaxel loaded vesicles at 445 nm .....	130
5.18	Time dependence of A549 and IGROV-1 cells in the presence of targeted catanionic vesicles .....	134
A.1	Chemical structure of curcumin and orientation in micelles. ....	138
A.2	Catanionic vesicles as protecting groups .....	139
A.3	Purification of CF-lipid vesicles reacted with NaOH and unreacted.....	142
A.4	CTAT-rich vesicles containing phenol red after SEC purification.....	144
A.5	Catanionic surfactant vesicles as protecting groups .....	146
A.6	Chemical structure of CF-lipid dye.....	146

## LIST OF SCHEMES

2.1	Binding scheme for Con A-induced vesicle aggregation .....	49
2.2	Preparation of bare cationic surfactant vesicles from the solid surfactants SDBS and CTAT .....	59
2.3	Surfactant vesicles functionalized with compounds containing hydrophobic moieties via hydrophobic interactions .....	64
3.1	Immune response of LOS vs. C <sub>12</sub> -PADRE/LOS conjugated cationic vesicles.....	75
3.2	Preparation of LOS conjugate from <i>N. gonorrhoeae</i> .....	76
3.3	Synthesis of C <sub>12</sub> -PADRE peptide conjugate.....	78
3.4	Preparation of TRIAD vaccine formulated with cationic surfactant vesicles containing the C <sub>12</sub> -PADRE peptide conjugate and LOS from <i>N. gonorrhoeae</i> ...	79
3.5	Synthesis of N-dodecanoylsuccinimide.....	84
3.6	Synthesis of dodecanoic acid tethered to PADRE peptide .....	85
4.1	Reconstitution of purified membrane proteins into liposomes compared to extraction procedure using cationic vesicles.....	90
A.1	Chemistry at the surface of cationic surfactant vesicles .....	138
A.2	Hydrolysis reaction of CF-lipid in cationic vesicles via NaOH.....	140
A.3	CF monoanion and dianion chemical structures.....	141

A.4	Deprotonation of protons at the surface of cationic surfactant vesicles.....	142
A.5	Phenol red monoanion and dianion chemical structures.....	143
A.6	Phenol red loaded in CTAT-rich vesicles .....	143
A.7	Determining the amount of dye incorporated within the internal region of vesicles .....	145

## LIST OF ABBREVIATIONS

Abs.	absorbance
aq.	aqueous
C	Celsius
cac	critical aggregation concentration
CaCl <sub>2</sub>	calcium chloride
CaCO <sub>3</sub>	calcium carbonate
CDCl <sub>3</sub>	deuterated chloroform
CF	carboxyfluorescein
CH <sub>2</sub> Cl <sub>2</sub>	methylene chloride
cmc	critical micelle concentration
Con A	concanavalin A
cps	counts per second
Cryo-TEM	cryogenic transmission electron microscopy
CTAB	cetyltrimethylammonium bromide
CTAT	cetyltrimethylammonium tosylate
DLS	dynamic light scattering
DMF	dimethylformamide
DMSO	dimethyl sulfoxide
DNA	deoxyribose nucleic acid
EDC	1-ethyl-3-(3-dimethylaminopropyl)-carbodiimide
ELISA	enzyme-linked immunosorbent assay

EM	electron microscope
Et	ethyl
EtOH	ethanol
EYPC	egg-yolk phosphatidylcholine
FT	fourier transform
g	gram
Glu	glucose
H	proton
h	hour
HCl	hydrochloric acid
HEPES	4-(2-hydroxyethyl)-1-piperazineethanesulfonic acid
HIV	human immunodeficiency virus
HM	hydrophobically modified chitosan
HPLC	high performance liquid chromatography
HUVEC	human umbilical vein endothelial cells
IgG	immunoglobulin G
IgM	immunoglobulin M
IR	infrared
$K_d$	dissociation constant
KV	kilovolt
LOS	lipid oligosaccharide
LPS	lipid polysaccharide
M	molar

m	medium
mf	mole fraction
mg	milligram
MgCl <sub>2</sub>	magnesium chloride
MgSO <sub>4</sub>	magnesium sulfate
MHz	megahertz
min	minute
mL	milliliter
mM	milimolar
mmol	milimole
MnCl <sub>2</sub>	manganese chloride
mp	melting point
mV	milivolt
MW	molecular weight
mW	miliwatt
N <sub>2</sub>	nitrogen
NaCl	sodium chloride
NaHCO <sub>3</sub>	sodium bicarbonate
NaOH	sodium hydroxide
NHS	N-hydroxysuccinimide
nm	nanometer
NMR	nuclear magnetic resonance
OMV	outer membrane vesicles

PADRE	Pan DR helper T cell epitope
PEG	poly(ethylene glycol)
PNA	peanut agglutinin
R <sub>f</sub>	retention factor
RGD	arginine-glycine-aspartic acid
RNA	ribonucleic acid
rpm	rate per minute
RT	room temperature
s	sharp
s	seconds
SDBS	sodium dodecylbenzene sulfonate
SEC	size exclusion chromatography
SOS	sodium octyl sulfate
STD	standard deviation
TEM	transmission electron microscopy
THF	tetrahydrofuran
TLC	thin layer chromatography
μg	microgram
μM	micromolar
UV	ultra violet
WST	water-soluble tetrazolium salts
wt	weight
w/w	weight by weight

# Chapter 1: Comparison of Cationic Surfactant Vesicles to Conventional Liposomes

## 1.1 Introduction

For decades, nanoparticles have been studied for their potential use as drug delivery systems because of their stability, biocompatibility, and ability to distribute a drug *in vivo*. Nanoparticles that incorporate a drug have shown longer circulation time in the body, have improved the therapeutic index of the drug, and have decreased side effects from the drug.<sup>1</sup> Liposomes, or phospholipid vesicles, have achieved status as drug carriers due to their ability to encapsulate an aqueous environment and mimic cellular membranes.<sup>1-6</sup> Liposomal formulations are utilized as targeted drug delivery vehicles, biosensors, and vaccines.

Liposomes were discovered in the 1960's when Bangham *et al.* demonstrated that double-tailed amphiphilic molecules self-assembled into colloidal vesicles.<sup>7</sup> Since their discovery, liposomal formulations of clinically approved drugs have been used in drug delivery to increase a drug's solubility and efficacy. By adding a protective coating, such as polyethylene glycol (PEG), to the liposomal surface, circulation time *in vivo* can be further enhanced. Targeting agents have also been added to liposomes including carbohydrates, antibodies, folate, and peptides in order to direct the liposomal carrier to a specific tissue.<sup>8-11</sup>

Despite their extensive use and success, liposomal preparations have shortcomings for drug delivery: 1) their components are costly, 2) their formation requires the input of mechanical energy, and 3) the resulting systems are not

thermodynamically stable. Liposomes are kinetically trapped aggregates that eventually fuse together to form lamellar phases, thereby releasing their encapsulated materials.<sup>4, 12</sup> In addition, their phospholipid components are chemically unstable, where hydrolysis and oxidative degradation occur readily.<sup>4</sup> Various improvements have been considered to overcome these deficiencies.<sup>13</sup> For example, cholesterol has been added to liposomes to improve the mechanical properties and flexibility of the bilayer.<sup>13</sup>

A more promising alternative to classical liposomes is cationic surfactant vesicles.<sup>14</sup> Similar to liposomes, these cationic surfactant vesicles form a bilayer with an aqueous compartment, but in contrast are formed from single-tailed, charged surfactant molecules (Figure 1.1). This system was first reported by Kaler and it has many advantages over conventional liposomes.<sup>14</sup> Most notably, cationic vesicles form spontaneously from inexpensive materials and are thermodynamically stable for long periods of time. Alternatively, few reports exist that describe the formation of liposomes that do not require extensive preparation techniques.<sup>15-17</sup> Liposomes are formed by reverse-phase evaporation, dehydration-rehydration, ultrasonication, and freeze-thaw extrusion.<sup>4</sup> The general film method, originally used by Bangham *et al.*, is one of the simplest approaches, but yields liposomes with low encapsulation efficiencies.<sup>7</sup>

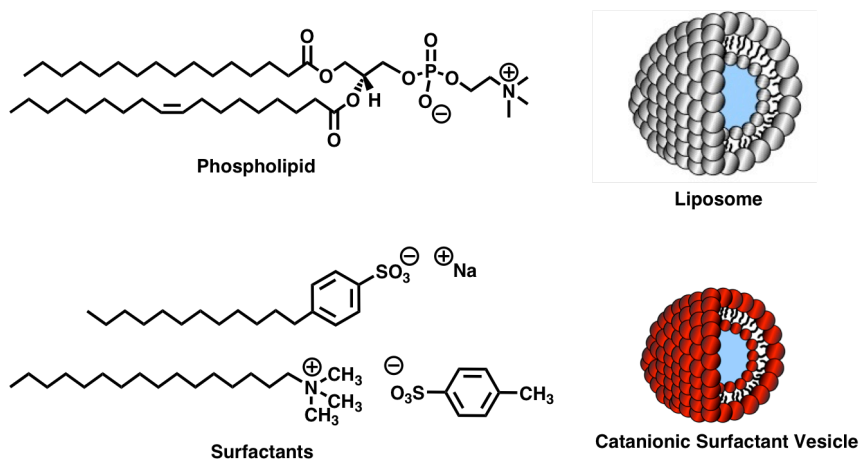


**Figure 1.1.** Chemical structures of a phospholipid and anionic and cationic surfactants and their aggregates.

Controlling surface charge is another characteristic that is extremely important when considering *in vivo* applications for colloids. Particles with especially low zeta potentials will be stable in solution because they are less likely to aggregate. Furthermore, highly negatively charged particles will not fuse with cells. An excess of one surfactant is used in the preparation of cationic vesicles, thereby resulting in vesicles with highly charged surfaces. In the case of anionic-rich cationic vesicles, the resulting negatively charged bilayer carries a charge similar to a eukaryotic cell and should not aggregate with other vesicles in solution. Many liposomes, on the other hand, are prepared from neutral phospholipids and exhibit a zeta potential of zero.<sup>18</sup> It is therefore not surprising that within the last decade, research using cationic surfactant vesicles has increased significantly, with dozens of cationic mixtures being studied.<sup>19-36</sup>

A detailed comparison between the properties of cationic vesicles and liposomes is outlined in Table 1.1.

	<b>Liposomes</b>	<b>Catanionic Vesicles</b>
<b>Constituents</b>	Expensive phospholipids (EYPC \$177)	Inexpensive ionic surfactants (SDBS \$1.10)
<b>Formation</b>	Input of mechanical energy (sonication, extrusion, etc.)	Spontaneous
<b>Stability</b>	Limited from days to weeks (hydrolysis, oxidative degradation, liposomal fusion)	Stable for years
<b>Encapsulation Efficiency</b>	Inefficient	Highly efficient
<b>Sterilization Techniques</b>	None	Pasteurization at 65 °C and autoclaving

**Table 1.1.** Comparison of catanionic vesicles to liposomes.

In order to understand how catanionic vesicles spontaneously form, are stable, and have high encapsulation efficiencies, the properties and capabilities of catanionic will be discussed in more detail.

### 1.2 *Physical Properties of Surfactants*

Hydrocarbon-based amphiphiles, referred to as surfactants, are the constituents of catanionic surfactant vesicles and are extensively used in commercial applications such as textiles, paint products, cosmetics, and soaps.<sup>13</sup> These amphiphilic molecules either orient their hydrophilic head group or hydrophobic tail toward a polar or nonpolar

solvent, respectively. Depending on the charge of the head group, surfactants are considered anionic, cationic, nonionic, or zwitterionic.

The term “surfactant” originates from surface-active agents and their unique ability to form aggregates at the air/solvent interface in order to minimize hydrophobic interactions with water (Figure 1.2, A). When surfactants are added to water, the surface tension is lowered as tails assemble in one-direction at the interface. After maximum saturation is achieved at the surface, addition of any excess surfactant only leads to the formation of micelles (Figure 1.2, C). At this point, known as the critical micelle concentration (cmc), aggregates form where tails assemble a lipophilic core. This aggregate structure minimizes the interaction between the hydrophobic tails with water.

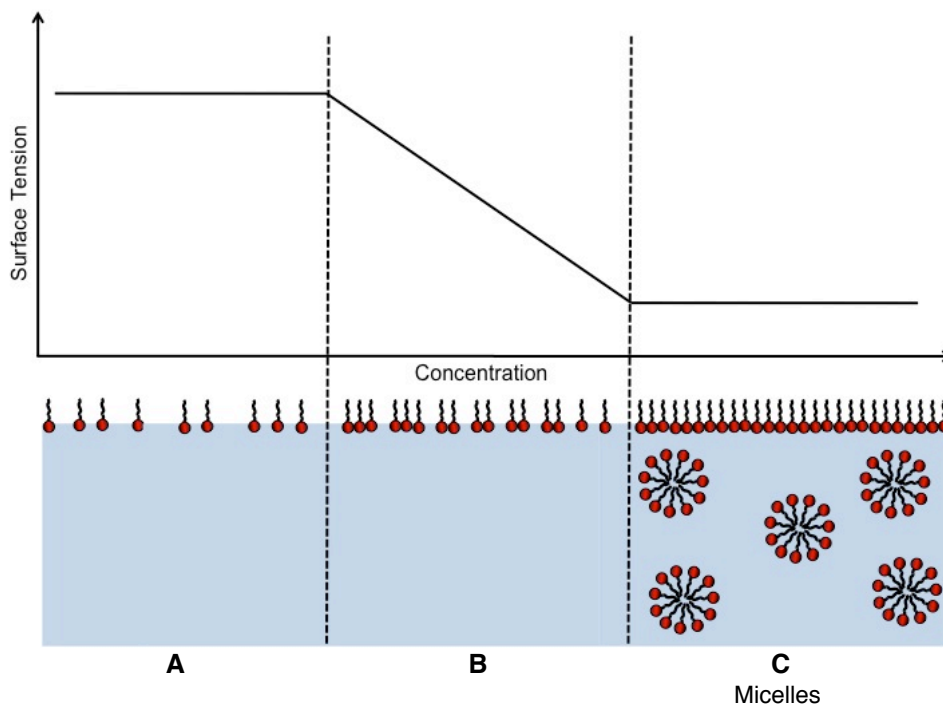


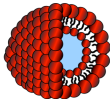
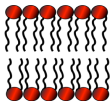
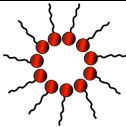
**Figure 1.2.** Critical micelle concentration (cmc) in solution. Surfactant molecules are oriented at the air/water interface with hydrophobic tails and head groups, respectively.

Geometric considerations of amphiphiles influence the type of aggregates and ordered-structures that will form in solution (Table 1.2). Depending on the cross-sectional area of the head group and tail, the packing of amphiphiles controls the type of aggregate that forms.<sup>13</sup> This principle is introduced by the packing parameter,  $P$ , defined as:

$$P = \frac{\nu}{a_o l} = \frac{a_{o(tail)}}{a_{o(head)}} \quad \text{Eq. 1.1}$$

where  $\nu$  is the volume of the tail,  $a_{o(head)}$  is the area of the head group,  $a_{o(tail)}$  is the area of the tail, and  $l$  is the optimal chain length (Figure 1.3).<sup>37</sup>

Highly curved structures ultimately form when  $a_{o(head)} > a_{o(tail)}$ . Depending on the ratio of the head group and tail areas, spherical micelles, cylindrical micelles, or vesicles form under aqueous conditions. When both head and tail regions are comparable in size, bilayers (i.e. lamellar phases) are most stable. As the tail becomes far larger than the head ( $a_{o(head)} \ll a_{o(tail)}$ ), structures with inverse curvature, such as inverse micelles, form (Table 1.2).

Packing Parameter	Geometric Shape	Predicted Aggregate Structure
$< 1/3$		 spherical micelles
$1/3 - 1/2$		 cylindrical micelles
$1/2 - 1$		 curved bilayers – vesicles
1		 planar bilayers
$1 >$		 inverse micelles

**Table 1.2.** Effect of amphiphile geometry on aggregate structure. Estimate of packing parameters for amphiphiles leads to the most likely formed structure in solution. Table adapted from ref. 13.

The phospholipid components of liposomes have two tails and head group of comparable size, where  $P \approx 1$  (Table 1.2). Therefore, bilayers are the most favorable structures for phospholipid aggregates. In order to form spherical liposomes, phospholipids must be forced into their curved aggregate structures, and as a result, are

not thermodynamically favorable. For this reason, liposomes eventually revert back to lamellar phases over time.

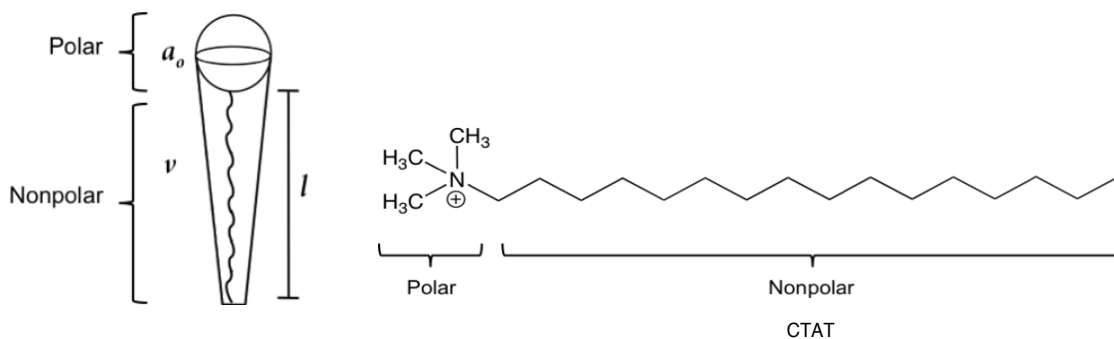


**Figure 1.3.** Hydrophobic and hydrophilic moieties on amphiphiles. The structure of a cationic surfactant molecule is shown above.

In the case of cationic surfactant vesicles, individual single-tailed surfactant molecules are cone-like in geometry, where  $P \approx 1/3$  (Table 1.2). Differential to their individual counterparts, the polar portion of cationic and anionic surfactants associate with one another to form a zwitterion head group with two tails. This ion pairing of surfactants mimics the characteristic nature of phospholipids (Figure 1.4). Thus,  $a_{o(head)}$  is reduced due to the electrostatic interactions of head groups and  $\nu$  is increased by the addition of a second tail, resulting in  $P \approx 1$ .<sup>37</sup> One would therefore expect cationic surfactant vesicles to be similar to liposomes with regard to their formation and stability. Yet, cationic surfactant vesicles spontaneously form and are thermodynamically stable.

### 1.3 Formation of Cationic Surfactant Vesicles

Spontaneous formation of cationic vesicles cannot be explained by merely considering their electrostatic and geometric characteristics. Extensive studies on the

phase behavior of catanionic vesicles have revealed that an excess of one surfactant must be present in order to spontaneously form vesicles.<sup>14, 37-45</sup> The excess of one surfactant causes spontaneous curvature of catanionic vesicles where the inner and outer monolayer are equal and opposite in curvature (Figure 1.4). Each leaflet of the resulting curved bilayer has a different composition. A higher mole fraction of the excess surfactant leads to less efficient packing and causes the outer leaflet to have a larger head group spacing. As a result, the inner leaflet is composed of ion pairs, thereby reducing the head group separation, leading to inverse curvature.

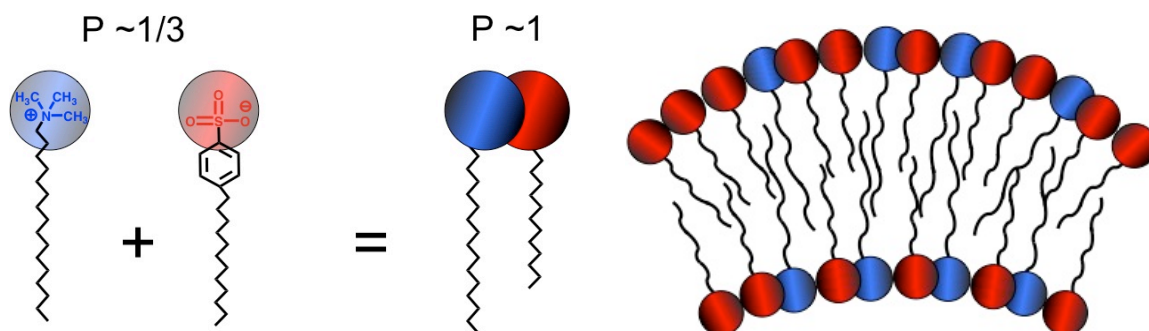


**Figure 1.4.** Association of cationic and anionic surfactants. One surfactant must be in excess to spontaneously form catanionic vesicles. Figure adapted from ref. 46.

Differences in the composition of the bilayer results in the ability to control surface charge and the zeta potential of the resulting colloidal solutions. For example, catanionic vesicles containing an excess of the anionic surfactant form highly negatively charged surfaces. The highly charge surface prevents aggregation of anionic-rich vesicles in solution and would also prevent the fusion of catanionic vesicles with anionic cell membranes.

For the original surfactant system studied by Kaler, optimal vesicle formation occurs at 7:3 and 3:7 w/w of the cationic surfactant cetyltrimethylammonium tosylate (CTAT) and anionic surfactant sodium dodecylbenzenesulfonate (SDBS), respectively (Figure 1.5). By using 1-3 wt % total concentration of the two surfactants with water, catanionic vesicles predominate (Figure 1.6).<sup>14</sup>

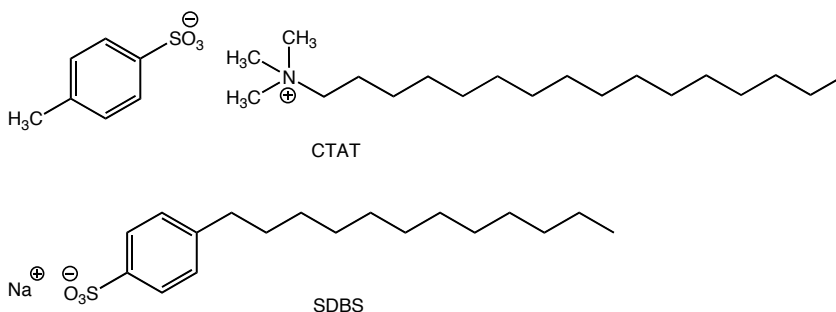


**Figure 1.5.** Chemical structures of CTAT and SDBS.

The critical aggregation concentration (cac) of catanionic vesicles is far lower than the cmc of either of the pure surfactant in water. For example, solutions of CTAT form rod-like micelles at a cmc of 0.01 wt % while SDBS forms spherical micelles at a cmc of 0.1 wt %. Surface tension measurements show that a mixture of SDBS/CTAT gives rise to a cac of 0.00017 wt %. Therefore, the combination of components, where one surfactant is in excess, forms more favorable structures compared to individual surfactants that form micelles.

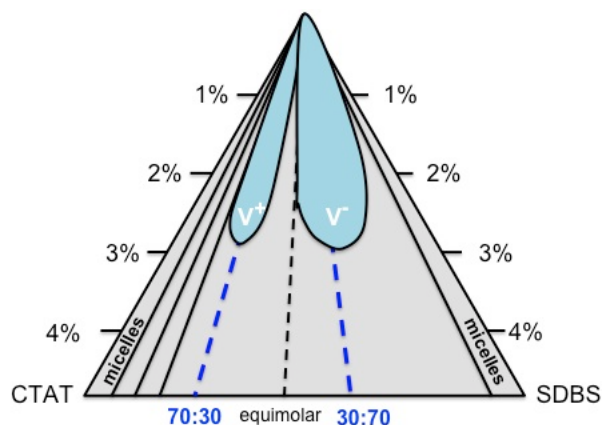


**Figure 1.6.** Phase diagram of CTAT/SDBS in water. Vesicles are present in the two lobes, denoted by  $V^+$  for CTAT-rich vesicles and  $V^-$  for SDBS-rich vesicles. The bottom axis is the weight ratio of the surfactants and the side axes indicate a total concentration (wt %) of the two surfactants in  $H_2O$ . Adapted from ref. 42.

Others have built upon Kaler's work by studying surfactants of various chain lengths with a variety of ionic head groups.<sup>37, 39-41, 43, 44, 47-49</sup> For example, Regev and coworkers showed that the relative length of alkyl chains affects self-assembly, forming either micelles, planar bilayers, or vesicles.<sup>37</sup> As a result, the quantities needed for each surfactant to form vesicles changes as the chain length is adjusted.<sup>23</sup>

#### 1.4 Loading of Cationic Surfactant Vesicles

Cationic surfactant vesicles have the potential to be loaded with a variety of molecules and used as alternatives over conventional liposomes due to their facile preparation and ready functionalization with additional components.<sup>21-23, 27</sup> Since Kaler's initial work on loading SDBS/CTAT vesicles with glucose<sup>14</sup>, efforts have expanded to improve the loading of molecules into cationic systems. While the authors report a considerable amount of glucose was retained within vesicles, no quantitative data was reported.

As seen in the three-dimensional structure (Figure 1.1), the vesicle bilayer surrounds an internal aqueous cavity, which has been utilized for the encapsulation of water-soluble molecules. Caillet found that only 0.2% of glucose could be encapsulated in cationic vesicles composed of sodium octyl sulfate (SOS) and cetyltrimethylammonium bromide (CTAB). The authors tried loading other biomolecules, but found that only 0.4% of riboflavin could be loaded and carboxyfluorescein (CF) could not be encapsulated.<sup>47</sup> Other work using SDBS/CTAT vesicles revealed that glucose leaks out over time, thereby reducing the promise of loading the internal aqueous cavity of cationic vesicles.<sup>19</sup>

Danoff *et al.* showed that the encapsulation efficiency of SDBS/CTAT vesicles was improved by loading a molecule opposite in charge with the vesicle surface charge.<sup>35</sup> Specifically, negatively charged vesicles were found to selectively encapsulate cationic dyes and positively charged vesicles selectively encapsulate anionic dyes.<sup>36</sup> SDBS-rich (anionic) vesicles were loaded with the cationic dye rhodamine B and anionic dye CF. Purification of vesicles by gel filtration showed retention of rhodamine B in vesicles while CF was separated from the vesicle solution. Therefore, cationic vesicles preferentially sequester molecules of opposite charge (Figure 1.7). In contrast, similarly charged molecules are inefficiently incorporated into cationic vesicles due to electrostatic repulsion with the vesicle bilayer.<sup>36</sup> Further studies showed the successful loading of other charged molecules such as rhodamine 6G, Lucifer yellow, and doxorubicin hydrochloride.

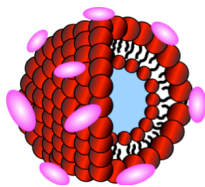


**Figure 1.7.** Electrostatic adsorption of charged molecules into oppositely charged vesicles.

Although cationic vesicles can be modified by the incorporation of molecules using electrostatic interactions, charged molecules can eventually detach or be replaced by molecules that bind more efficiently. An alternative method is to functionalize surfactant vesicles by adding a hydrophobic linker to molecules of interest. Using the hydrophobic effect, long alkyl chains are inserted into the vesicle bilayer to reduce unfavorable interactions in an aqueous environment (Figure 1.8). As a result, vesicles can be functionalized with virtually any molecule that contains a hydrophobic moiety. The first realization of this idea was by Walker and Zasadzinski when they functionalized the outer membrane of cationic vesicles with biotin-lipid conjugates.<sup>20</sup> PEG has also been inserted into the bilayer of cationic surfactant vesicles in order to improve their circulation time *in vivo*.<sup>38, 50</sup> Modification of the bilayer with PEG provides a lipophilic barrier that prevents immune system recognition and clearance of vesicles by the renal system.<sup>2</sup>

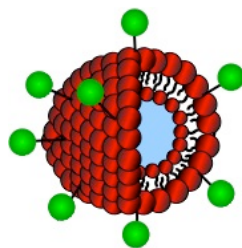


**Figure 1.8.** Functionalizing cationic surfactant vesicles with molecules containing hydrophobic moieties.

Catanionic vesicles have also been prepared with glycoconjugates, where the carbohydrate is modified with a lipid tail.<sup>51-53</sup> Functionalization of catanionic vesicles with glycoconjugates is particularly useful due to the involvement of carbohydrates in cell-cell adhesion, cell-cell signaling, and the immune response.<sup>54</sup> Furthermore, catanionic vesicles coated with specific carbohydrates can regulate cell recognition, allowing for the targeted delivery of payloads. The DeShong group reported the functionalization of SDBS-rich vesicles with the glycoconjugates glucose, maltose, maltotriose, and lactose.<sup>33</sup> Carbohydrates were proven to remain accessible by performing lectin-binding studies. Vesicles containing a monomer specific to a lectin selectively aggregated after the addition of the lectin.<sup>33</sup>

Catanionic vesicles can also be used for *in vitro* technology as diagnostic agents. The Raghavan and Payne *et al.* have adhered catanionic surfactant vesicles to a surface coated with hydrophobically-modified chitosan (HM chitosan) (Figure 1.9).<sup>55</sup> The hydrocarbon tails on the HM chitosan surface insert into the vesicle leaflet and anchor the vesicles. Functionalized catanionic vesicles anchored to a surface have also shown selective binding with molecules in solution.<sup>31</sup> Biotinylated catanionic vesicles were treated with fluorescently-labeled NeutrAvidin, which has a high binding affinity for biotin. Fluorescence of the tetramer NeutrAvidin remained associated with the anchored catanionic vesicles after washing. These results showed that biotinylated vesicle binding with NeutrAvidin occurred.<sup>31</sup>

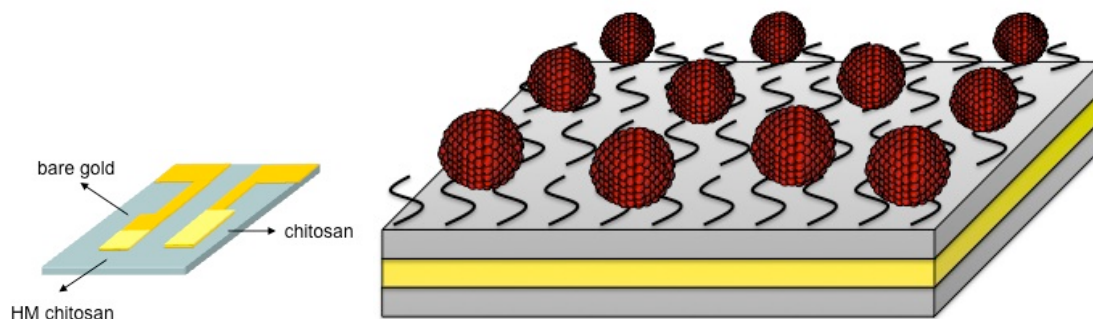


**Figure 1.9.** Cationic surfactant vesicles attached to a surface coated with HM chitosan.<sup>55</sup>

### 1.5 Conclusions

As previously indicated, the benefits of synthesizing cationic vesicles include lower cost, ease of synthesis, and significantly enhanced vesicle stability. In order to understand and determine the usefulness of cationic surfactant vesicles in biological applications, their loading and stability must first be researched. If cationic vesicles are to be used over conventional liposomes, they must have similar loading qualities, as well as enhanced stability, cost, and ease of preparation.

### 1.6 Research Goals

Research in the DeShong group has focused on functionalizing cationic surfactant vesicles for vaccine development and targeted delivery applications. Accordingly, it is critical that the methods of preparing functionalized vesicles can be optimized and that the stability of the resulting suspensions be characterized. The focus of this study was 1) to prepare, characterize, and functionalize cationic surfactant vesicles, 2) to use surfactant vesicles to extract biologically active molecules for use in

vaccine applications, and 3) to load drug molecules within vesicles for use as drug carriers.<sup>35, 36, 47, 33</sup>

Toward this goal, cationic surfactant vesicles were prepared with a wide range of bioconjugates and fully characterized. Results of these studies are discussed in Chapter 2. After full characterization, vesicles were loaded with complex molecules and were employed for *in vivo* applications. These vesicles systems were studied for their potential use in developing bacterial vaccines and will be discussed in Chapter 3. Finally, vesicle systems were incorporated with biologically active materials to determine their effectiveness as vaccines and targeted drug delivery vehicles. These results and studies are discussed in Chapters 4 and 5, respectively.

## References

1. Barratt, G., Colloidal drug carriers: Achievements and perspectives. *Cell. Mol. Life Sci.* **2003**, *60* (1), 21-37.
2. Allen, T. M.; Moase, E. H., Therapeutic opportunities for targeted liposomal drug delivery. *Adv. Drug Delivery Rev.* **1996**, *21* (2), 117-133.
3. Gregoriadis, G.; Leathwood, P. D.; Ryman, B. E., Enzyme entrapment in liposomes. *FEBS Letters* **1971**, *14* (2), 95-9.
4. Samad, A.; Sultana, Y.; Aqil, M., Liposomal drug delivery systems: an update review. *Curr. Drug Delivery* **2007**, *4* (4), 297-305.
5. Anabousi, S.; Bakowsky, U.; Schneider, M.; Huwer, H.; Lehr, C.-M.; Ehrhardt, C., In vitro assessment of transferrin-conjugated liposomes as drug delivery systems for inhalation therapy of lung cancer. *Eur. J. Pharm. Sci.* **2006**, *29* (5), 367-374.
6. Brochu, H.; Polidori, A.; Pucci, B.; Vermette, P., Drug delivery systems using immobilized intact liposomes: A comparative and critical review. *Curr. Drug Delivery* **2004**, *1* (3), 299-312.
7. Bangham, A. D.; Horne, R. W., Negative staining of phospholipids and their structural modification by surface-active agents as observed in the electron microscope. *J. Mol. Biol.* **1964**, *8* (5), 660-8.
8. Cheng, Z.; Al Zaki, A.; Hui, J. Z.; Muzykantov, V. R.; Tsourkas, A., Multifunctional nanoparticles: Cost versus benefit of adding targeting and imaging capabilities. *Science* **2012**, *338* (6109), 903-910.

9. Zhu, J.; Xue, J.; Guo, Z.; Zhang, L.; Marchant, R. E., Biomimetic glycoliposomes as nanocarriers for targeting P-selectin on activated platelets. *Bioconjugate Chem.* **2007**, *18* (5), 1366-1369.
10. Zhu, J.; Yan, F.; Guo, Z.; Marchant, R. E., Surface modification of liposomes by saccharides: Vesicle size and stability of lactosyl liposomes studied by photon correlation spectroscopy. *J. Colloid Interface Sci.* **2005**, *289* (2), 542-550.
11. Torchilin, V. P., Recent advances with liposomes as pharmaceutical carriers. *Nat. Rev. Drug Discovery* **2005**, *4* (2), 145-160.
12. Gregoriadis, G.; Editor, Liposome preparation and related techniques. Liposome technology, *3<sup>rd</sup> Ed., Volume 1.* **2007**; p 324 pp.
13. Lasic, D. D., Novel applications of liposomes. *Trends Biotechnol.* **1998**, *16* (7), 307-321.
14. Kaler, E. W.; Murthy, A. K.; Rodriguez, B. E.; Zasadzinski, J. A., Spontaneous vesicle formation in aqueous mixtures of single-tailed surfactants. *Science* **1989**, *245* (4924), 1371-4.
15. Talmon, Y.; Evans, D. F.; Ninham, B. W., Spontaneous vesicles formed from hydroxide surfactants: evidence from electron microscopy. *Science* **1983**, *221* (4615), 1047-8.
16. Hargreaves, W. R.; Deamer, D. W., Liposomes from ionic, single-chain amphiphiles. *Biochemistry* **1978**, *17* (18), 3759-68.
17. Gabriel, N. E.; Roberts, M. F., Spontaneous formation of stable unilamellar vesicles. *Biochemistry* **1984**, *23* (18), 4011-15.

18. Liui, A. L.; Tien, H. T.; Editors, Advances in planar lipid bilayers and liposomes, *Volume 4*. **2006**; p 325 pp.
19. Fischer, A.; Hebrant, M.; Tondre, C., Glucose encapsulation in catanionic vesicles and kinetic study of the entrapment/release processes in the sodium dodecyl benzene sulfonate/cetyltrimethylammonium tosylate/water system. *J. Colloid Interface Sci.* **2002**, *248* (1), 163-168.
20. Walker, S. A.; Zasadzinski, J. A., Electrostatic control of spontaneous vesicle aggregation. *Langmuir* **1997**, *13* (19), 5076-5081.
21. Boudier, A.; Castagnos, P.; Soussan, E.; Beaune, G.; Belkhef, H.; Menager, C.; Cabuil, V.; Haddioui, L.; Roques, C.; Rico-Lattes, I.; Blanzat, M., Polyvalent catanionic vesicles: Exploring the drug delivery mechanisms. *Int. J. Pharm.* **2011**, *403* (1-2), 230-236.
22. Bramer, T.; Dew, N.; Edsman, K., Catanionic mixtures involving a drug: a rather general concept that can be utilized for prolonged drug release from gels. *J. Pharm. Sci.* **2006**, *95* (4), 769-780.
23. Bramer, T.; Dew, N.; Edsman, K., Pharmaceutical applications for catanionic mixtures. *J. Pharm. Pharmacol.* **2008**, *59* (10), 1319-1334.
24. Chiruvolu, S.; Israelachvili, J. N.; Naranjo, E.; Xu, Z.; Zasadzinski, J. A.; Kaler, E. W.; Herrington, K. L., Measurement of forces between spontaneous vesicle-forming bilayers. *Langmuir* **1995**, *11* (11), 4256-66.
25. Coldren, B.; Van Zanten, R.; Mackel, M. J.; Zasadzinski, J. A.; Jung, H.-T., From vesicle size distributions to bilayer elasticity via cryo-transmission and freeze-fracture electron microscopy. *Langmuir* **2003**, *19* (14), 5632-5639.

26. Dey, S.; Mandal, U.; Sen Mojumdar, S.; Mandal, A. K.; Bhattacharyya, K., Diffusion of organic dyes in immobilized and free cationic vesicles. *J. Phys. Chem. B* **2010**, *114* (47), 15506-15511.
27. Jiang, Y.; Li, F.; Luan, Y.; Cao, W.; Ji, X.; Zhao, L.; Zhang, L.; Li, Z., Formation of drug/surfactant cationic vesicles and their application in sustained drug release. *Int. J. Pharm.* **2012**, *436* (1-2), 806-814.
28. Jiang, Y.; Luan, Y.; Qin, F.; Zhao, L.; Li, Z., Cationic vesicles from an amphiphilic prodrug molecule: a new concept for drug delivery systems. *RSC Adv.* **2012**, *2* (17), 6905-6912.
29. Li, H.; Xin, X.; Kalwarczyk, T.; Kalwarczyk, E.; Niton, P.; Holyst, R.; Hao, J., Reverse vesicles from a salt-free cationic surfactant system: A confocal fluorescence microscopy study. *Langmuir* **2010**, *26* (19), 15210-15218.
30. Marques, E. F.; Khan, A.; Lindman, B., A calorimetric study of the gel-to-liquid crystal transition in cationic surfactant vesicles. *Thermochim. Acta* **2002**, *394* (1-2), 31-37.
31. Pond, M. A.; Zangmeister, R. A., Carbohydrate-functionalized surfactant vesicles for controlling the density of glycan arrays. *Talanta* **2012**, *91*, 134-139.
32. Coldren, B. A.; Warriner, H.; van Zanten, R.; Zasadzinski, J. A.; Sirota, E. B., Lamellar gels and spontaneous vesicles in cationic surfactant mixtures. *Proc. Natl. Acad. Sci. U. S. A.* **2006**, *103* (50), 19213.
33. Park, J.; Rader, L. H.; Thomas, G. B.; Danoff, E. J.; English, D. S.; DeShong, P., Carbohydrate-functionalized cationic surfactant vesicles: preparation and lectin-binding studies. *Soft Matter* **2008**, *4* (9), 1916-1921.

34. Thomas, G. B.; Rader, L. H.; Park, J.; Abezgauz, L.; Danino, D.; De Shong, P.; English, D. S., Carbohydrate modified cationic vesicles: probing multivalent binding at the bilayer interface. *J. Am. Chem. Soc.* **2009**, *131* (15), 5471-5477.
35. Danoff, E. J.; Wang, X.; Tung, S.-H.; Sinkov, N. A.; Kemme, A. M.; Raghavan, S. R.; English, D. S., Surfactant vesicles for high-efficiency capture and separation of charged organic solutes. *Langmuir* **2007**, *23* (17), 8965-8971.
36. Wang, X.; Danoff, E. J.; Sinkov, N. A.; Lee, J.-H.; Raghavan, S. R.; English, D. S., Highly efficient capture and long-term encapsulation of dye by cationic surfactant vesicles. *Langmuir* **2006**, *22* (15), 6461-6464.
37. Regev, O.; Khan, A., Alkyl chain symmetry effects in mixed cationic-anionic surfactant systems. *J. Colloid Interface Sci.* **1996**, *182* (1), 95-109.
38. Berman, A.; Cohen, M.; Regev, O., Cationic vesicle-PEG-lipid system: Langmuir film and phase diagram study. *Langmuir* **2002**, *18* (15), 5681-5686.
39. Kondo, Y.; Uchiyama, H.; Yoshino, N.; Nishiyama, K.; Abe, M., Spontaneous vesicle formation from aqueous solutions of didodecyldimethylammonium bromide and sodium dodecyl sulfate mixtures. *Langmuir* **1995**, *11* (7), 2380-4.
40. Marques, E. F.; Regev, O.; Khan, A.; Da Graca Miguel, M.; Lindman, B., Vesicle formation and general phase behavior in the cationic mixture SDS-DDAB-water. The anionic-rich side. *J. Phys. Chem. B* **1998**, *102* (35), 6746-6758.
41. Herrington, K. L.; Kaler, E. W.; Miller, D. D.; Zasadzinski, J. A.; Chiruvolu, S., Phase behavior of aqueous mixtures of dodecyltrimethylammonium bromide (DTAB) and sodium dodecyl sulfate (SDS). *J. Phys. Chem.* **1993**, *97* (51), 13792-802.

42. Kaler, E. W.; Herrington, K. L.; Murthy, A. K.; Zasadzinski, J. A. N., Phase behavior and structures of mixtures of anionic and cationic surfactants. *J. Phys. Chem.* **1992**, *96* (16), 6698-707.
43. Edlund, H.; Sadaghiani, A.; Khan, A., Phase behavior and phase structure for catanionic surfactant mixtures: Dodecyltrimethylammonium chloride-sodium nonanoate-water system. *Langmuir* **1997**, *13* (19), 4953-4963.
44. Yacilla, M. T.; Herrington, K. L.; Brasher, L. L.; Kaler, E. W.; Chiruvolu, S.; Zasadzinski, J. A., Phase behavior of aqueous mixtures of cetyltrimethylammonium bromide (CTAB) and sodium octyl Sulfate (SOS). *J. Phys. Chem.* **1996**, *100* (14), 5874-9.
45. Marques, E. F.; Regev, O.; Khan, A.; Miguel, M. d. G.; Lindman, B., Vesicle formation and general phase behavior in the catanionic mixture SDS-DDAB-water. The cationic-rich side. *J. Phys. Chem. B* **1999**, *103* (39), 8353-8363.
46. Lioi, S. B.; Wang, X.; Islam, M. R.; Danoff, E. J.; English, D. S., Catanionic surfactant vesicles for electrostatic molecular sequestration and separation. *Phys. Chem. Chem. Phys.* **2009**, *11* (41), 9315-9325.
47. Caillet, C.; Hebrant, M.; Tondre, C., Sodium octyl sulfate/cetyltrimethylammonium bromide aatanionic vesicles: Aggregate composition and probe encapsulation. *Langmuir* **2000**, *16* (23), 9099-9102.
48. Tondre, C.; Caillet, C., Properties of the amphiphilic films in mixed cationic/anionic vesicles: a comprehensive view from a literature analysis. *Adv. Colloid Interface Sci.* **2001**, *93* (1-3), 115-134.

49. Zhao, G.-X.; Yu, W.-L., Vesicles from mixed sodium 10-undecenoate-decyltrimethylammonium bromide solutions. *J. Colloid Interface Sci.* **1995**, *173* (1), 159-64.
50. Working, P. K.; Newman, M. S.; Huang, S. K.; Mayhew, E.; Vaage, J.; Lasic, D. D., Pharmacokinetics, biodistribution and therapeutic efficacy of doxorubicin encapsulated in Stealth liposomes (Doxil). *J. Liposome Res.* **1994**, 667-87.
51. Menger, F. M.; Binder, W. H.; Keiper, J. S., Cationic surfactants with counterions of glucuronate glycosides. *Langmuir* **1997**, *13* (12), 3247-3250.
52. Blanzat, M.; Perez, E.; Rico-Lattes, I.; Prome, D.; Prome, J. C.; Lattes, A., New cationic glycolipids. 1. Synthesis, characterization, and biological activity of double-chain and gemini cationic analogues of galactosylceramide. *Langmuir* **1999**, *15* (19), 6163-6169.
53. Soussan, E.; Mille, C.; Blanzat, M.; Bordat, P.; Rico-Lattes, I., Sugar-derived tricatener cationic surfactant: Synthesis, self-assembly properties, and hydrophilic probe encapsulation by vesicles. *Langmuir* **2008**, *24* (6), 2326-2330.
54. Larsen, K.; Thygesen Mikkelsen, B.; Guillaumie, F.; Willats William, G. T.; Jensen Knud, J., Solid-phase chemical tools for glycobiology. *Carbohydr. Res.* **2006**, *341* (10), 1209-34.
55. Dowling, M. B.; Javvaji, V.; Payne, G. F.; Raghavan, S. R., Vesicle capture on patterned surfaces coated with amphiphilic biopolymers. *Soft Matter* **2011**, *7* (3), 1219-1226.

## Chapter 2: Loading and Characterization of Cationic Surfactant Vesicles

*Some parts of this chapter are related to the published article:*

Park, J.; Rader, L. H.; Thomas, G. B.; Danoff, E. J.; English, D. S.; DeShong, P., Carbohydrate-functionalized cationic surfactant vesicles: preparation and lectin-binding studies. *Soft Matter* **2008**, 4 (9), 1916-1921.

### 2.1 Introduction

Since the discovery of cationic surfactant vesicles, research has been performed on the loading and modification of these systems using dyes, drugs, and functionalizable materials.<sup>1-8</sup> For example, Walker and Zasadzinski added biotinylated phospholipids to the external leaflet of SDBS/CTAT vesicles.<sup>3,9</sup> By hydrophobic interactions, the biotin-lipid tail associated itself into the membrane of vesicles, thereby decorating the surface with biotin.<sup>3</sup> To determine the accessibility of biotin for binding, streptavidin, a protein that has a high binding affinity for biotin, was added. Addition of streptavidin induced biotinylated vesicles to aggregate in solution (Figure 2.1).

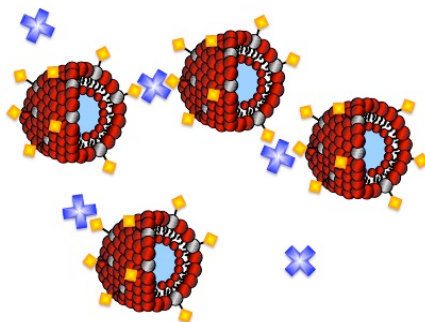


**Figure 2.1.** Biotinylated cationic surfactant vesicle binding with streptavidin. Binding of streptavidin to biotin leads to vesicle aggregation.

The DeShong group has shown that glucose, lactose, maltose, and maltotriose were incorporated (18-25%) into the outer leaflet of vesicles by conjugating molecules with a hydrophobic moiety employing glycosyl linkages.<sup>7</sup> Once glycoconjugates inserted, lectins, proteins that are highly specific for carbohydrates, were added. The accessibility of carbohydrates was shown by vesicle aggregation (Figure 2.2). This proved that glycoconjugates remained bioactive by selective binding to their lectins.<sup>7</sup> For example, the tetrameric lectins, concanavalin A (Con A) and peanut agglutinin (PNA) selectively bind to glucose residues and galactose residues, respectively. Vesicles containing terminal glucose monomers showed increased aggregation as the concentration of Con A was increased, but lacked agglutination after the addition of PNA. Furthermore, bare vesicles and lactose conjugated vesicles showed no significant increase in turbidity when titrated with Con A.

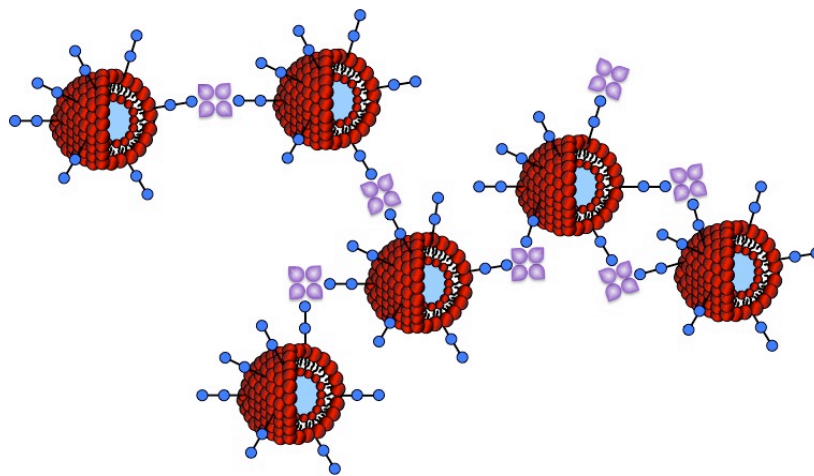


**Figure 2.2.** Con A aggregation of glucosyl-modified cationic surfactant vesicles.

Depending on the chemical structure of these glycoconjugates, surface density of cationic vesicles can be controlled. Thomas *et al.* showed that N-linked versus O-

linked glucosyl conjugates (Figure 2.3) showed significant differences in binding to Con A.<sup>8</sup> The O-linked conjugates exhibited binding kinetics consistent with a Poisson distribution of residues on the vesicle surface (Figure 2.3, A). N-linked conjugates gave rates of aggregation that were consistent with the formation of lipid rafts (Figure 2.3, B). This behavior of conjugate clustering at the surface of cationic vesicles is similar to what is observed on a solid surface.<sup>10</sup> N-linked glycoconjugates have been shown to align on gold surfaces where hydrogen bonding facilitates aggregation.<sup>10</sup> The same is proposed in a lipid bilayer, causing ligand clustering at the surface of vesicles.

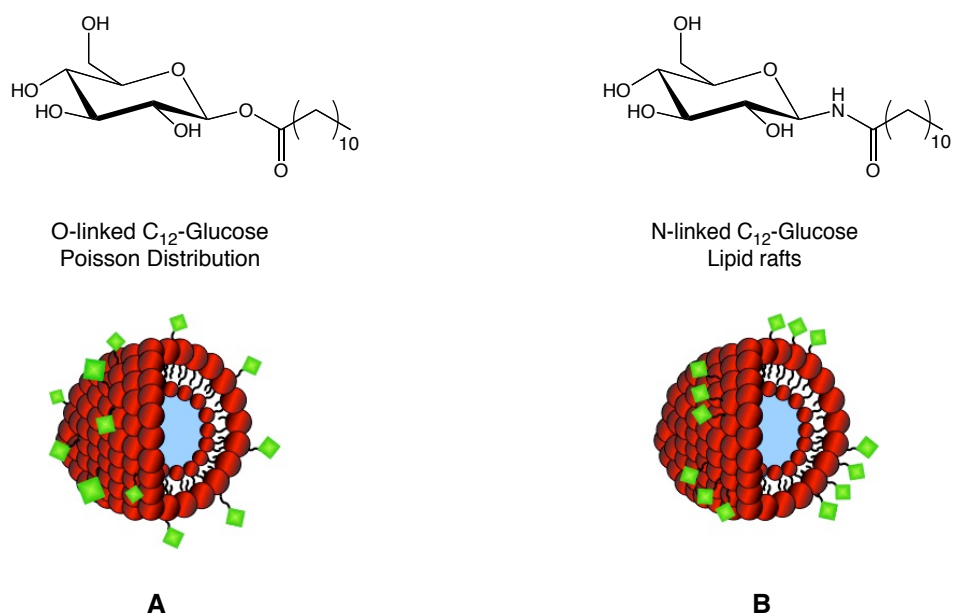


**Figure 2.3.** Poisson distribution and lipid rafts of glycoconjugates at the surface of cationic vesicles.

Functionalization of vesicles with glycoconjugates is particularly useful due to the involvement of carbohydrates in numerous biological processes.<sup>11</sup> Carbohydrates are also useful in vesicle technology because of their high degree of specificity and rapid

interaction with cell surface receptors. Catanionic vesicles coated with specific carbohydrate derivatives should elicit an immune response and target to specific tissues. These functionalized vesicles would allow for the recognition of catanionic vesicles as vaccines and as targeted delivery vehicles.

## 2.2 *Specific Aims, Results, and Discussion*

The specific aims for this research were 1) to develop methods to prepare bare catanionic surfactant vesicles and to examine the reproducibility and stability of each method, 2) to characterize catanionic vesicles functionalized with carbohydrates, peptides, dyes, drugs, and carotenoids, and 3) to study the use of functionalized catanionic vesicles in lectin-carbohydrate binding.

### 2.2.1 *Synthesis and Characterization of Bare Catanionic Surfactant Vesicles*

Bare catanionic vesicles were initially prepared according to the Wang procedure: dry surfactants were mixed by gently stirring in water and the colloidal solution equilibrated for 48 h.<sup>5</sup> Vesicle formation was monitored by measuring the average hydrodynamic radius using dynamic light scattering (DLS; see Experimental Section for details). Results showed that vesicles formed after 1 h and were essentially the same size as vesicle suspensions that were allowed to develop for 48 h (Table 2.1). These vesicle suspensions were also sonicated in a water bath and remained equal in size before and after sonication. This result showed that once all surfactants dissolved, catanionic vesicles spontaneously formed and did not require equilibration.

Time (h)	Hydrodynamic Radius (nm) ( $\pm < 0.5$ nm)*
1	54
3	54
6	55
24	56
48	56

**Table 2.1.** Monitoring vesicle equilibrium by DLS over time. A stock solution of bare catanionic vesicles was prepared by stirring the dry surfactants in water for 1 h and analyzing the size of vesicles by DLS. \*The standard deviation of all vesicle suspensions were  $< 0.5$  nm.

Next, catanionic vesicles were monitored over an extended period to determine their shelf life and thermodynamic stability. Vesicle suspensions that formed after 1 h were comparable in size and opacity to vesicle samples stored for  $> 6$  months. (Table 2.2). This result was important because it meant that catanionic vesicles would be stable indefinitely at room temperature.

Time	Hydrodynamic Radius (nm) ( $\pm < 0.5$ nm)*
1 week	57
1 month	57
5 months	58
8.5 months	57

**Table 2.2.** Monitoring temporal stability of vesicles by DLS. A stock solution of bare catanionic vesicles was analyzed to determine the shelf life of solutions stirred at room temperature. \*The standard deviation of all vesicle suspensions were  $< 0.5$  nm.

The previously reported sizes of vesicle suspensions only reported the average size. These results did not confirm whether the vesicles that were produced were monodisperse. For example, the average radius cannot be used for polydisperse samples because larger particles scatter light to a greater degree than smaller particles, as indicated by eq. 2.1.

$$I \propto d^6 \quad \text{Eq. 2.1}$$

In other words, if more than one population of vesicles exists, the larger particles will contribute more to the hydrodynamic radius measurement. By varying the scattering angle in DLS, if more than one size of particles is present, the hydrodynamic radius will not remain constant. For this reason vesicle suspensions were analyzed by multi-angle DLS to determine their polydispersity.

As vesicle suspensions were analyzed at scattering angles  $\theta$  45 to 150, two populations of vesicles were observed (Table 2.3). The hydrodynamic radii of smaller vesicles were  $\sim 35 \pm 10$  nm and larger vesicles were  $\sim 100 \pm 20$  nm.

Angle	Hydrodynamic Radius (nm)
45	34, 114, 133
55	32, 101, 102
65	46
75	36, 100, 140
85	58, 40
95	35, 98, 114
105	29, 79, 84
115	63
125	43
135	43
150	33, 91, 103

**Table 2.3.** Confirmation of size distribution of bare cationic vesicles studied by multi-angle DLS. A diluted solution of cationic bare vesicles was studied varying the scattering angle  $\theta = 45^\circ$  to  $150^\circ$ .

To confirm these two sizes quantitatively, the diffusion coefficient of each population was determined. If the relaxation time is related to the diffusion of vesicles in solution, then the decay rate is

$$\frac{1}{\tau} = Dq^2 \quad \text{Eq. 2.2}$$

where  $\tau$  is the relaxation of vesicles,  $q = (4\pi n/\lambda) (\sin\theta/2)$  is the wavenumber ( $n$  is the refractive index of the solution,  $\lambda$  is the wavelength of the laser beam, and  $\theta$  is the scattering angle), and  $D$  is the diffusion coefficient. By  $1/\tau$  versus  $q^2$ , the size of the two

populations was confirmed. Assuming Brownian, monodisperse, spherical, non-interactive particles, the Stokes-Einstein equation was used

$$D = \frac{k_B T}{6\pi\eta R_H} \quad \text{Eq. 2.3}$$

where  $k_B$  is the Boltzmann constant,  $T$  is temperature,  $\eta$  is viscosity of the solution, and  $R_H$  is the hydrodynamic radius. By using the diffusion coefficient in the Stokes-Einstein equation, the hydrodynamic radius for each population was determined (Figure 2.4). The diffusion coefficients from the small and large vesicles confirmed that bare cationic vesicles were either 80 or 180 nm in diameter.

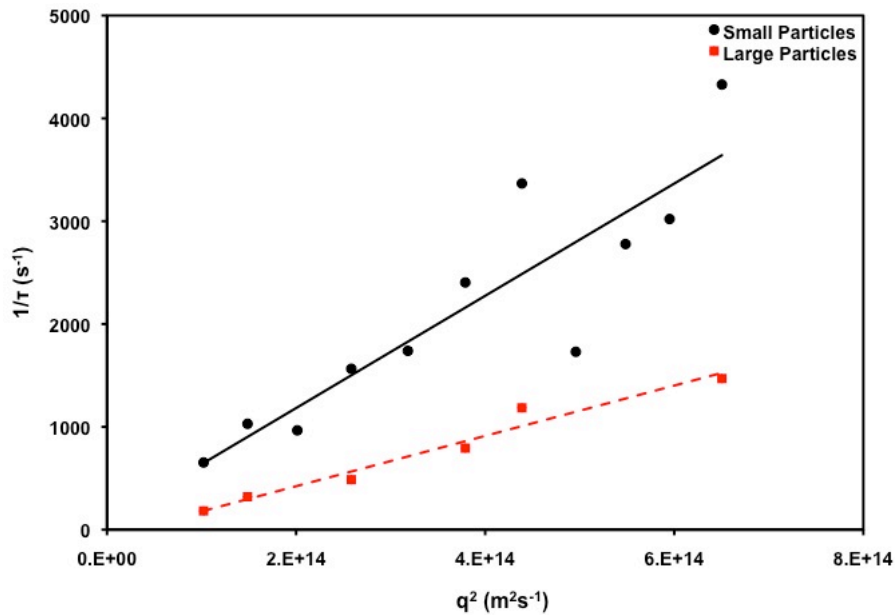


**Figure 2.4.** Confirmation of size distribution of bare cationic vesicles studies by multi-angle DLS. The hydrodynamic radii were calculated to be 40 nm and 89 nm. Wavenumber dependence of the decay rate  $1/\tau$  of the vesicle diffusion mode in bare vesicles at 25 °C. The initial slope yielded a diffusion coefficient  $D = 5.460 \times 10^{-8} \text{ cm}^2 \text{ s}^{-1}$  for smaller particles and  $D = 2.447 \times 10^{-8} \text{ cm}^2 \text{ s}^{-1}$  for larger particles in accordance with eq. 3. The large deviation from linearity at larger wavenumbers is attributed to polydispersity of the smaller vesicles.

Next, we wanted to determine which population of vesicles dominated. As the scattering angle increased, the amplitude of smaller particles increased and larger particles decreased. This result indicated that by increasing the angle, a greater amount of light was scattered by smaller particles. By plotting the amplitude of vesicles at each angle, the distribution of the two populations showed a majority of the smaller particles (Figure 2.5). As seen in Figure 11, the diffusion coefficient for small particles did not fit well at large scattering angles. This result indicated that smaller particles were polydisperse. In contrast, larger particles were fit well to a linear curve, which showed that larger particles were monodisperse. Unfortunately, the precise ratio of each population could not be determined unless standard solutions of 80 and 180 nm particles are utilized for calibration.

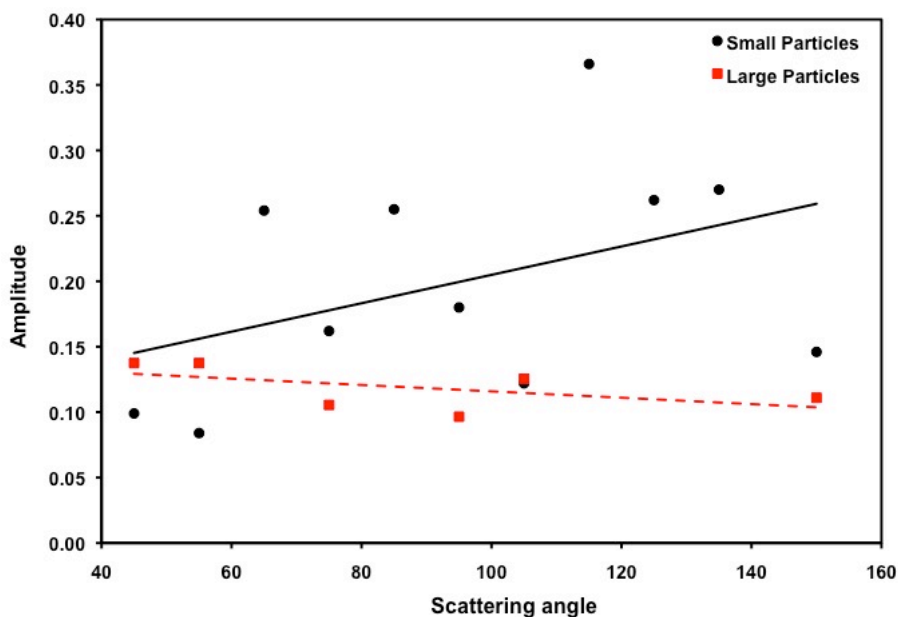


**Figure 2.5.** Amplitude of small and large particle populations as the scattering angle increased.

While cationic vesicle size can be determined by DLS, an actual snapshot of vesicles in solution would give a more accurate picture. For this reason, cryogenic-transmission electron microscopy (cryo-TEM) was used to confirm our measurements reported from DLS. Dr. Douglas English vitrified bare vesicles in liquid ethanol and observed vesicle suspensions by cryo-TEM. The majority of vesicles appeared to be  $80 \pm 20$  nm (Figure 2.6). This result matched the data that we reported from multi-angle DLS.

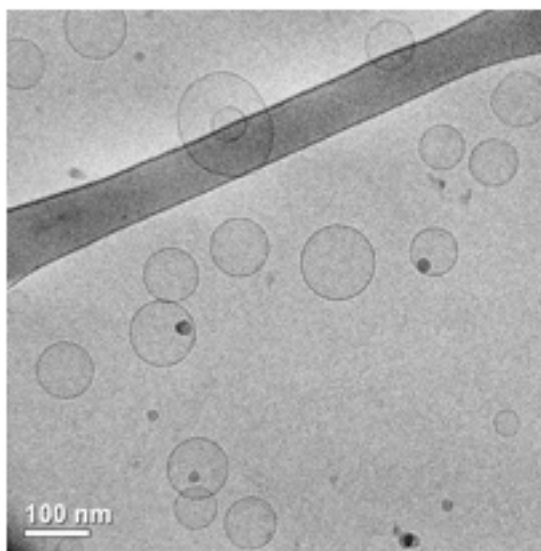


**Figure 2.6.** Cryo-TEM of bare cationic vesicles (performed by Dr. Douglas English, Wichita State University). The suspension contained two populations, where smaller particles were in majority. Smaller vesicles were approximately  $80 \pm 20$  nm in diameter.

Next, we wanted to further characterize cationic vesicles to determine other factors that are responsible for their stability. For example, zeta potential measures the charge at the surface of particles. Zeta potential is important with regard to colloidal solutions because highly charged particles are less likely to aggregate with one another above  $\pm 30$  mV (e.g. most cells). Zeta potentials were taken on bare cationic vesicles

in order to determine the stability of vesicle suspensions. Zeta potential measurements conducted by Dr. Sara Lioi, Dr. Matthew Hurley, and Neeraja Dashaputre showed that SDBS-rich (anionic) vesicles were  $-57$  mV. SDBS-rich vesicles contain highly negatively charged surfaces as a result of an excess of the anionic surfactant SDBS. Therefore, SDBS-rich vesicles are stable in solution and will not aggregate because of electrostatic repulsion with other vesicles. Similarly, SDBS-rich vesicles should not fuse with cells because of this repulsion. In contrast, CTAT-rich (cationic) vesicles would rapidly fuse with cells as a result of electrostatic attraction. For this reason, SDBS-rich vesicles are the focus of this study.

Next, we investigated several different vesicle preparation methods in order to compare the ease of preparation, reproducibility, scalability, and stability of each method. A number of factors influenced the characteristics of the vesicles that were produced. These factors included the purity of the initial components, the solubility of the surfactants in water or buffer, and the hygroscopic nature of the solid surfactants SDBS and CTAT. Formation of cationic vesicles was studied using four different methods: 1) dissolving solid surfactants together in water, 2) blending surfactants together using a grinder followed by dissolution in water, 3) combining surfactant solutions, and 4) adding solid CTAT to a solution of SDBS. Specific preparations for each method can be found in the Experimental Section. Each method produced vesicles and each sample of vesicles was examined by DLS for their average hydrodynamic radius. The results from each method are summarized in Table 2.4.

Method 1 demonstrated limited ability for production of cationic vesicles due to the difficulty in precisely weighing small quantities of hygroscopic surfactants. While

solid CTAT is less hygroscopic after recrystallization and can be easily weighed reproducibly without restrictions in handling, SDBS becomes gummy from water adsorption. Therefore, a procedure that required reproducible weighing of a hygroscopic reagent was not viable.

Preparation Method	Hydrodynamic Radius (nm)	Hydrodynamic Radius (nm)
	( $\pm < 0.5$ nm)*	( $\pm < 0.5$ nm)*
	Initial	After 8.5 Months
1	57	57
2	146 $\pm$ 3	— <sup>#</sup>
3	43	40
4	59	54

**Table 2.4.** Various sizes of cationic vesicles prepared by various techniques. Stock solutions of bare cationic vesicles were prepared by 1) dissolving solid surfactants together in water, 2) blending surfactants together using a grinder followed by dissolution in water, 3) combining surfactant solutions, and 4) adding solid CTAT to a solution of SDBS. Samples were reanalyzed again after 8.5 months to compare stability to the traditional Method 1. \*The standard deviation of unreported vesicle suspensions was  $< 0.5$  nm. <sup>#</sup>Sample precipitated on standing.

Method 2 was not acceptable for the production of vesicles because the resulting vesicles lacked reproducibility in size and stability. Vesicles prepared using this method were more opaque than vesicles prepared using solid surfactants, indicating the larger size of the vesicles produced by this method. Since light scattering of larger particles is more efficient, the solution containing the larger particles appeared more opaque, as seen qualitatively in Figure 15. More important was that the resulting colloidal solution was not thermodynamically stable and after several months the vesicles had precipitated (Table 2.4). The lack of stability and variations in size are likely due to the inaccurate

addition of the required amount of each component. As seen in the phase diagram for SDBS/CTAT, vesicles only form at specific ratios in water (Figure 1.6). Straying from the 7:3 w/w values leads to either precipitation of components or formation of other lamellar phases. In addition, as the surfactants were blended together, the resulting mixture became gummy from adsorption of water, which prevented the ability to accurately weight out 100 mg of the mixture. Also, vesicles prepared under this method could not be filtered through a sterile filter due to shearing forces from the filter.



**Figure 2.7.** Solutions of cationic bare vesicles formed from 1) solid surfactants and 2) blended surfactants. The University of Maryland seal can be seen behind vesicles prepared using dry surfactants. Vesicles prepared by blended surfactants yielded significantly cloudier solutions containing larger vesicles, which scattered light to a greater degree.

Method 3 was limited by the solubility of the components and vesicle size. SDBS is readily soluble in water, whereas CTAT is only slightly soluble, which caused difficulty preparing stock solutions. The viscosity of the CTAT solution prevented the addition of the CTAT solution to SDBS, leaving residual CTAT in the vial. Therefore, the SDBS solution must always be added directly to the CTAT solution. Vesicles formed immediately upon pipetting the solutions together and remained stable over time.

Catanionic vesicles that formed from mixing surfactant solutions were reproducibly smaller in size than vesicles prepared under the traditional method of Wang.<sup>5</sup> Additional studies including multi-angle DLS and cryo-TEM are needed to further characterize vesicles made in this manner in order to compare their morphology to vesicles formed using Method 1. However, this method would be appropriate for reproducibility, ease of preparation, and scalability of production, assuming that smaller catanionic vesicles were required.

Method 4 was found to produce catanionic vesicles of similar characteristics to the traditionally used vesicle forming method. Catanionic vesicles prepared using either Method 1 or Method 4 had comparable properties with regard to their hydrodynamic radii (Table 2.4) and stability. Vesicles prepared using either method produced vesicles with a hydrodynamic radius of approximately  $56 \pm 3$  nm. Suspensions proved to be thermodynamically stable in water and vesicle size remained constant over a period of 6 months at room temperature.

The average zeta potential was used to determine the electrical potential on the surface of the vesicles to determine if these two suspensions were equivalent. Average zeta potentials of vesicles prepared using solid surfactants, Method 1, was -57 mV, while Method 4 produced vesicles of -56 mV (Table 2.5). Both preparation methods yielded vesicles that were equivalent in size and surface potential, which showed that vesicle formation likely occurs by similar mechanisms.

Preparation Method	Zeta Potential (mV)
1	-57
4	-56

**Table 2.5.** Average zeta potentials of bare cationic surfactant vesicles; performed by Dr. Sara Lioi. Solutions of cationic bare vesicles were formed from 1) solid surfactants and 4) adding solid CTAT to a solution of SDBS.

As indicated earlier, the average hydrodynamic radius does not provide information regarding the distribution of vesicle sizes in suspension, but only the average size. Samples prepared by Methods 1 and 4 were analyzed by the English lab. Both suspensions had hydrodynamic radii of ~55 nm and contained two similar populations of vesicles (Table 2.6). Further studies by multi-angle DLS and cryo-TEM would provide more accurate data to further confirm these results.

Preparation Method	Hydrodynamic Radius (nm)
1	30-40, 100-130
4	35-40, 100-150

**Table 2.6.** Size distribution of vesicles studied by DLS; performed by a student in the English group (Wichita State University). Solutions of cationic bare vesicles were formed from (1) solid surfactants and (4) adding solid CTAT to a solution of SDBS, where both yield two populations of vesicles.

Cationic surfactant vesicles prepared by Methods 1, 3, and 4 were shown to be thermodynamically stable while vesicle size was dependent upon the method of preparation. The comparison of different methods for the production of cationic

vesicles indicated that vesicle size can be controlled. Furthermore, different preparation methods for vesicle formation may prove more useful than others under special conditions. For example, when loading hydrophobic drugs into vesicles, different vesicle preparation methods may incorporate molecules more efficiently. For example, using Method 1, where dry surfactants are dissolved in water, causes difficulty for the incorporation of molecules that cannot be solubilized in water. Whereas Methods 3 and 4, where a solution of surfactant is prepared, may be used to initially solubilize a drug within micelles. Research has shown that micelles incorporate insoluble molecules inside the hydrophobic region of the aggregate.<sup>12, 13</sup> After the addition of the second surfactant, the hydrophobic molecule may be incorporated into vesicles because of the molecule's association with the initial surfactant. These methods provide a plethora of opportunities to cater to the solubility requirements of individual molecules during loading into cationic vesicles.

#### *2.2.1.1 Stability of Bare Cationic Surfactant Vesicles under Drug Formation Conditions*

In order for vesicles to be considered for *in vivo* applications, their stability under various physiological conditions were studied. Vesicles were prepared in buffered solutions, saline solutions, and tested at different pH values. Cationic prepared in HEPES buffer at pH 7.4 yielded vesicles of equal size and opacity to vesicle suspensions prepared in water. Specifically, vesicles had a hydrodynamic radius of 55 nm and remained this size over time. Previous studies report that cationic vesicles remained intact after the addition of NaCl solutions. Vesicles even remained stable beyond

physiological saline concentrations (0.15 M).<sup>6</sup> Next, solutions of HCl and NaOH were added dropwise to vesicle suspensions. Vesicles remained intact at a pH of 2 to 11 and remained equivalent in size at each pH. These results indicated that catanionic vesicles are robust systems that are stable at high ionic strength and extreme pH.

Next, the long-term storage of vesicles at -20 °C was studied. Vesicle suspensions were frozen in a -20 °C freezer and in liquid N<sub>2</sub>. After immediate freezing of both samples, surfactants precipitated and the suspensions were no longer cloudy and opalescent. Even upon standing, the bare catanionic vesicles that eventually formed from freezing at -20 °C and in liquid N<sub>2</sub> had hydrodynamic radii of 195 ± 5 nm and 358 ± 14 nm, respectively. These results indicated that vesicles were disrupted and freezing likely ruptured vesicles upon formation of ice crystals.

Next, we studied the ability to sterilize vesicle suspensions by removing bacterial contamination for their potential use in clinical applications. We sterilized vesicles by filtration through sterile filters (0.22 μm) and by autoclaving. The hydrodynamic radius before and after filtration was 57 and 56 nm, respectively. While vesicle size did not change, shearing forces of the vesicles could be an issue if there are ever vesicles larger than the membrane. This would release free surfactant into solution and cause toxicity of the surfactant that is not associated with vesicles. Autoclaved vesicle suspensions remained opaque and appeared to be intact, yet increased in size slightly (Table 2.7). Since the size of vesicles changed, vesicles may be disrupted under these conditions and reform upon cooling and a decrease in pressure. Further studies were conducted with loaded materials in order to determine whether vesicles were disrupted during autoclaving. These results will be discussed later.

Sample	Hydrodynamic Radius (nm)	
	Non-sterile	Sterile
Bare Vesicles	87 ± 3	114 ± 3

**Table 2.7.** Purified vesicle-containing fractions by SEC before and after autoclaving. Samples were analyzed by DLS to determine whether vesicles were present and to determine their stability.

While the stability and robustness of bare cationic vesicles has been reported, vesicles require disruption for certain studies. For example, absorbance measurements cannot be conducted in the presence of cationic vesicles due to their light scattering. For this reason, we studied disruption of vesicles by addition of different solvents. Gradual addition of ethanol to vesicle solutions disrupted the vesicle suspensions. Qualitatively, one could see the disruption since the turbidity of the colloidal suspension disappeared (Figure 2.8). Quantitatively, the intensity of cationic vesicles measured by DLS diminished after the addition of 1 mL of ethanol to 1 mL of a vesicle suspension (Figure 2.9). This disruption method is effective when absorption measurements are required for vesicles loaded with chromophores.

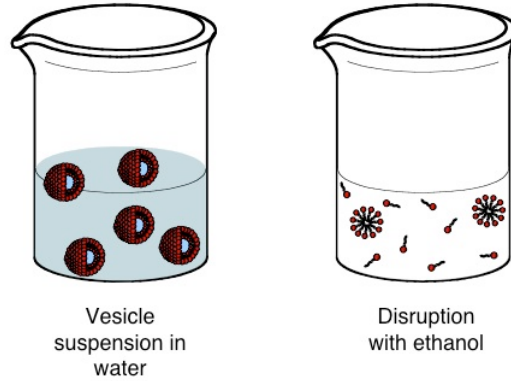


**Figure 2.8.** Cloudy vesicle suspensions compared to vesicles disrupted with ethanol. Cationic vesicle suspensions were cloudy due to light scattering compared to vesicles disrupted with ethanol. Vesicles initially scattered light and after the addition of ethanol, the solution became clear and colorless. Vesicles were broken and surfactants formed micelles or free surfactant, which did not scatter light significantly, due to their smaller size.

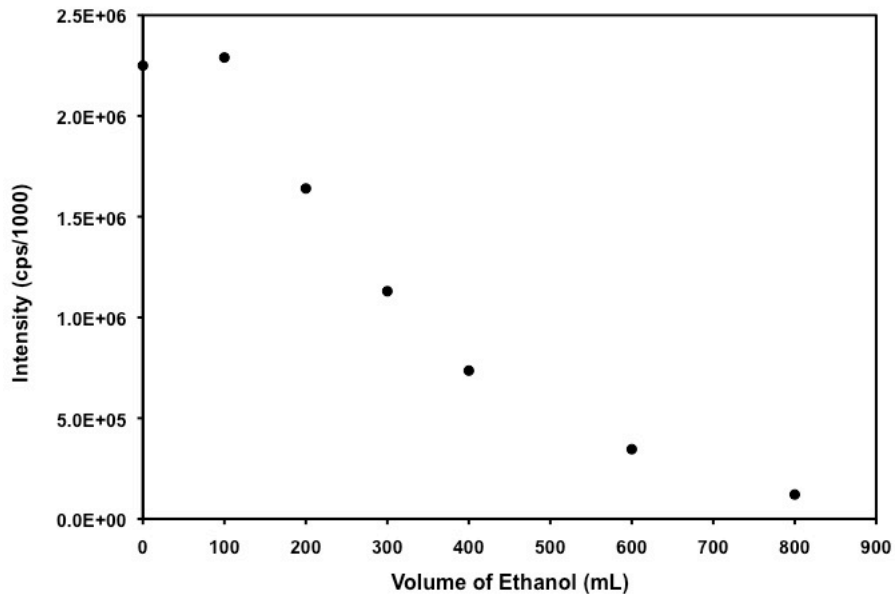


**Figure 2.9.** DLS intensity of a 1 mL colloidal solution of cationic vesicles disrupted with an increasing volume of ethanol. Decreasing intensity resulted from the decrease in light scattering by vesicle disruption with ethanol.

The studies described above indicated that unfunctionalized (bare) SDBS-rich cationic vesicles were prepared reproducibly and that the resulting suspensions exhibited excellent long-term stability. For vaccine production or drug delivery applications, functionalized, SDBS-rich cationic vesicles would be required. Accordingly, we extended our study of vesicle stability to these systems. The major questions to be addressed were 1) whether vesicles could be loaded with molecules containing various properties, 2) whether vesicles could be characterized to determine the amount conjugate incorporated and the size of the resulting suspensions, and 3) whether the surface of the conjugates remained active.

### *2.2.2 Surface Functionalization and Characterization of Cationic Vesicles*

Cationic surfactant vesicles have been functionalized and loaded with a variety of molecules with the aim to study them in biological processes. We studied the incorporation of hydrophilic and hydrophobic molecules, molecules containing a hydrophobic linker, and charged molecules into cationic vesicles (Figure 2.10). For hydrophilic molecules, it was necessary to attach a hydrophobic linker that would embed itself into the leaflet. This generalized strategy was successfully applied to the functionalization of cationic vesicles with carbohydrates, peptides, dyes, drugs, and carotenoids.

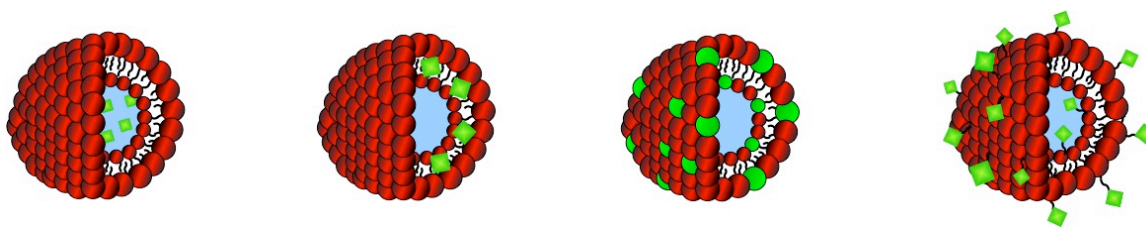


**Figure 2.10.** Vesicles modified with molecules that insert via different mechanisms. Representation of hydrophilic, hydrophobic, charged, and conjugated molecules and their incorporation into cationic vesicles.

### 2.2.2.1 Carbohydrate Functionalized Cationic Vesicles

Cationic vesicles were loaded with glycoconjugates (i.e. C<sub>12</sub>-glucose, C<sub>8</sub>-glucose, C<sub>8</sub>-maltose and C<sub>8</sub>-maltotriose) that contained an alkyl chain (Figure 2.11) that inserted into the bilayer. Functionalized vesicles were purified by size exclusion chromatography (SEC) to purify excess glycoconjugate from vesicles. Vesicle-containing fractions were determined by DLS, where fractions 3 and 4 showed the greatest scattering intensity (Figure 2.12, black solid line).

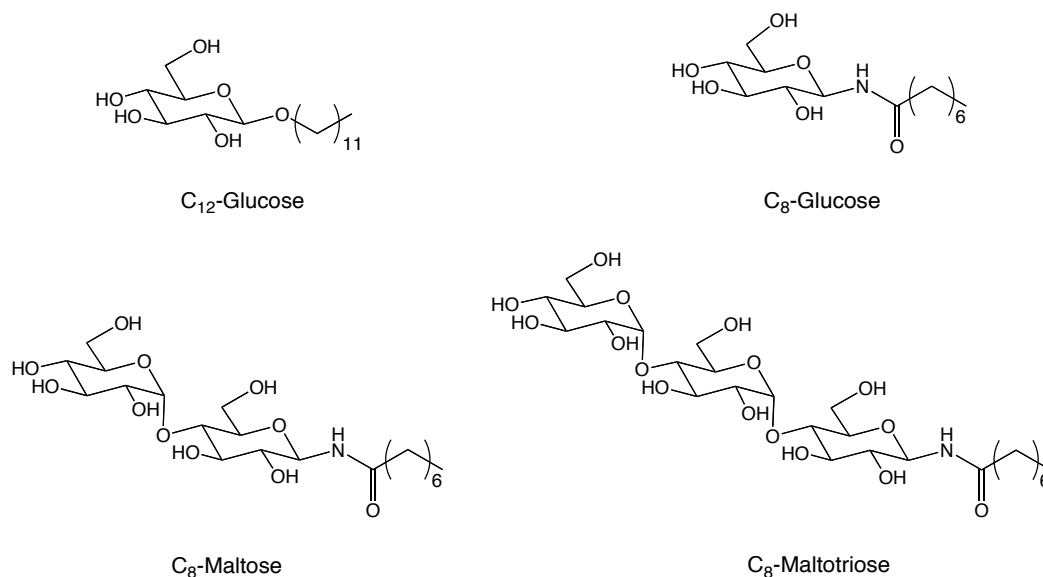


**Figure 2.11.** Glycoconjugates functionalized to vesicles C<sub>12</sub>-glucose, C<sub>8</sub>-glucose, C<sub>8</sub>-maltose, and C<sub>8</sub>-maltotriose, prepared by Dr. Juhee Park.

A colorimetric phenol/sulfuric acid analysis was performed for each fraction in order to detect carbohydrate. Vesicle-containing fractions, 3 and 4, as well as later fractions, primarily 9 and 10, turned yellow in color (Figure 2.12, red dashed line). This result showed that glycoconjugate was successfully incorporated into vesicles (Table 2.8) and that any unincorporated glycoconjugate was removed.

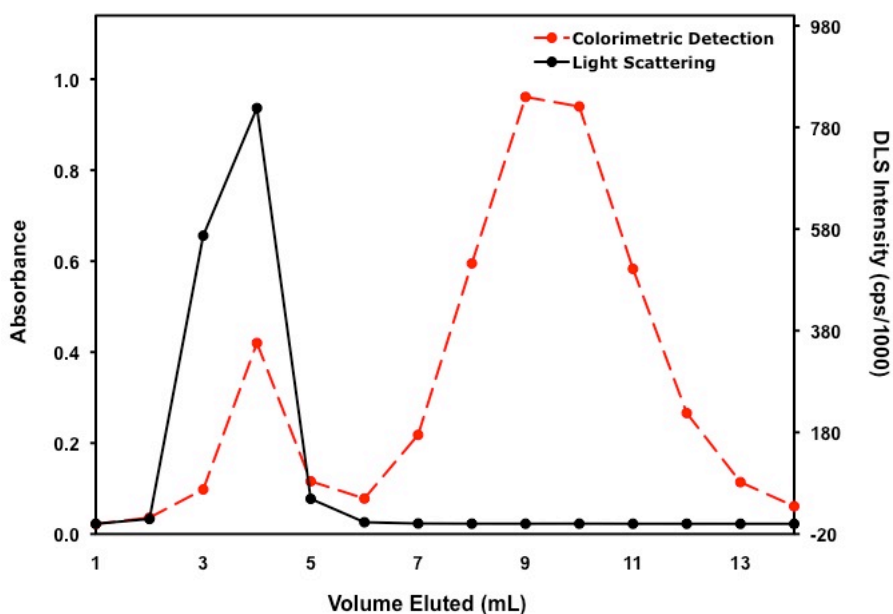


**Figure 2.12.** Results from SEC carbohydrate-functionalized cationic vesicles evaluated by DLS and colorimetric assay of carbohydrate-loaded vesicles. SEC fractions were evaluated by DLS (solid black line) to identify vesicle-containing fractions. Fractions containing carbohydrates were identified with colorimetric detection at 490 nm (dashed red line). (See Experimental Section for details.)

Glycoconjugates	Hydrodynamic Radius (nm) ( $\pm < 0.5$ nm)*	Percent Incorporation <sup>#</sup>
C <sub>8</sub> -Glucose	81	18
C <sub>8</sub> -Maltose	70	25
C <sub>8</sub> -Maltotriose	58	19

**Table 2.8.** Glycoconjugate incorporation into cationic vesicles and DLS results. <sup>#</sup>Incorporation percentage is the fraction of a 1 mM solution of glycoconjugate that eluted with vesicles during SEC. Hydrodynamic radii were determined by DLS prior to SEC. \*The standard deviation of all vesicle suspensions were  $< 0.5$  nm.

Next, we wanted to determine if the glycoconjugates that were loaded into cationic vesicles remained accessible at the surface. Carbohydrate functionalized vesicles were incubated with a sugar-binding protein, lectin, to determine if the anchored glycoconjugates will bind. The lectin concanavalin A (Con A), derived from the jack bean plant (*Conavalia ensiformis*), selectively binds to glucose monosaccharides.<sup>14, 15</sup> In this case, binding of the lectin to its cognate sugar should lead to the aggregation of the vesicles. After the addition of Con A to vesicles containing terminal glucose monomer units (Figure 2.13), the turbidity of the suspension increased. These turbid solutions indicated that vesicles bound to the lectin and caused aggregation with other vesicles (Figure 2.12).

Next, we studied the binding kinetics of Con A vesicle aggregation in solution. Specifically, we studied the effect of glucose monomer length (monosaccharide, disaccharide, and trisaccharide) on the rate of carbohydrate binding. Con A was added to vesicles functionalized with glucose, maltose, and maltotriose conjugates. Maltose showed the fastest rate of binding while glucose and maltotriose were comparable to one

another (Table 2.9). The trisaccharide showed the least binding to Con A. This result indicated that the number of monomer units or length of the polysaccharide did not make the carbohydrate more accessible to lectin binding. Since maltotriose contained the most monomer units, the trisaccharide flexibility may have decreased the likelihood of lectin binding. Maltotriose may interact with the bilayer or fold back onto itself, thus causing decreased binding at the terminal glucose unit. Furthermore, C<sub>8</sub>-maltotriose showed a smaller hydrodynamic radius than the other glycoconjugated vesicles (Table 2.8). Measurement of the hydrodynamic radius of the cationic vesicles by DLS includes molecules protruding from the surface of vesicles. Maltotriose vesicles were of smaller size, indicating that maltotriose is not as elongated as one would expect compared to the shorter glycoconjugates. We hypothesized that maltose showed the fastest and greatest binding capability because the disaccharide extends from the surface. These results indicated that carbohydrates were bound to the vesicle surface and remained available for interaction.

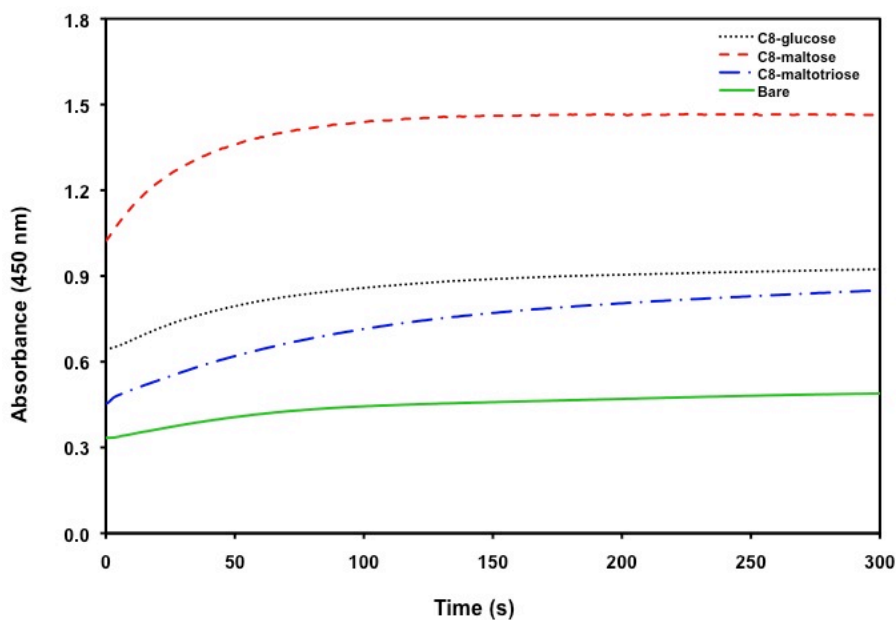


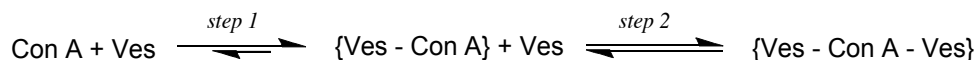
**Figure 2.13.** Effect of carbohydrate subunit length on Con A agglutination. Samples were studied at RT by turbidity as a function of time,  $[\text{Con A}] = 5 \mu\text{M}$  (see Experimental Section for details). Adapted from ref. 7.

Glycoconjugates	Initial Rate ( $\text{Abs s}^{-1}$ )
Bare vesicles	—
C <sub>8</sub> -glucose	0.003
C <sub>8</sub> -maltose	0.012
C <sub>8</sub> -maltotriose	0.005

**Table 2.9.** Initial rate of vesicle agglutination at RT using  $[\text{Con A}] = 5 \mu\text{M}$  (see Experimental Section for details).

Next, we wanted to get a snapshot of Con A-vesicle binding. Cationic C<sub>12</sub>-glucose functionalized vesicles were also examined with and without Con A using cryo-TEM by the English group. Images showed that vesicles aggregated and even fused after the addition of Con A (Figure 2.14). Furthermore, vesicles appeared to form multi-lamellar structures. These studies with glycoconjugated vesicles shows their ability

toward the targetability of cationic vesicles to cell receptors for antigen recognition in vaccines and targeted drug delivery vehicles.



**Scheme 2.1.** Binding scheme for Con A-induced vesicle aggregation.<sup>8</sup>

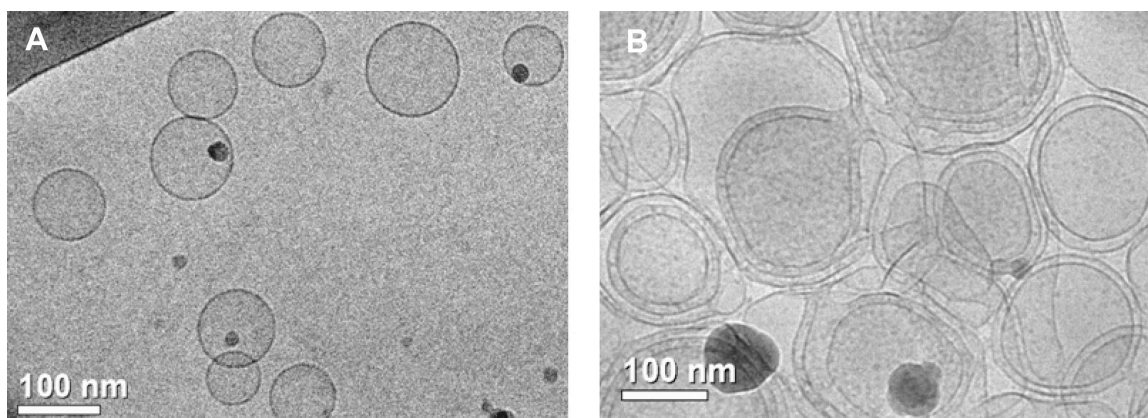


**Figure 2.14.** Representative cryo-TEM micrographs of vesicles with C<sub>12</sub>-glucose. (A) Before mixing with Con A the vesicles were unilamellar and spherical. (B) After mixing with 10 μM Con A the vesicles aggregated and became multilamellar. Experiment performed by Dr. English and was taken from ref. 8.

#### 2.2.2.1.1 Stability of Carbohydrate Functionalized Cationic Surfactant Vesicles

Subsequently, we wanted to determine if functionalized vesicles had the same stability as bare cationic vesicles under various conditions. C<sub>12</sub>-glucose vesicles were prepared and their stability was studied in saline solutions and after autoclaving. C<sub>12</sub>-glucose vesicles were prepared at different mole fractions and solutions of increasing concentrations of NaCl were added to each sample. All mole fractions of C<sub>12</sub>-glucose vesicles remained stable at physiological saline, but became unstable at higher saline

concentrations of 1.2 M and eventually precipitated (Table 2.10). This result showed that the size remained the same for both functionalized and bared vesicles even when prepared at high salt concentrations (0.6 M).

Mole fraction	NaCl concentration*				
	0 M	0.15 M	0.3 M	0.6 M	1.2 M
0.05	80	64	64	62	206 ± 5
0.1	73	58	57	63	166 ± 3
0.2	81	61	61	67	252 ± 7
0.3	77	62	61	65	262 ± 7
0.4	67	64	64	62	206 ± 5

**Table 2.10.** Hydrodynamic radius (nm) of C<sub>12</sub>-Glucose vesicles at increasing NaCl concentrations analyzed by DLS. \*The standard deviation of all unreported vesicle suspensions were < 0.5 nm.

As discussed earlier, bare vesicles increased in size after being autoclaved. This increase in vesicle size could have resulted from breaking and reforming vesicles. To study this hypothesis, C<sub>12</sub>-glucose vesicles were autoclaved to determine if carbohydrate was retained. C<sub>12</sub>-glucose vesicles were purified by SEC. Two aliquots were taken from vesicle-containing fractions; one sample was autoclaved while the other served as a control. Each sample was purified a second time by SEC to determine if glucose leaked out with or without autoclaving. After autoclaving, carbohydrate-conjugated vesicles increased in size (Table 2.11). In addition, no excess carbohydrate was seen in later fractions of SEC (Figure 2.15). This result showed that even though the size of C<sub>12</sub>-

glucose vesicles changed after being autoclaved, the autoclaved vesicles retained carbohydrate as efficiently as unsterilized vesicles.

Sample	Hydrodynamic Radius (nm)	
	Non-sterile	Sterile
Bare Vesicles	$87 \pm 3$	$114 \pm 3$
0.01 mf C <sub>12</sub> -Glucose	$99 \pm 2$	$158 \pm 3$

**Table 2.11.** Purified vesicle-containing fractions before and after autoclaving. Samples were analyzed by DLS.

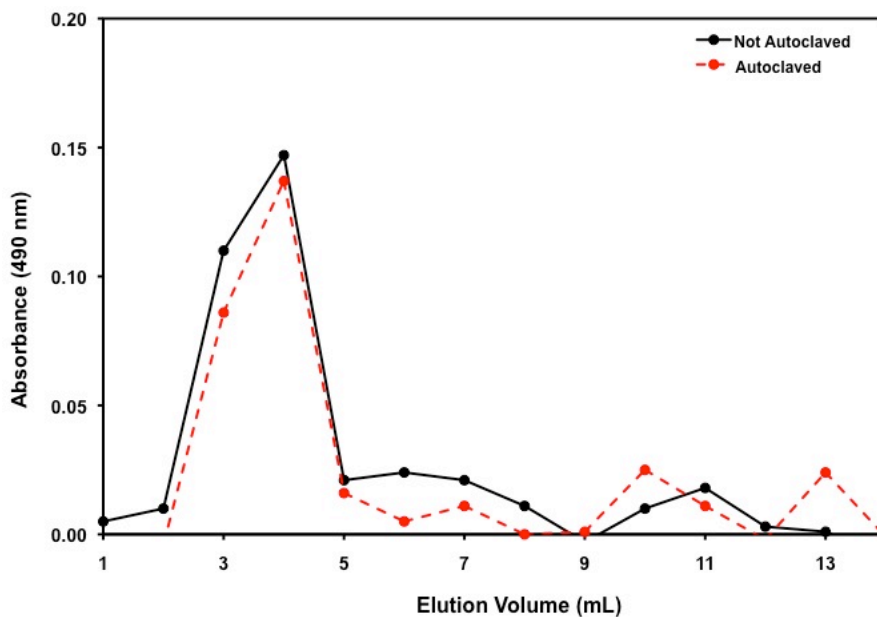
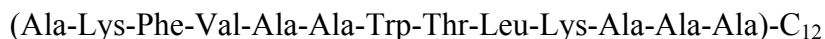


**Figure 2.15.** Comparison of sterile and non-sterile C<sub>12</sub>-glucose vesicles' second purification by SEC.

### 2.2.2.2 Loading of Peptides and Chromophores into Catanionic Vesicles

At this point, we have demonstrated that hydrophilic carbohydrate derivatives required the attachment of a hydrophobic tail before they could be incorporated into catanionic vesicles. Next, we showed that a variety of other molecules could be incorporated into catanionic vesicles, including lutein, carboxyfluorescein, maytansine, taxol derivative, PADRE peptide-conjugate, and lipid oligosaccharides. All molecules incorporated formed vesicles of similar dimensions and were characterized after purification by SEC. These molecules will be discussed in detail in later chapters.

Vesicles were loaded with a 13-mer peptide, PADRE. Before incorporation of the peptide, a hydrophobic linker was added to form a C<sub>12</sub>-PADRE conjugate (Figure 2.16). C<sub>12</sub>-PADRE conjugate was added to solid SDBS and CTAT and the suspension was stirred with water. Vesicles were purified by SEC and analyzed for the presence of peptide using a modified procedure of the Pierce bicinchoninic acid (BCA) assay.<sup>16</sup> The absorbance was measured at 562 nm and compared to a bovine serum albumin standard curve to determine the total protein concentration in each sample. Vesicle-containing fractions appeared purple in color. This result indicated the presence of peptide conjugate peptide in vesicles that inserted via the hydrophobic linker.



C<sub>12</sub>-PADRE peptide conjugate

**Figure 2.16.** Sequence of C<sub>12</sub>-PADRE peptide conjugate. The 13-mer contains a C<sub>12</sub> hydrophobic amide linker that inserted into the vesicle lipid bilayer.

Vesicles were also loaded with chromophores. These chromophores contained a hydrophobic linker, were charged, or were neutral (Figures 2.17-2.19). Qualitatively, after purification by SEC, vesicle-containing fractions clearly incorporated the chromophore and were evident by colored solutions. However, quantitative measurements could not be conducted on vesicles containing a chromophore due to the interference of light scattering from the vesicles. Ethanol was added to all fractions to disrupt vesicles and to prevent light scattering. After disruption, the chromophores were detected by UV/VIS. When a phospholipid component was used, vesicle-containing fractions were the only fractions where chromophore was observed. For example, vesicles were prepared with lissamine rhodamine B-lipid. After purification by SEC, no residual dye came through later fractions of the column, but was retained on the top of the column (Figure 2.20). This result indicated that not all of the lipid dye was incorporated into cationic vesicles and any remaining lipid dye was insoluble in water. Lipid dye retained on the column was removed by washing the column with a surfactant solution, solubilizing the molecule in detergent. When a linker was not used, excess dye was often found in later fractions, indicating that the dye was not incorporated into vesicles.

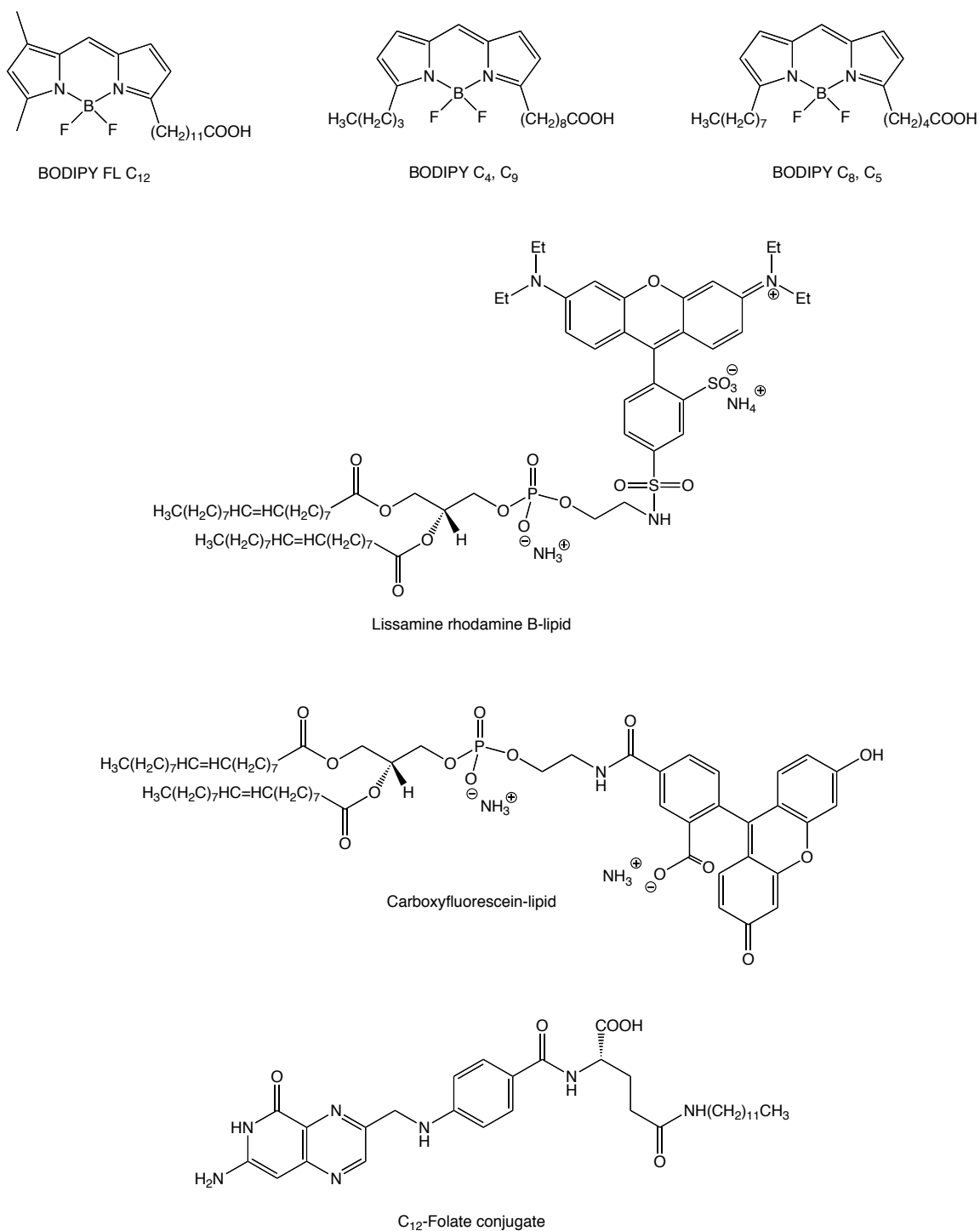


**Figure 2.17.** Chemical structure of chromophores containing a hydrophobic linker. BODIPY conjugates, lissamine rhodamine B-lipid, CF-lipid, and C<sub>12</sub>-folate conjugate.

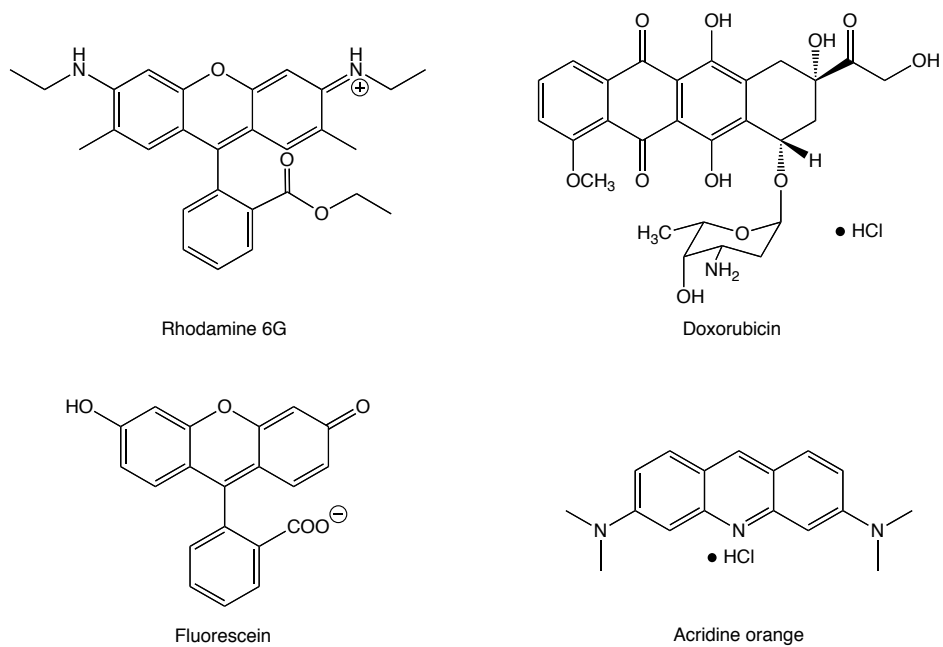


**Figure 2.18.** Chemical structure of dyes containing a charge. Rhodamine 6G, doxorubicin, fluorescein, and acridine orange.

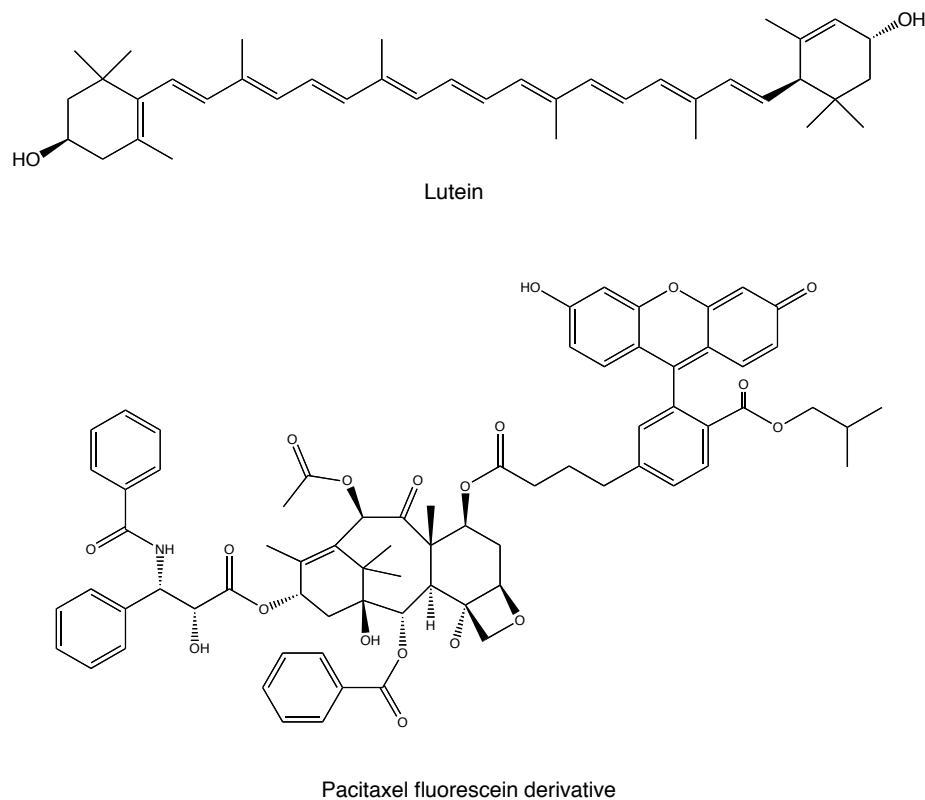


**Figure 2.19.** Chemical structure of hydrophobic molecules containing a chromophore. Structures of lutein and paclitaxel fluorescein derivative.

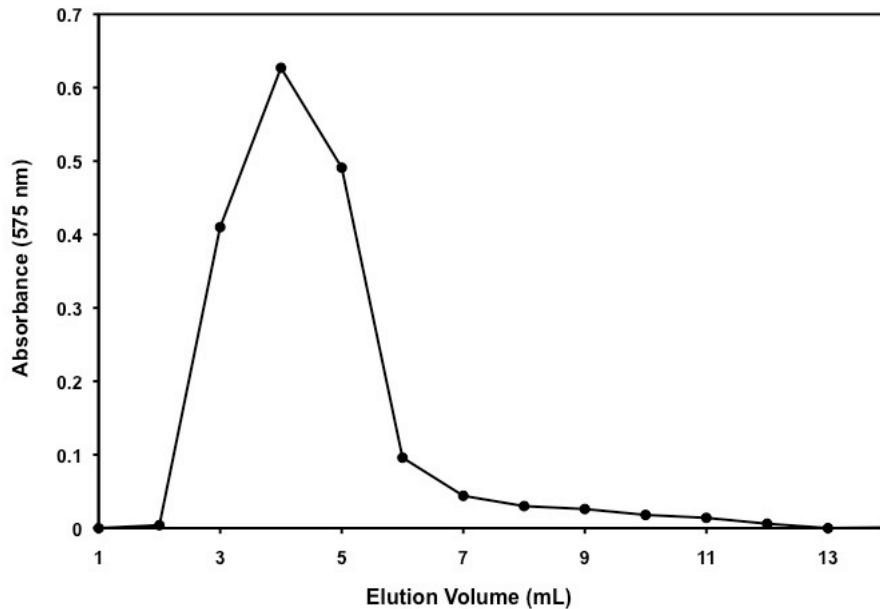


**Figure 2.20.** Absorption of lissamine rhodamine B-lipid vesicles after purification by SEC. Fractions were disrupted with ethanol and the absorbance was measured at 575 nm. Pink color in vesicle-containing fractions indicated the presence of lipid dye incorporated into cationic vesicles.

### 2.2.3 Dialysis

Removal of surfactant components is also important if molecules loaded into vesicles need to be retrieved. Cationic vesicle suspensions were disrupted with ethanol and added to dialysis tubing placed into water. As ethanol was removed, vesicles reformed, preventing the removal of surfactants. To alleviate this issue, vesicles were disrupted with the addition of the detergent Triton-X 100 and dialyzed in water. After one day, soapy bubbles were still present in the dialysis tubing. The soapy bubbles indicated the presence of the detergent. The sample was also analyzed by UV-VIS, which contained a characteristic absorption at 260 nm. This absorption corresponds to the UV chromophore of the surfactant aryl functional groups. Finally, after additional dialyze washes, all detergent was removed.

### 2.3 *Conclusions*

We have hypothesized that functionalized cationic vesicles could be used in vaccine development and drug delivery for *in vivo* applications. Vesicles remained intact between a pH of 2 to 12 and could be autoclaved without releasing their contents. Vesicles have also been functionalized with a variety of materials and characterized accordingly. Their increased stability, ease of preparation, and cost show an improvement over conventional liposomes. These robust properties of cationic surfactant vesicles make them excellent candidates for applications that currently employ the use of liposomes.

### 2.4 *Experimental*

#### 2.4.1 *General Experimental*

Thin-layer chromatography (TLC) was performed on 0.25 mm Merck silica-coated glass plates treated with a UV-active binder. Compounds were identified using UV (254 nm), vanillin/sulfuric acid charring,  $\text{KMnO}_4$ , or iodine detection.

Melting points were taken in Kimax soft glass capillary tubes using a Thomas-Hoover Uni-Melt capillary melting point apparatus equipped with a calibrated thermometer.

Infrared spectra were recorded on a Nicolet 5DXC FT-IR spectrophotometer. Band positions are given in reciprocal centimeters ( $\text{cm}^{-1}$ ) and relative intensities are listed as br (broad), s (strong), m (medium) or w (weak).

$^1\text{H}$  NMR spectra were recorded on a Bruker DRX-400 MHz spectrometer. Chemical shifts are reported in parts per million (ppm) relative to the solvent. Coupling

constants ( $J$  values) are given in hertz (Hz). Spin multiplicities are indicated by the following symbols: s (singlet), d (doublet), t (triplet), q (quartet), or m (multiplet).

Absorbance measurements were performed on a CHEM2000-UV-Vis-spectrometer, Ocean Optics, Inc. and fluorescence measurements on an RF-1501 Spectrofluorophotometer, Shimadzu.

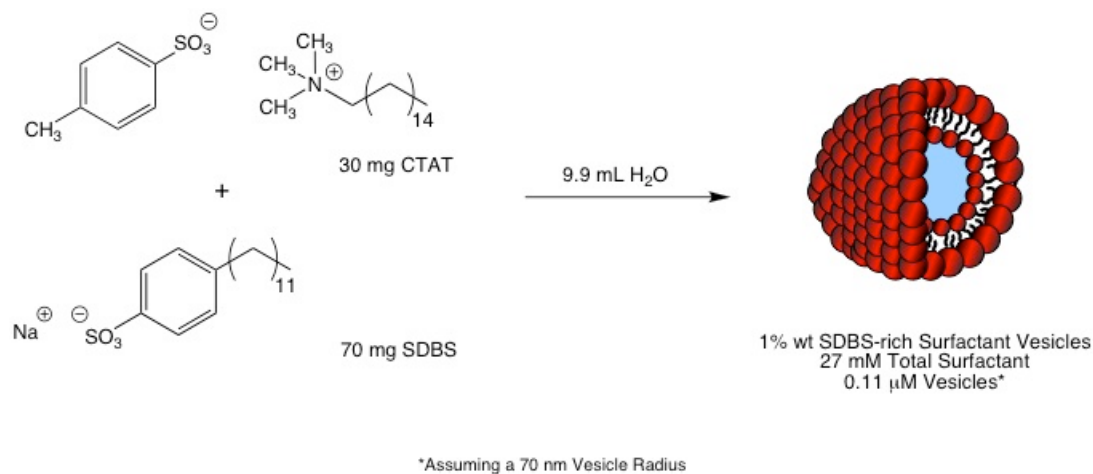
TEM samples were viewed using a ZEISS EM 10CA Transmission Electron Microscope with an accelerating voltage of 80 KV.

All chemicals and solvents were purchased from commercial suppliers unless otherwise noted. CTAT was purified by recrystallization from ethanol/acetone and yielded white shiny crystals.

#### 2.4.2 *Synthesis of Bare Surfactant Vesicles*

Vesicles prepared with a molar excess of SDBS will be referred to as SDBS-rich (anionic). The surfactants CTAT and SDBS were monitored by TLC using 7:3 petroleum ether/EtOH as the solvent to determine the presence of surfactants.

**Method 1:** Anionic surfactant vesicles, 1 wt % total surfactant (26.9 mM total surfactant), were prepared by adding 9.90 mL of 18 M $\Omega$  Millipore water to 70.0 mg of SDBS (0.200 mmol) and 30.0 mg of CTAT (0.0658 mmol) (Scheme 2.1).<sup>5</sup> The solution was stirred for 60 min. The resulting colloidal suspension was milky in appearance. The concentration of vesicles was determined to be 0.11  $\mu$ M by using a bilayer of 3.5 nm, which was determined by cryo-TEM (Figure 2.21).<sup>8</sup> Vesicles were always prepared using this method unless otherwise stated.



**Scheme 2.2.** Preparation of bare catanionic surfactant vesicles from the solid surfactants SDBS and CTAT. The colloidal suspension of vesicles is cloudy and opalescent in appearance. Vesicles have an overall negative charge on the surface from the resulting excess of SDBS.

$$N_{total} = \frac{4\pi(R_1^2 + R_2^2)}{0.48}$$

$$[\text{vesicles}] = \frac{[\text{surfactant}] - \text{cac}}{N_{total}}$$

$$[\text{vesicles}] = 0.11 \mu\text{M}$$

**Figure 2.21.** Determination of vesicle concentration in solution. The total surface area per surfactant =  $0.48 \text{ nm}^2$ .<sup>3</sup> Analysis is based on using a bilayer measurement of 3.5 nm determined by cryo-TEM by Dr. Douglas English. A cac of 2.5 to 3.0 mM and a surfactant concentration of 26.9 mM was used.<sup>17</sup>

Three additional methods for vesicle formation were studied:

**Method 2:** The surfactants, 7.00 g of SDBS (20.0 mmol) and 3.00 g of CTAT (6.58 mmol), were blended in a grinder for 3 min. Then, 100 mg of the surfactant mixture was added to 9.90 mL of water and stirred for 60 min.

**Method 3:** Stock solutions of 0.291 M SDBS (101 mg/mL) and 0.219 M CTAT (100 mg/mL) were prepared. Then, 6.90 mL of the SDBS solution (0.200 mmol) was added to 3.0 mL of the CTAT solution (0.0658 mmol) and mixed.

**Method 4:** A 0.0203 M stock solution of SDBS (7.07 mg/mL) in water was prepared. Then, 9.90 mL of the SDBS solution (0.200 mmol) was added to 30.0 mg of solid CTAT (0.0658 mmol) and stirred for 60 min.

### 2.4.3 Dynamic Light Scattering

The mean hydrodynamic radius of vesicles was determined by dynamic light scattering (DLS), where a Photocor-FC light scattering device equipped with a 5 mW laser (633 nm) was used (Figure 2.22). All measurements were performed at a 90° scattering angle at 25 °C unless otherwise stated. An autocorrelation function was used to determine the hydrodynamic radius and polydispersity index, assuming a Gaussian distribution of vesicle size. The cumulant method was used for single angle measurements.<sup>18</sup>

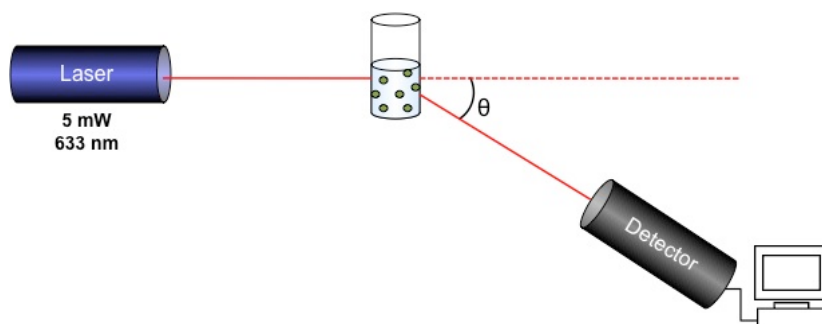


**Figure 2.22.** Set-up used for dynamic light scattering (DLS).

For multi-angle DLS, samples were made by diluting vesicles in water and then submerging the optical cell containing the sample in silicone oil at 25 °C. Samples were allowed to equilibrate for at least 30 min before taking a reading. The scattering angles were varied from 45° to 150° and samples were run for 5 to 10 min. The intensity auto-correlation function  $g_2(t)$  for a single-exponential relaxation mode is

$$g_2(t) - 1 = A \exp(-2\Gamma t) \quad \text{Eq. 2.4}$$

where  $A$  is the amplitude,  $t$  is the lag time, and  $\Gamma$  is the decay rate related to the relaxation time  $\tau$  of the fluctuations by  $\Gamma = 1/\tau$ .

#### 2.4.4 *Sonication of Bare Vesicles*

Bare cationic vesicles were sonicated in a water bath sonicator (Proequip.com 3510 Branson) for 5 min at room temperature. DLS (described below) was taken on the sample before and after sonication to determine whether the size of vesicles changed.

#### 2.4.5 *Zeta Potential Measurements*

Zeta potential measurement were analyzed by Dr. Sara Lioi. Methods for the measurements are reported in ref. 19.

#### 2.4.6 *Preparation of Cationic Vesicles in Buffered Solutions*

Bare cationic vesicles were prepared according to the methods reported in 2.6.2 accept with the modification of using buffer instead of water. A 0.1 M solution of 4-(2-hydroxyethyl)-1-piperazineethanesulfonic acid (HEPES) buffer was prepared (pH 7.4) and was added in the replacement of water.

#### 2.4.7 *Saline Studies*

Standard solutions of NaCl were prepared. Vesicles were prepared under different saline concentrations. DLS was measured on each samples to determine the effects of salt concentration on vesicle formation.

#### 2.4.8 *pH Studies*

The pH of vesicles was measured using a standardized pH meter (Denver Instrument). Concentrated HCl (12 M) was added to vesicles to decrease the pH and concentrated NaOH (19 M) was added to vesicles to increase the pH. DLS was performed afterward on all vesicle samples to determine the average hydrodynamic radius.

#### 2.4.9 *Freezing Studies on Bare Catanionic Vesicles*

A 1 mL vesicle suspension was added to a -20 °C freezer for 1 h or added to liquid N<sub>2</sub> until the sample froze. Each sample was removed and warmed to room temperature followed by measurements taken by DLS.

#### 2.4.10 *Sterilization of Vesicles*

Vesicles were sterilized using a sterile filter (0.22 μm). The syringe and filter were first rinsed with water followed by the filtration of the vesicle suspension.

Vesicles were autoclaved at 120°C for 1 h. Samples were measured by DLS to determine their robustness before and after sterilization.

Cationic vesicles were pasteurized by heating vesicle suspensions in a 65 °C water bath for 4 h.

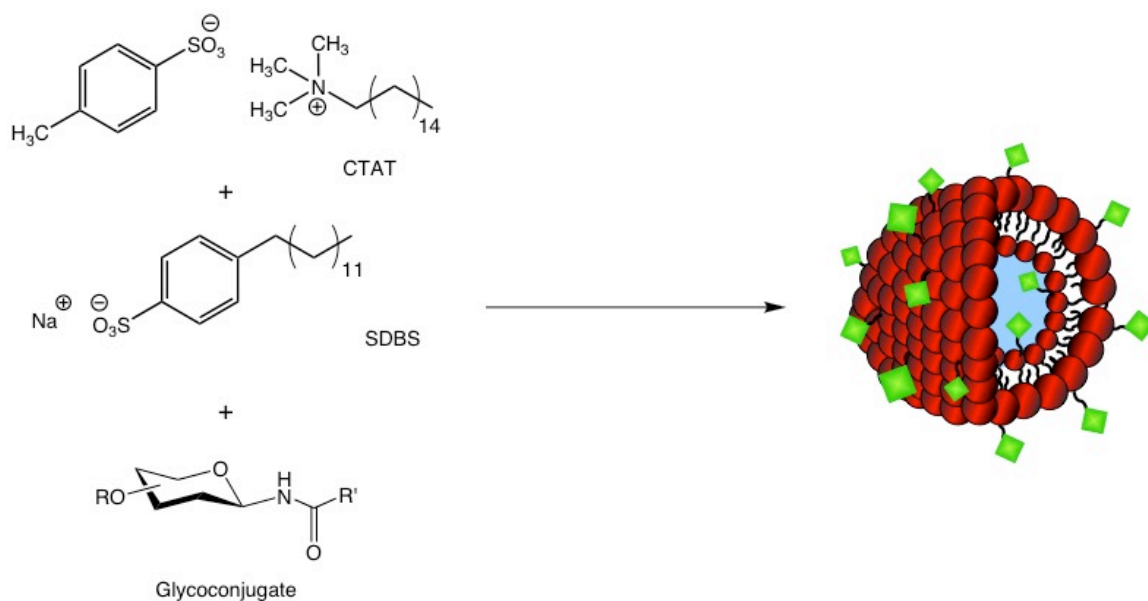
#### *2.4.11 Measuring Disruption of Bare Vesicles with Ethanol*

A 1.00 mL portion vesicles was transferred to an empty vial. Increasing amounts of absolute ethanol were added to the vesicle suspension and vortexed. Each ethanol/vesicle mixture was measured by DLS to determine the amount of light scattering occurring. The intensity of light reaching the detector was measured .

#### *2.4.12 Surface Functionalization of Surfactant Vesicles*

To prepare vesicles incorporating glycoconjugates shown in Figure 19, 9.90 mL of a 1 mM aqueous solution of glycoconjugate was added to 70.0 mg of SDBS (0.200 mmol) and 30.0 mg of CTAT (0.0658 mmol) and stirred for 60 min. Vesicles contained glycoconjugate on the inner and outer leaflet (Scheme 2.3). Vesicles were purified from free conjugate by SEC (details reported below).

To prepare conjugated vesicles with other conjugates shown in Figures 25 – 27, the molecule was either weighed directly into a vial or an aliquot was added to the vial, followed by removal of the solvent *in vacuo*. Then, 70.0 mg of SDBS (0.200 mmol) and 30.0 mg of CTAT (0.0658 mmol) was weighed into the vial followed by the addition of 9.90 mL of water and stirring for 60 min. Vesicles were purified from free conjugate by SEC (details below).



**Scheme 2.3.** Surfactant vesicles functionalized with compounds containing hydrophobic moieties via hydrophobic interactions. Addition of glycoconjugate during vesicles formation yielded glycoconjugate both on the internal and external leaflet.

#### 2.4.13 Size Exclusion Chromatography

After vesicle formation, vesicles were purified using size exclusion chromatography (SEC), using a column (5.5 cm; 1.5 cm diameter) packed with Sephadex G-100 (Sigma). To the column, 1.00 mL of the colloidal solution was added and collected as the first fraction. Then, 1.00 mL aliquots of Millipore water were added and collected in separate vials until the total volume reached 14.00 mL. After SEC, fractions 3 and 4 gave the highest intensity of scattered light determined by DLS and therefore, corresponded to vesicle containing fractions.

In the case of functionalized vesicles, samples were analyzed to determine the retention of the material by purification a second time through SEC. A 1.00 mL portion of vesicle-containing fractions was added to the column and purified as stated above.

#### 2.4.14 Colorimetric Assay for Carbohydrate

A colorimetric assay<sup>20</sup> using phenol and sulfuric acid was used to detect the presence of glycoconjugates in fractions 1-14 from SEC. A 0.50 mL portion of each SEC fraction was transferred to an empty vial where 0.25 mL of 0.530 M aqueous phenol (13.3 mmol) was added to the sample, followed by the addition of 1.25 mL of concentrated sulfuric acid (18 M) that was introduced as a stream of liquid directly to the liquid surface. The samples were vortexed and allowed to sit at room temperature for 1 h to allow the color to develop. Yellow containing fractions indicated the presence of glycoconjugate in solution. Then, 0.50 mL of ethanol was added and mixed thoroughly. After 10 min, the absorbance was measured at 490 nm and compared to a standard curve.

#### 2.4.15 Binding Studies

Agglutination studies were performed using the lectins concanavalin A (Con A, Type V, lyophilized powder) and peanut agglutinin (PNA, lyophilized powder). Lectin stock solutions were prepared by dissolving the lectin in HEPES-buffered saline (HEPES 10 mM, NaCl 150 mM, CaCl<sub>2</sub> 1 mM, and MnCl<sub>2</sub> 1 mM adjusted to pH 7.4 for Con A) and (HEPES 10 mM, NaCl 150 mM, CaCl<sub>2</sub> 1 mM, MnCl<sub>2</sub> 1 mM, and MgCl<sub>2</sub> 1 mM adjusted to pH 7.4 for PNA) which was incubated overnight. The resulting solution was filtered through a 0.22 μm syringe filter and the absorbance at 280 nm ( $A_{280} = 1.37 \times [\text{mg mL}^{-1} \text{ Con A}]^{14}$ ,  $A_{280} = 0.96 \times [\text{mg mL}^{-1} \text{ PNA}]^{21}$ ) was measured to determine the concentration of PNA in solution.

For the Con A kinetics binding assay, a 150  $\mu\text{L}$  aliquot of vesicle sample was added to a cuvette followed by addition of 150  $\mu\text{L}$  of buffered Con A. The sample was mixed for 5 s and the absorption at 450 nm was measured at 1 s intervals for 30 min.

#### *2.4.16 Transmission Electron Microscopy*

Vesicle-containing fractions from SEC were diluted with water (1:10). To a Formvar Carbon Support Film Mesh 200 (Electron Microscopy Sciences), 3  $\mu\text{L}$  of the diluted vesicle sample was added and allowed to dry to a thin film. Then, 5  $\mu\text{L}$  of 2% uranyl acetate stain was applied to the coated grid. After 30 s, the stain was wicked off to form a thin film and was allowed to dry before microscopy. Samples were then viewed by TEM. These TEM results did not match the vesicle sizes reported by DLS or cryo-TEM. Therefore, the size of vesicles changed when suspensions dried to form a thin film. For this reason, cryo-TEM images were performed by Dr. Douglas English and the methods can be found in ref. 8 (Figures 14 and 22).

#### *2.4.17 Bicinchoninic Acid Assay for Protein*

Vesicles were also analyzed for the presence of protein using a modified procedure of the Pierce bicinchoninic acid (BCA) protein assay (Thermo Scientific) (Table 1).<sup>16</sup> The working reagent was prepared using a 50:1 v/v ratio of Reagent A (sodium carbonate, sodium bicarbonate, bicinchoninic acid, and sodium tartrate in 0.1 M sodium hydroxide) to Reagent B (4% copper (II) sulfate). The test-tube protocol was used in which 2.00 mL of working reagent was added to 0.10 mL of the sample. To prevent intact vesicles from scattering light and interfering with the absorbance of

samples, 0.10 mL of 1-propanol was added to each sample to break up vesicles. After the addition of the working reagent, the samples were vortexed and incubated at 37 °C in a water bath for 30 min. The absorbance was measured at 562 nm and compared to a bovine serum albumin standard curve to determine the total protein concentration in each sample. While each sample was read, the remaining samples were incubated in the refrigerator at 4 °C in order to prevent the reaction from progressing further.

#### *2.4.18 Quantifying Dye Incorporation into Catanionic Vesicles*

A 0.50 mL portion of each vesicle fraction was transferred to an empty vial where 0.50 mL absolute ethanol was added to the sample to prevent light scattering during absorption measurements. Vesicle solutions appeared clear after the addition of ethanol (Figure 16). The samples were vortexed and the absorbance was measured at the specified wavelength for the desired molecule. The absorbance of each chromophore is as follows: lutein (446 nm), CF and CF- lipid (500 nm), lissamine rhodamine B-lipid (575 nm), doxorubicin (480 nm), and paclitaxel fluorescein derivative (445 nm).

#### *2.4.19 Dialysis*

Vesicle solutions (1 mL) were added to a dialysis membrane (MW 1,000) and equilibrated against 500 mL of water while stirring at room temperature. Several dialyzate changes occurred every several hours and then the solution was left to stir overnight.

To remove surfactants from solution, vesicles were first disrupted with Triton-X 100 until the solution became clear and colorless.

## References

1. Bramer, T.; Dew, N.; Edsman, K., Pharmaceutical applications for cationic mixtures. *J. Pharm. Pharmacol.* **2008**, *59* (10), 1319-1334.
2. Fischer, A.; Hebrant, M.; Tondre, C., Glucose encapsulation in cationic vesicles and kinetic study of the entrapment/release processes in the sodium dodecyl benzene sulfonate/cetyltrimethylammonium tosylate/water system. *J. Colloid Interface Sci.* **2002**, *248* (1), 163-168.
3. Walker, S. A.; Zasadzinski, J. A., Electrostatic control of spontaneous vesicle aggregation. *Langmuir* **1997**, *13* (19), 5076-5081.
4. Jiang, Y.; Li, F.; Luan, Y.; Cao, W.; Ji, X.; Zhao, L.; Zhang, L.; Li, Z., Formation of drug/surfactant cationic vesicles and their application in sustained drug release. *Int. J. Pharm.* **2012**, *436* (1-2), 806-814.
5. Wang, X.; Danoff, E. J.; Sinkov, N. A.; Lee, J.-H.; Raghavan, S. R.; English, D. S., Highly efficient capture and long-term encapsulation of dye by cationic surfactant Vesicles. *Langmuir* **2006**, *22* (15), 6461-6464.
6. Danoff, E. J.; Wang, X.; Tung, S.-H.; Sinkov, N. A.; Kemme, A. M.; Raghavan, S. R.; English, D. S., Surfactant vesicles for high-efficiency capture and separation of charged organic solutes. *Langmuir* **2007**, *23* (17), 8965-8971.
7. Park, J.; Rader, L. H.; Thomas, G. B.; Danoff, E. J.; English, D. S.; DeShong, P., Carbohydrate-functionalized cationic surfactant vesicles: preparation and lectin-binding studies. *Soft Matter* **2008**, *4* (9), 1916-1921.

8. Thomas, G. B.; Rader, L. H.; Park, J.; Abezgauz, L.; Danino, D.; De Shong, P.; English, D. S., Carbohydrate modified cationic vesicles: Probing multivalent binding at the bilayer interface. *J. Am. Chem. Soc.* **2009**, *131* (15), 5471-5477.
9. Soussan, E.; Mille, C.; Blanzat, M.; Bordat, P.; Rico-Lattes, I., Sugar-derived tricationic cationic surfactant: Synthesis, self-Assembly properties, and hydrophilic probe encapsulation by vesicles. *Langmuir* **2008**, *24* (6), 2326-2330.
10. Kadalbajoo, M.; Park, J.; Opdahl, A.; Suda, H.; Kitchens, C. A.; Garno, J. C.; Batteas, J. D.; Tarlov, M. J.; DeShong, P., Synthesis and structural characterization of glucopyranosylamide films on gold. *Langmuir* **2007**, *23* (2), 700-707.
11. Larsen, K.; Thygesen Mikkel, B.; Guillaumie, F.; Willats William, G. T.; Jensen Knud, J., Solid-phase chemical tools for glycobiology. *Carbohydr. Res.* **2006**, *341* (10), 1209-34.
12. Rangel-Yagui, C. O.; Pessoa, A., Jr.; Tavares, L. C., Micellar solubilization of drugs. *J. Pharm. Pharm. Sci.* **2005**, *8* (2), 147-163.
13. Wang, Z.; Leung, M. H. M.; Kee, T. W.; English, D. S., The role of charge in the surfactant-assisted stabilization of the natural product curcumin. *Langmuir* **2010**, *26* (8), 5520-5526.
14. Cairo, C. W.; Gestwicki, J. E.; Kanai, M.; Kiessling, L. L., Control of multivalent interactions by binding epitope density. *J. Am. Chem. Soc.* **2002**, *124* (8), 1615-1619.
15. Neurohr, K. J.; Young, N. M.; Mantsch, H. H., Determination of the carbohydrate-binding properties of peanut agglutinin by ultraviolet difference spectroscopy. *J. Biol. Chem.* **1980**, *255* (19), 9205-9.

16. Smith, P. K.; Krohn, R. I.; Hermanson, G. T.; Mallia, A. K.; Gartner, F. H.; Provenzano, M. D.; Fujimoto, E. K.; Goeke, N. M.; Olson, B. J.; Klenk, D. C., Measurement of protein using bicinchoninic acid. *Anal. Biochem.* **1985**, *150* (1), 76-85.
17. Kaler, E. W.; Herrington, K. L.; Murthy, A. K.; Zasadzinski, J. A. N., Phase behavior and structures of mixtures of anionic and cationic surfactants. *J. Phys. Chem.* **1992**, *96* (16), 6698-707.
18. Frisken, B. J., Revisiting the method of cumulants for the analysis of dynamic light-scattering data. *Appl Opt* **2001**, *40* (24), 4087-91.
19. Nieves, W.; Asakrah, S.; Qazi, O.; Brown, K. A.; Kurtz, J.; AuCoin, D. P.; McLachlan, J. B.; Roy, C. J.; Morici, L. A., A naturally derived outer-membrane vesicle vaccine protects against lethal pulmonary *Burkholderia pseudomallei* infection. *Vaccine* **2011**, *29* (46), 8381-8389.
20. Dubois, M.; Gilles, K. A.; Hamilton, J. K.; Rebers, P. A.; Smith, F., Colorimetric method for determination of sugars and related substances. *Anal. Chem.* **1956**, *28*, 350-6.
21. Miller, R. L., Purification of peanut (*Arachis hypogaea*) agglutinin isolectins by chromatofocusing. *Anal. Biochem.* **1983**, *131* (2), 438-46.

## Chapter 3: Loading Complex Carbohydrates and Peptides into Cationic Surfactant Vesicles for Use in Vaccine Applications

### 3.1 *Introduction*

The previous chapter described the preparation and characterization of cationic surfactant vesicles functionalized with simple, small, organic molecules. We have shown that glycolipids could be incorporated into the leaflet of the cationic vesicle with control of both the density and aggregation of the glycolipid. The goal of the next phase of this study was to incorporate multiple bioconjugates (i.e. liposaccharides and peptides) into cationic vesicles. We were interested in determining whether complex bioconjugates loaded into cationic surfactant vesicles would work toward applications in vaccine technology, specifically for the formulation of vaccines against bacterial pathogens. In addition, we studied the ability of loading more than one conjugate together during vesicle formation. This loading would allow for the ability to adjust the ratio of each component when controlled addition is required.

#### 3.1.1 *Vaccine Formulation*

Currently, the different methods employed for vaccine development include using killed pathogens, attenuated strains, inactivated toxoids, and formulated conjugates.<sup>1</sup> To avoid safety concerns that may arise from attenuated or killed pathogens, protein subunits have been employed for viral vaccines. These proteins are found on the capsid of the virus and are utilized to generate an immune response. In bacterial vaccines, carbohydrates are used as antigens. Unfortunately, carbohydrates from the cell surface

are poorly immunogenic. Therefore, a variety of bacterial vaccines have lacked the ability to generate effective formulations, including meningitis, gonorrhea, and tularemia.<sup>1</sup>

### *3.1.2 Bacterial Vaccines*

Efforts toward generating vaccines against pathogenic bacteria include using capsular polysaccharides that are specific to their bacterial pathogens.<sup>2</sup> For example, glycolipids, such as lipopolysaccharide (LPS) or lipooligosaccharide (LOS), are prevalent on the exterior cell surface of Gram-negative bacteria. These antigens play a pivotal role in cellular recognition and have been studied in vaccine development.<sup>3</sup> For example, the lipid A region of liposaccharide has been shown to elicit an immune response (Figure 3.1).<sup>4</sup> For this reason, vaccine formulations have included liposaccharides or lipid A alone. Unfortunately, lipid A is extremely toxic. However, research has shown that incorporating the lipid A of liposaccharides into liposomes greatly reduces its toxicity, while still generating an immune response.<sup>5-7</sup> Unfortunately, these carbohydrate-based vaccines against bacteria are poorly immunogenic and fail to trigger helper-T cell recognition.<sup>8</sup> Therefore, long-term protection against bacterial pathogens is not achieved.

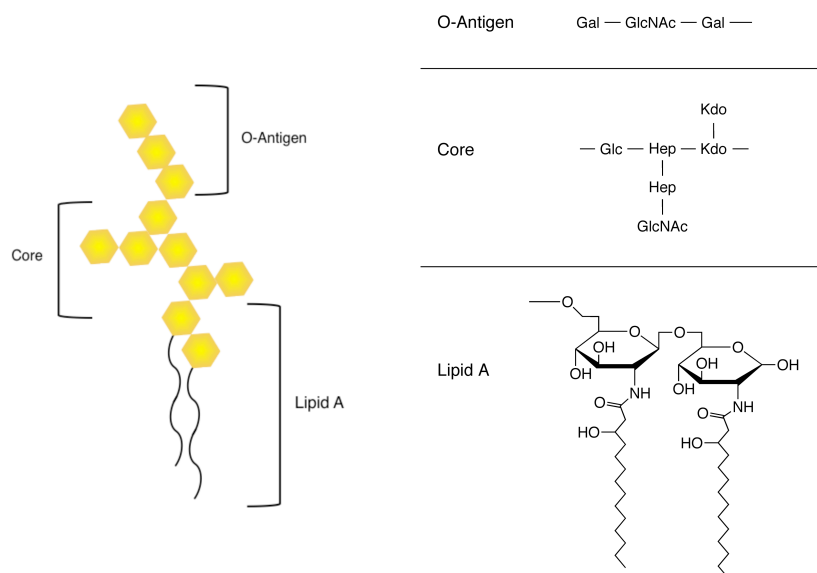


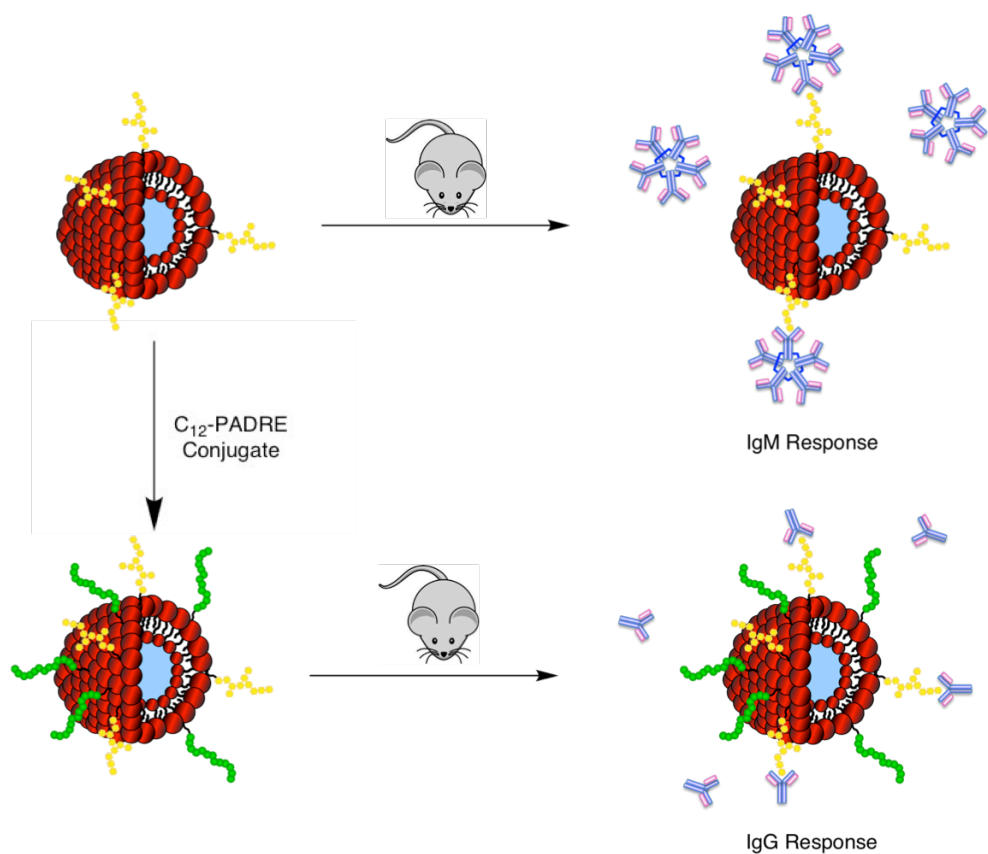
**Figure 3.1.** Chemical structure of lipooligosaccharide components from the Gram-negative bacteria *N. gonorrhoeae*. The various regions include the O-antigen, core, and lipid A.

Since polysaccharides are poorly immunogenic, efforts have also been devoted toward conjugating carbohydrates directly to large proteins such as tetanus or diphtheria toxoids that are known to elicit an immune response.<sup>9</sup> However, the inability to control the ratio of the carbohydrate antigen to the protein has hampered development in using this approach.

### 3.1.3 Catanionic Surfactant Vesicles as Vaccines

We were interested in developing carbohydrate-based vaccines against Gram-negative bacteria, specifically *N. gonorrhoeae* and *F. tularensis* by utilizing catanionic surfactant vesicles for incorporation of surface antigens onto the outer leaflet. The resulting functionalized vesicles would display the antigens on the surface of the vesicle in a manner analogous to their presence in bacterial pathogens. Vaccine studies by our

lab were performed using cationic surfactant vesicles that contained bacterial liposaccharides (i.e. LOS and LPS) and Pan DR helper T cell epitope (PADRE) peptide conjugate. The peptide PADRE was chosen for co-incorporation into vesicles because the peptide is a synthetic epitope that has been shown to stimulate the production of IgG antibodies.<sup>10</sup> Specifically, PADRE has been shown to augment the potency of vaccines designed to stimulate T-cells in developing a potent immune response against the carbohydrate antigens that could be presented. We undertook this study to determine if liposaccharides and PADRE inserted into a cationic vesicles would be capable of eliciting an immune response against the carbohydrate component (Scheme 3.1).



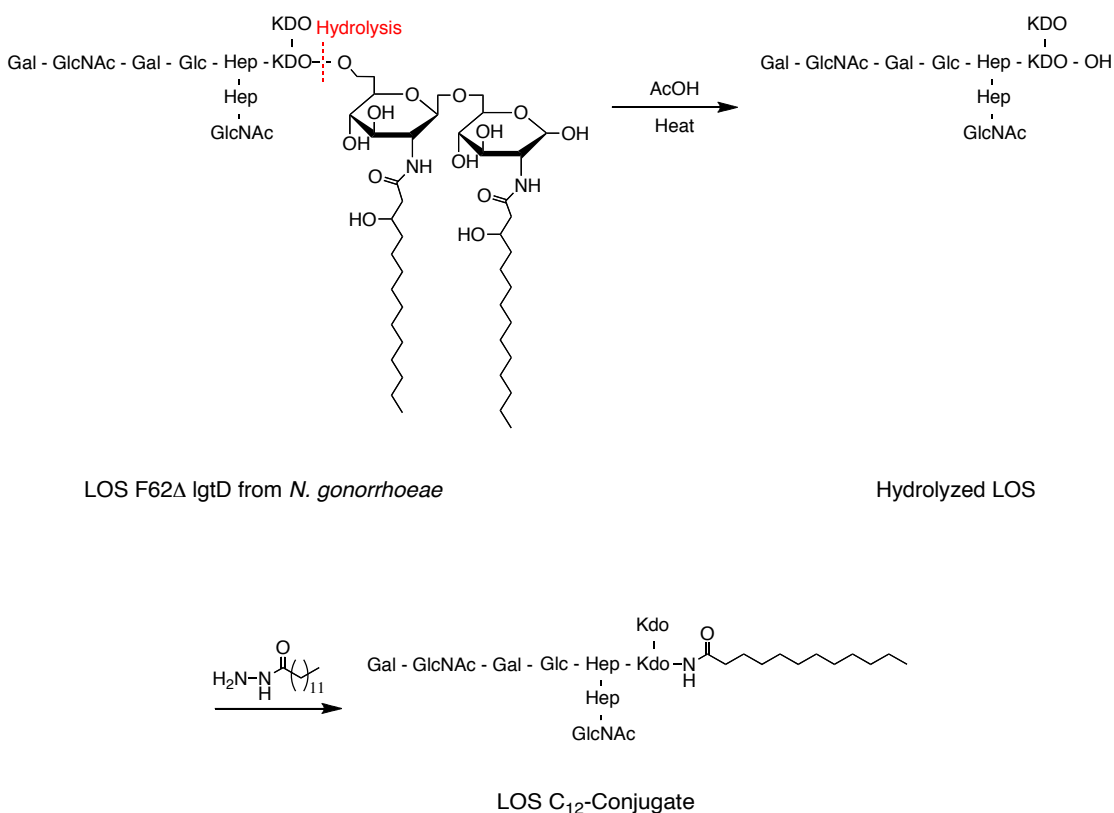
**Scheme 3.1.** Immune response of LOS vs. C<sub>12</sub>-PADRE/LOS conjugated catanionic vesicles. Vesicles loaded with only carbohydrate would generate IgM antibodies. Addition of the epitope C<sub>12</sub>-PADRE to LOS functionalized vesicles would generate IgG antibodies.

### 3.2 Results and Discussion

#### 3.2.1 Catanionic Vaccines for *Neisseria gonorrhoeae*

Surface antigens from Gram-negative bacteria trigger the immune response and therefore offer the potential to be used in vaccine development. Components on the *N. gonorrhoeae* cell membrane that trigger immune stimulation are LOS, porins (PorA and PorB), pili, and OPA.<sup>11</sup> To date, no one has been able to exploit the immunological potential of neisserial LOS as a vaccine candidate.

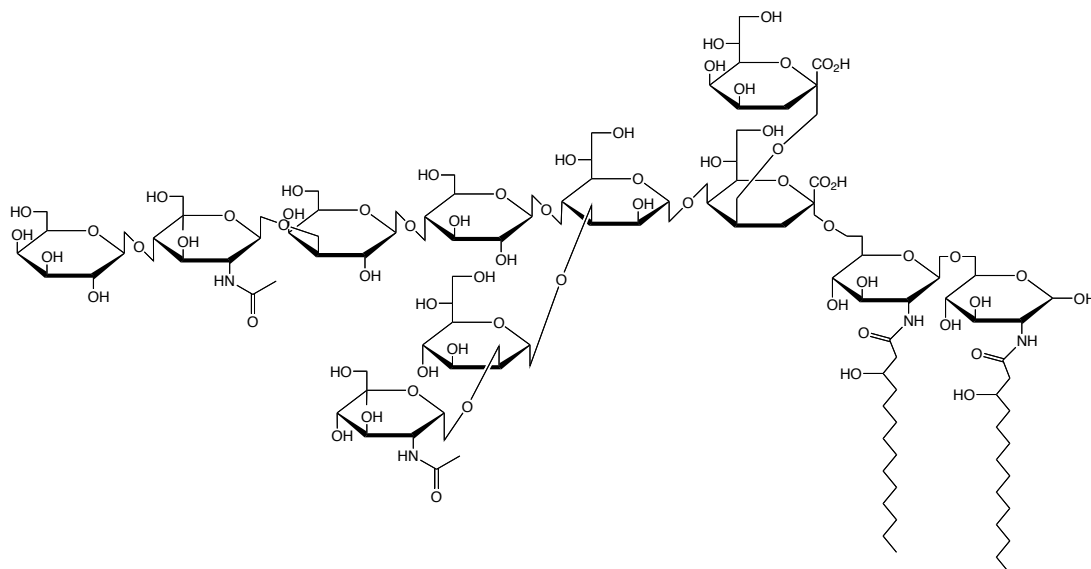
Previous research in the DeShong group utilized LOS from *N. gonorrhoeae* for its incorporation into cationic vesicles. In order to avoid toxicity associated with lipid A, the lipid A region was cleaved (Scheme 3.2).<sup>12</sup> A C<sub>12</sub>-conjugate was added to the oligosaccharide to provide an anchor for insertion into vesicles. While this method was effective when preparing functionalized vesicles, incorporation of the lipid A region into liposomes is known to lower its toxicity. Consequently, we studied vesicles loaded with the entire liposaccharide unit to determine if lipid A toxicity is removed after incorporation into cationic systems.



**Scheme 3.2.** Preparation of LOS conjugate from *N. gonorrhoeae*. The toxic lipid A portion was cleaved from the oligosaccharide using hot acetic acid and a hydrophobic C<sub>12</sub>-linker was added.

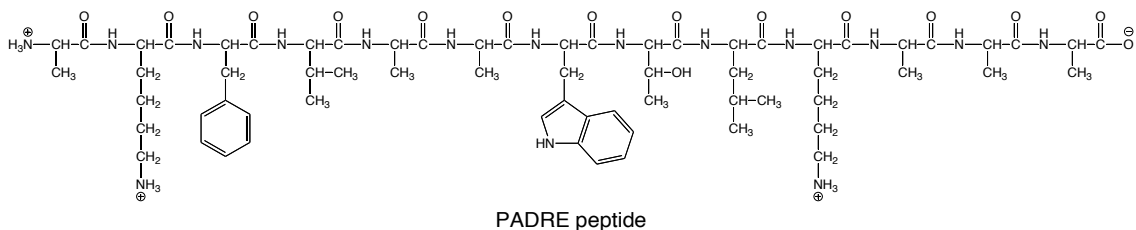
Cationic vesicles were prepared by adding native LOS derived from *N. gonorrhoeae* F62Δ lgtD (a strain that produces lacto-N-neotetraose LOS), which was provided by Dr. Daniel Stein's Group (Figure 3.2). Addition of this isolated pathogenic component should decorate the exterior membrane of vesicles (Scheme 3.1). Vesicles were purified by SEC and the presence of saccharide in the vesicle-containing fractions was confirmed using the phenol/sulfuric acid assay (described previously) (Table 3.1).<sup>13</sup>

Next, we developed a glycoconjugate-based vaccine (TRIAD) that contained the liposaccharide component and an epitope unit that would trigger the immune system. We utilized LOS and Pan DR helper T cell epitope (PADRE) peptide conjugate that possesses the ability to bind to a large number of HLA class II molecules. PADRE (Figure 3.3) was coupled with N-dodecanoylsuccinimide to form dodecanoic acid tethered PADRE conjugate that inserted into the vesicle bilayer (Scheme 3.3).<sup>14</sup> Both components were inserted into surfactant vesicles using a 10:1 w/w of LOS and C<sub>12</sub>-PADRE, respectively, and were purified by SEC (Scheme 3.4). Vesicle-containing fractions were analyzed by the phenol/sulfuric acid carbohydrate assay (described in Chapter 2) and by fluorescence. Results confirmed the presence of carbohydrate and phenylalanine and tryptophan residues in vesicle-containing fractions from SEC. These cationic surfactant vesicle formulations were stable at room temperature for years, unlike typical liposomal vaccine formulations. Furthermore, TRIAD is so robust that it can be autoclaved without any appreciable loss of structural integrity.



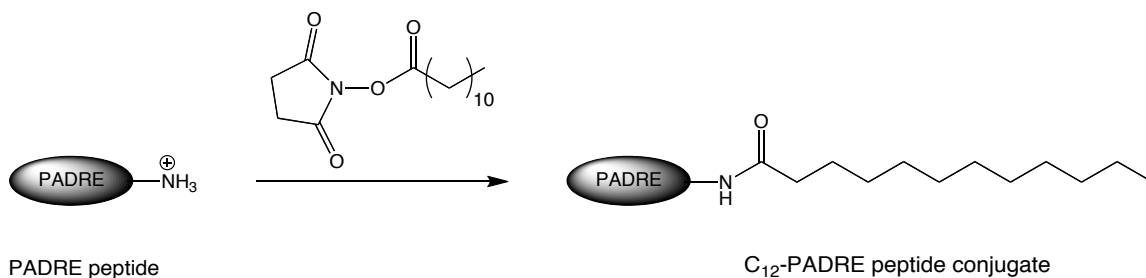
LOS F62Δ IgtD from *N. gonorrhoeae*

**Figure 3.2.** Chemical structure of lipooligosaccharide (LOS) F62Δ IgtD purified from *N. gonorrhoeae*. O-Antigen: Galβ1-4GlcNAcβ1-3Galβ1-; Core: -4Glcβ1-4Hepα1-(-3Hepα1-GlcNAcα1)5Kdo4-(-2αKdo); lipid A.



PADRE peptide

**Figure 3.3.** Chemical structure of unconjugated PADRE peptide (AKFVAAWTLKAAA).



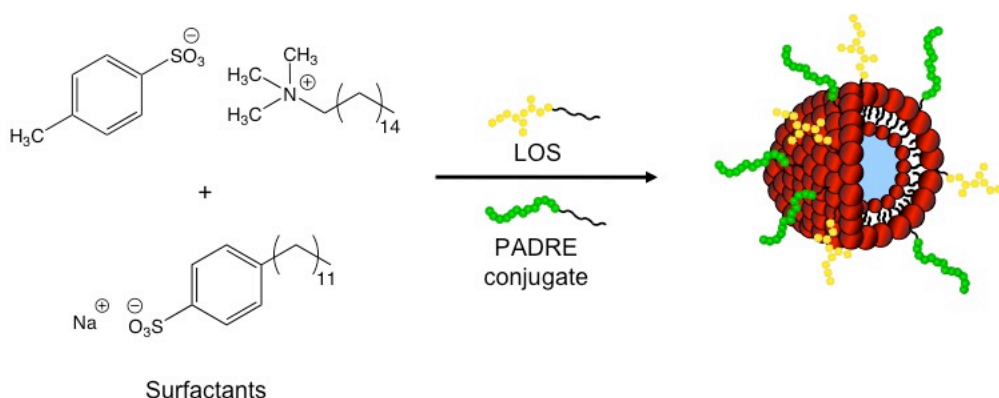
PADRE peptide

C<sub>12</sub>-PADRE peptide conjugate

**Scheme 3.3.** Synthesis of C<sub>12</sub>-PADRE peptide conjugate. Conjugated PADRE peptide contains a hydrophobic moiety, which allows for incorporation into the membrane of vesicle bilayers.

	Carbohydrate ( $\mu\text{g/mL}$ )	% Incorporation
TRIAD Vaccine	$51 \pm 7$	$96 \pm 16$

**Table 3.1.** Average amount of carbohydrate in TRIAD vaccine from two batches. Carbohydrate determined by phenol/sulfuric acid colorimetric assay.



**Scheme 3.4.** Preparation of TRIAD vaccine formulated with cationic surfactant vesicles containing the C<sub>12</sub>-PADRE peptide conjugate and LOS from *N. gonorrhoeae*. Ratio of conjugate components can be adjusted during vesicle formation to control the surface decoration of antigens.

### 3.2.1.1 Animal Studies with Vesicle Antigens

Lindsey Zimmerman in the Stein lab performed immunization studies. Mice were treated with TRIAD vaccine that contained LOS and C<sub>12</sub>-PADRE at a ratio of 10:1. Antibody levels were determined by ELISA immunoassay by immunizing with 2 mg of LOS equivalent. Antibody titers for both LOS and LOS/C<sub>12</sub>-PADRE vesicles showed the generation of antibodies after mice were inoculated. Treatment with LOS vesicles showed that only primary antibodies were present (IgM). These results indicated that only a primary immune response was achieved. Inoculation with LOS/C<sub>12</sub>-PADRE

showed that our vaccine induced a high titer anti-LOS antibody response, with the majority of the elicited antibody being IgG (Table 3.2). Intraperitoneal immunization of mice with our vaccine construct produced no observable adverse effects in mice, while intraperitoneal immunization with equivalent amounts of purified LOS induced significant adverse effects. Therefore, cationic vesicles loaded with LOS/C<sub>12</sub>-PADRE may have generated IgG antibodies that recognize LOS (Scheme 3.1). Immunogenic recognition of LOS in our TRIAD carbohydrate-based vaccine and may offer protection against *N. gonorrhoeae* in challenged mice. Furthermore, the LOS from the strain F62Δ lgtD contains the same LOS found in *N. meningitidis*. We have not tested protection of vaccinated mice against gonorrhea and meningitis, but a vaccine derived from F62Δ lgtD LOS could offer protection against both gonorrhea and meningitis. This would allow a method to make vaccines against both pathogens without having to work directly with *N. meningitidis*.

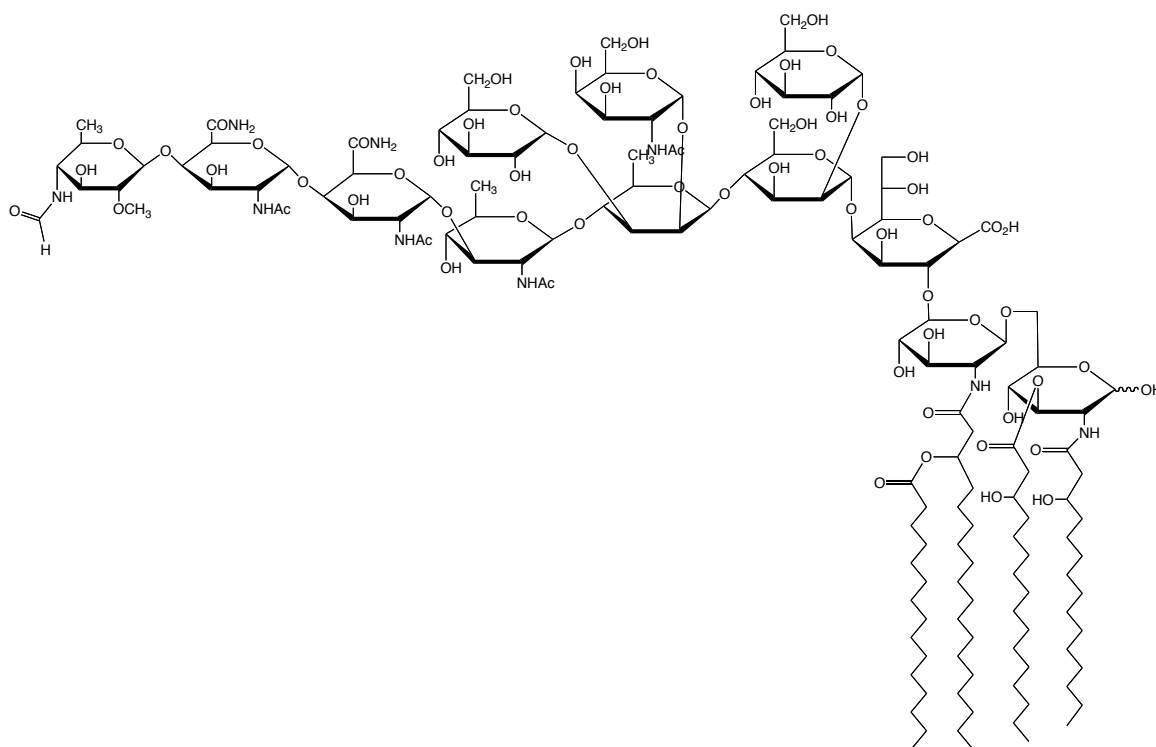
	Inoculation	Antibody Titer	IgG:IgM
LOS/PADRE Vesicles	Initial	1:1500	75:25
	Booster (2 weeks)	1:2000	
LOS Vesicles (Control)	Initial	1:100	0:100

**Table 3.2.** Antibody titer results in mice inoculated with LOS and LOS/ C<sub>12</sub>-PADRE functionalized surfactant vesicles; performed by a student in the Stein group (unpublished results).

### 3.2.2 Cationic Vaccines for *Francisella tularensis*

Similar cationic vaccines were performed in *F. tularensis*. Cationic vesicles were prepared in the same manner as reported in section 2.2.1, but native LPS from *F.*

*tularensis* was substituted for LOS (Figure 3.4). Vaccine studies were performed by Dr. Stefanie Vogel. After inoculation of LPS control vesicles, mice challenged with the virulent strain of *F. tularensis* died within four hours. Conversely, four out of five mice inoculated with LPS/C<sub>12</sub>-PADRE vesicles survived for four days after being challenged. One mouse even survived for two weeks. These results showed that mice vaccinated using LPS/C<sub>12</sub>-PADRE vesicles survived longer than the control group. These vaccines offer promise toward the development of vesicle-based vaccines to combat tularemia infections. Further vaccine studies are currently underway to determine the antibody titers using the ELISA immunoassay. Furthermore, the ratio of peptide conjugate to saccharide can be controlled in vesicle-based vaccines in order to control the immune system's response to the peptide.



LPS from *F. tularensis*

**Figure 3.4.** Chemical structure of lipopolysaccharide (LPS) from *F. tularensis*.

### 3.3 *Conclusions*

We have devised a safe and effective way of generating a large IgG titer against carbohydrate with a small dose of vaccine. A single dose of TRIAD injected intraperitoneally induced a robust antibody response against carbohydrate without adverse effects. The generated response was mostly IgG and reached a maximum titer with one dose of the vaccine. We believe that this will allow us to generate a universal vaccine capable of protecting against all serotypes of *N. meningitidis*. This vaccine platform also readily lends itself to further modifications in that it is possible to include additional neisserial proteins. In Chapter 4 we report incorporation of neisserial proteins and LOS via a novel whole cell extraction protocol, which offers the ability to load a variety of membrane components into vesicles.

### 3.4 *Future Work*

Vaccine studies will be continued by functionalizing vesicles with other liposaccharides and peptides. By coating surfactant vesicles with liposaccharides from the outer envelope of bacteria, vesicles were shown to elicit an immune response as mentioned above. Studies will be performed to determine how much C<sub>12</sub>-PADRE conjugate and liposaccharide can be loaded into vesicles. Varying ratios of C<sub>12</sub>-PADRE conjugate and liposaccharide will be prepared and tested for antibody titers using ELISA analysis. This work is important because the relative ratio of liposaccharide to peptide required to trigger a long-term immune response is unknown.

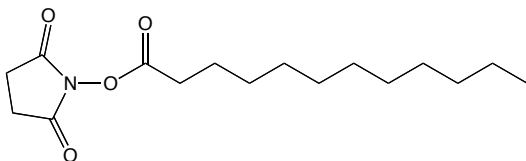
### 3.5 *Experimental*

Animal studies were performed by under the direction of Dr. Daniel Stein in the Department of Cell Biology and Molecular Genetics at the University of Maryland and Dr. Stefanie Vogel in the Department of Microbiology and Immunology at the University of Maryland School of Medicine.

#### 3.5.1 *Materials*

All chemicals and solvents were purchased from commercial suppliers unless otherwise noted. CTAT was purified by recrystallization in ethanol/acetone prior to use.

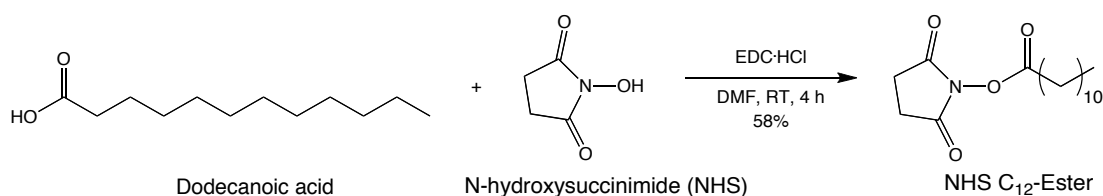
#### 3.5.2 *Synthesis of Conjugates*



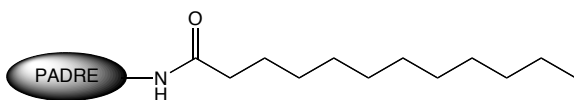
#### **N-Dodecanoylsuccinimide**

A solution of dodecanoic acid (0.539 mmol, 0.108 g), N-hydroxysuccinimide (NHS) (0.573 mmol, 0.0660 g), 1-ethyl-3-(3-dimethylaminopropyl)-carbodiimide hydrochloride (EDC·HCl) (0.574 mmol, 0.110 g) in DMF was stirred at room temperature for 4 h (Scheme 3.5). The solution was diluted with ethyl acetate (20 mL) and washed with H<sub>2</sub>O (20 mL), saturated aqueous NaHCO<sub>3</sub> (20 mL), and H<sub>2</sub>O (20 mL x 2). The organic layer was dried over MgSO<sub>4</sub>, filtered, and concentrated *in vacuo*. Purification after recrystallization (diethyl ether/hexane) afforded 0.0977 g (58%) of N-dodecanoylsuccinimide as white shiny crystals: R<sub>f</sub> = 0.85 (diethyl ether/hexane); mp 78 –

79 °C (lit.<sup>15</sup> 78-81°C); IR (thin film, NaCl) 2929 (m), 2852 (m), 1744 (s); <sup>1</sup>H NMR (CDCl<sub>3</sub>, 400 MHz) δ 2.84 (s, 4H), δ 2.61 (t, *J* = 8 Hz, 2H), δ 1.75 (m, *J* = 8 Hz, 2H), δ 1.41 (m, 16H), δ 0.89 (t, *J* = 8 Hz, 3H).

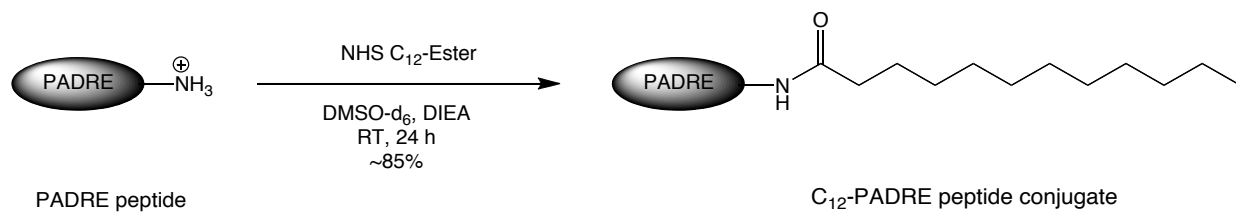


**Scheme 3.5.** Synthesis of N-dodecanoylsuccinimide.



### Dodecanoic Acid Tethered PADRE Peptide Conjugate

To a solution of PADRE peptide (Figure 3.4) (GenScript) (1.445 μmol, 1.950 mg, 2.890 μM) in 0.5 mL of DMSO-d<sub>6</sub> was added a solution of N-dodecanoylsuccinimide (1.445 μmol, 0.430 mg, 2.89 μM) in 0.5 mL of DMSO-d<sub>6</sub> followed by a solution of diisopropylethylamine (50 μL, 1.44 μmol, 28.7 mM) in DMSO-d<sub>6</sub>. The resulting solution was mixed well by vortexing and stirred at room temperature for 24 h. <sup>1</sup>H NMR analysis of the reaction mixture indicated that approximately 85% of NHS C<sub>12</sub>-ester was reacted with PADRE by comparing the integration of starting material to product. The reaction mixture was concentrated *in vacuo* and stored at -20 °C.



**Scheme 3.6.** Synthesis of dodecanoic acid tethered to PADRE peptide.

### 3.5.3 Isolation and characterization of LOS

LOS was obtained from Lindsey Zimmerman and Amanda Mahle in the Stein Lab. The LOS was purified from *N. gonorrhoeae* F62Δ lgtD, a strain genetically modified to produce only the lacto-N-neotetraose LOS (L7 immunotype), using a hot phenol/water extraction.<sup>16</sup>

### 3.5.4 Synthesis and Characterization of Surfactant Vesicles

Vesicles prepared with a molar excess of SDBS will be referred to as SDBS-rich (anionic).

To prepare vesicles with the liposaccharides shown in Figures 3.3 and 3.4, the liposaccharide was weighed directly into a vial containing 70.0 mg of SDBS (0.200 mmol) and 30.0 mg of CTAT (0.0658 mmol). Specifically, 1 mg of LOS or LPS and 0.2 mg of C<sub>12</sub>-PADRE conjugate were used to give a 10:1 w/w ratio of antigens in vesicles. Then 9.90 mL of water was added and samples were stirred for 60 min. Vesicles were purified from free conjugate by SEC, described previously.

The incorporation of carbohydrate and C<sub>12</sub>-PADRE-conjugate were determined by colorimetric assays to determine the quantity retained in vesicle-containing fractions (See Chapter 2 for details). The phenol/sulfuric acid colorimetric assay is described

previously.<sup>13</sup> The absorbance was measured at the  $\lambda_{\text{max}}$  (~490 nm) and compared to a standard curve, prepared for LOS and LPS to determine the total carbohydrate concentration in each sample.

### 3.5.5 *Animal Trials*

Mice were immunized by the Stein lab intraperitoneally with either 10  $\mu\text{g}$  of purified LOS alone, or 8.5  $\mu\text{g}$  of conjugated vaccine (Vs-OS-PADRE). On day 21 and 42, mice were boosted with an equivalent amount of vaccine or oligosaccharide and blood samples were taken. Serum was recovered from all mice on day 51 in a terminal bleed.

## References

1. Corbel, M. J., Reasons for instability of bacterial vaccines. *Dev. Biol. Stand.* **1996**, 87,113-124.
2. Foster, K. A.; Gorringer, A. R.; Hudson, M. J.; Reddin, K. M.; Robinson, A. Preparation of outer membrane vesicles from Gram negative bacteria and uses thereof as vaccines. 2002-GB57182003051379, 20021217., **2003**.
3. Varki, A., Biological roles of oligosaccharides: All of the theories are correct. *Glycobiology* **1993**, 3 (2), 97-130.
4. Gupta, R. K.; Siber, G. R., Adjuvants for human vaccines - current status, problems and future prospects. *Vaccine* **1995**, 13 (14), 1263-76.
5. Alving, C. R., Lipopolysaccharide, lipid A, and liposomes containing lipid A as immunologic adjuvants. *Immunobiology* **1993**, 187 (3-5), 430-46.
6. Dijkstra, J.; Mellors, J. W.; Ryan, J. L., Altered in vivo activity of liposome-incorporated lipopolysaccharide and lipid A. *Infect. Immun.* **1989**, 57 (11), 3357-63.
7. Tamauchi, H.; Tadakuma, T.; Yasuda, T.; Tsumita, T.; Saito, K., Enhancement of immunogenicity by incorporation of lipid A into liposomal model membranes and its application to membrane-associated antigens. *Immunology* **1983**, 50 (4), 605-12.
8. Stallforth, P.; Lepenies, B.; Adibekian, A.; Seeberger Peter, H., Carbohydrates: A frontier in medicinal chemistry. *J. Med. Chem.* **2009**, 52 (18), 5561-77.
9. Robbins, J. B.; Schneerson, R., Polysaccharide-protein conjugates: a new generation of vaccines. *J. Infect. Dis.* **1990**, 161 (5), 821-32.
10. Alexander, J.; Del Guercio, M.-F.; Maewal, A.; Qiao, L.; Fikes, J.; Chesnut, R. W.; Paulson, J.; Bundle, D. R.; DeFrees, S.; Sette, A., Linear PADRE T helper epitope

and carbohydrate B cell epitope conjugates induce specific high titer IgG antibody responses. *J. Immunol.* **2000**, *164* (3), 1625-1633.

11. Stein, D. C.; Patrone, J. B.; Bish, S., Innate immune recognition of *Neisseria meningitidis* and *Neisseria gonorrhoeae*. *Neisseria* **2010**, 95-122.
12. Yamasaki, R.; Bacon, B. E.; Nasholds, W.; Schneider, H.; Griffiss, J. M., Structural determination of oligosaccharides derived from lipooligosaccharide of *Neisseria gonorrhoeae* F62 by chemical, enzymatic, and two-dimensional NMR methods. *Biochemistry* **1991**, *30* (43), 10566-75.
13. Park, J.; Rader, L. H.; Thomas, G. B.; Danoff, E. J.; English, D. S.; DeShong, P., Carbohydrate-functionalized cationic surfactant vesicles: preparation and lectin-binding studies. *Soft Matter* **2008**, *4* (9), 1916-1921.
14. Anderson, G. W.; Zimmerman, J. E.; Callahan, F. M., N-Hydroxysuccinimide esters in peptide synthesis. *J. Am. Chem. Soc.* **1963**, *85* (19), 3039.
15. Rothman, E. S.; Serota, S.; Swern, D., Enol esters. II. N-Acylation of amides and imides. *J. Org. Chem.* **1964**, *29* (3), 646-50.
16. Westphal, O.; Jann, K.; Himmelsbach, K., Chemistry and immunochemistry of bacterial lipopolysaccharides as cell wall antigens and endotoxins. *Prog Allergy* **1983**, *33*, 9-39.

## Chapter 4: Methodology for the Extraction of Membrane Components from *Neisseria gonorrhoeae*

*This chapter is taken from the prepared article:*

Stocker, L. H.; Horn, A.; Zimmerman, L.; Dhabaria, A. P.; Fenselau, C.; Stein, D. C; and DeShong, P., Extraction of membrane components from *Neisseria gonorrhoeae* using cationic surfactant vesicles. *In preparation.*

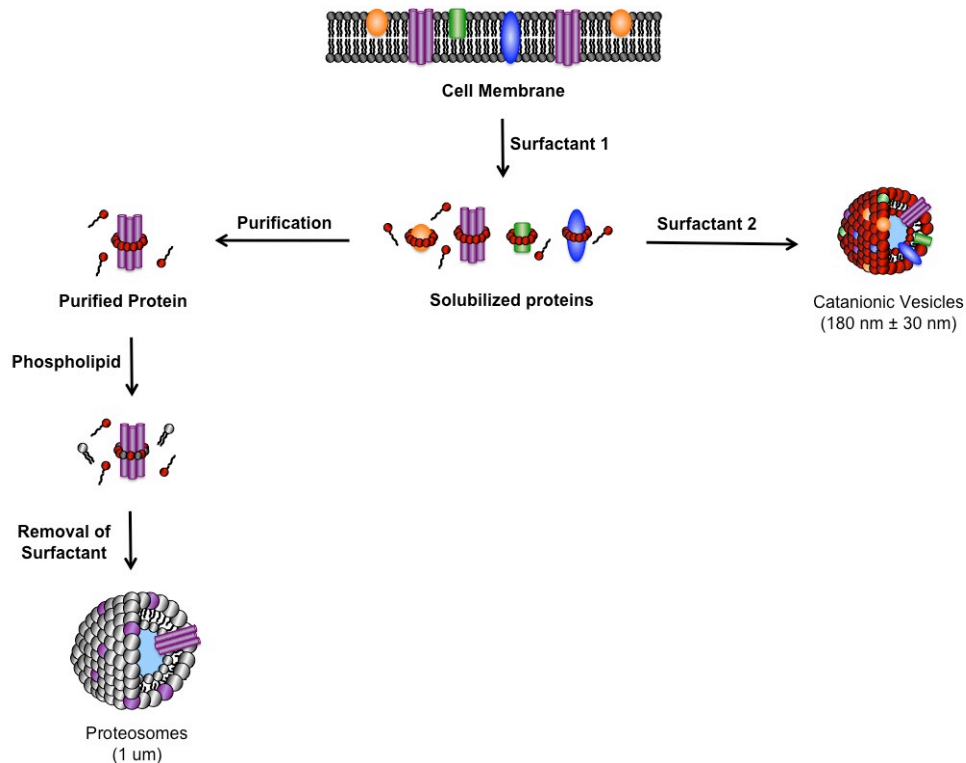
### 4.1 Introduction

Cell surface receptors play a crucial role in cell-cell communication and recognition.<sup>1</sup> In Gram negative bacteria, cell-cell recognition is a key feature of pathogen virulence<sup>2</sup> and biofilm formation.<sup>3</sup> Accordingly, methods for the extraction and purification of carbohydrates and proteins from cellular membranes, followed by reconstitution of cellular components into stable hydrophobic matrices has been widely investigated as a model system for studying surface-mediated phenomena.<sup>4-13</sup> Due to the complexity of biological membranes, cell surface components are often studied in artificial membranes in order to determine their specific role and mechanism of action.<sup>12</sup> However, when solubilizing and reconstituting membrane proteins, special consideration must be taken in order to retain the orientation and biological activity of the protein.<sup>11</sup>

#### 4.1.1 Reconstitution of Membrane Proteins into Liposomes

There are a number of strategies employed for the insertion of proteins into liposomes, including mechanical means, freeze-thaw methods, organic solvent-mediated reconstitution, direct incorporation into preformed liposomes, or detergent-mediated reconstitution.<sup>12, 13</sup> Detergent-mediated reconstitution is the most commonly used

method because detergents are often involved during the initial solubilization step for cellular membrane proteins. As outlined in Scheme 4.1, the detergent-mediated reconstitution procedure developed by Rigaud begins with the addition of detergent to the native membrane to solubilize proteins in a lipid-detergent solution.<sup>12, 13</sup> After protein purification, excess detergent is removed by dialysis, gel chromatography, or absorption onto hydrophobic resins to form a closed lipid vesicle.<sup>7</sup> Due to the lipophilic nature, membrane proteins embed themselves within the liposomal bilayer to form proteoliposomes.



**Scheme 4.1.** Reconstitution of purified membrane proteins into liposomes compared to extraction procedure using cationic vesicles. Incorporation of membrane components into liposomes requires purification, addition of phospholipid, and removal of surfactant. Extraction using cationic surfactants only requires the addition of a second surfactant to form cationic vesicles that contain membrane components.

Other methods of protein incorporation into liposomes have been conducted where preformed liposomes are incubated in the presence of cells<sup>14</sup> or proteoliposomes.<sup>15</sup> One study focused on extracting membrane-bound proteins from human erythrocytes by incubating cells with sonicated phospholipid liposomes.<sup>14</sup> The resulting liposomes were shown to contain cell surface proteins by subjecting cells to lactoperoxidase iodination prior to incubation with liposomes followed by detection of <sup>125</sup>I-labeled proteins in liposomal extracts.<sup>14</sup> Another study reported the transfer of proteins from proteoliposomes into giant unilamellar vesicles (15-120 μm).<sup>15</sup> Proteoliposomes were prepared and incubated in the presence of giant unilamellar vesicles, where spontaneous transfer of a mitochondrial proteins occurred within 24 h.<sup>15</sup>

#### 4.1.2 Liposomal Bacterial Vaccines

Outer membrane proteins from bacteria have been incorporated into liposomes for vaccines and the immune response of the resulting liposomal preparations has been reported.<sup>8-10, 16-18</sup> Liposomal formulations of antigens have particularly significant advantages in vaccine formulation over cell-based formulations since they avoid safety concerns that may arise from attenuated or killed pathogens. Previous research has demonstrated that PorA from *Neisseria meningitidis* incorporated into liposomes induced an immune response against many serotypes of meningococci.<sup>17</sup> In a recent study, Zollinger *et al.* reported a liposomal vaccine currently in a Phase I study containing major outer membrane proteins from *N. meningitidis*.<sup>10</sup> In this study, surface antigens of *N. meningitidis* were presented in three manners: adhesion to aluminum hydroxide, insertion

into proteoliposomes, and insertion into liposomes: the latter preparation gave the most effective immune response in humans.<sup>10</sup>

Lipopolysaccharide (LPS) present in Gram negative bacteria have been shown to act as adjuvants, resulting from the lipid A portion of the molecule.<sup>19</sup> While vaccines have been formulated that contain LPS or lipid A alone, the toxicity of LPS has limited its use in vaccine formulation.<sup>20</sup> Incorporating LPS or lipid A into liposomes<sup>21-26</sup> has been shown to greatly reduce toxicity.<sup>27-29</sup> Unfortunately, carbohydrate-based vaccines are poorly immunogenic and fail to trigger helper-T cell recognition.<sup>30</sup> Therefore, long-term protection of the carbohydrate is not achieved.

#### 4.1.3 *Outer Membrane Vesicles for Vaccines*

Another formulation of bacterial vaccines are outer membrane vesicles (OMV), also referred to as blebs.<sup>31</sup> OMV bud off from bacterial cells and are comprised of several membrane components from the original cell that are incorporated into the OMV lipid bilayer structure. Research has shown that OMV from *N. meningitidis* generate an immune response directed to PorA.<sup>32</sup> For example, the commercially available vaccine HexaMen is used against bacterial meningitis and is derived from OMV.<sup>33 34-36</sup>

Liposomal formulations of cell surface components have several limitations as vehicles for displaying cell surface proteins and lipids in a stable membrane-like environment. First, since cell surface components typically reside in the hydrophobic bilayer, the solubilization and purification of these substances from the membrane often results in denaturation of the protein. Second, it is unclear if insertion of the purified protein into the membrane of a liposome results in the presentation of the protein in its

"natural" form.

Another major limitation of the liposomal formulation approach is related to the general physicochemical characteristics of liposomes. Liposome production requires either sonication or passage through a membrane. This results in the addition of mechanical stress to the system that also may lead to denaturation of sensitive biological components. Liposomal preparations prepared by either sonication or membrane extrusions are very heterogeneous with respect to size (300 nm to 20  $\mu$ m). Finally, liposomal formulations are typically unstable in biological media and are thermodynamically unstable.

#### 4.1.4 *Catanionic Vesicle Bacterial Vaccines*

We have investigated the use of cationic surfactant vesicles<sup>37</sup> to extract membrane components from pathogenic bacteria directly into these systems without further purification of cellular components (Scheme 4.1). Most notably, these vesicles are formed from inexpensive, commercially available surfactants, form spontaneously with only mixing involved, and possess long-term and enhanced stability when compared to their liposomal counterparts.<sup>38, 39</sup> These properties make them attractive for vaccine formulations due to ease of handling, preparation, and storage.

In this chapter, we describe the extraction of cell surface components from *N. gonorrhoeae* directly into cationic vesicles. Mass spectral analysis of the proteins contained within these vesicles demonstrated that key cell surface components were effectively incorporated into the vesicles. To our knowledge, this is the first study in which membrane components were directly extracted from bacteria into vesicles without

purification prior to incorporation into the lipid bilayer structure. The resulting extraction method creates an "artificial pathogen", which can be used for the development of vaccines.

#### 4.2 *Results and Discussion*

Vesicle extractions of *N. gonorrhoeae* were prepared using the methods described in the Experimental Section. After purification of cationic vesicles by column chromatography, vesicles were characterized using a colorimetric carbohydrate assay, a BCA protein assay, silver staining after gel electrophoresis, Western blotting, and mass spectrometry-based proteomics. The results indicated that membrane components from this bacterium were incorporated into cationic vesicles.

Five different methods were used to construct the vesicles in order to determine if protein and carbohydrate were incorporated better by a specific method (Table 4.1). Details for each preparation method can be found in Experimental Section 2.4.2. After purification by gel filtration, the resulting vesicle-containing fractions were tested for the presence of carbohydrate and protein using a carbohydrate colorimetric assay<sup>39</sup> and the BCA protein assay<sup>40</sup> (Table 4.1). While the total amount of protein and carbohydrate varied with the purification method, each method was able to incorporate significant levels of cellular proteins and carbohydrates. While these assays quantitatively determined the amount of carbohydrate and protein contained within vesicles, they lacked the ability to determine which Gonococcal component were present in the vesicles.

Method	Protein ( $\mu\text{g/mL}$ )	Carbohydrate ( $\mu\text{g/mL}$ )	Ratio
1	333	38	8.76
2	309	62	4.98
3	408	56	7.29
4	346	44	7.86
5	341	26	13.12

**Table 4.1.** Total protein and carbohydrate concentrations in vesicle extract samples determined by colorimetric BCA and carbohydrate assays. All five extraction methods yielded similar quantities of protein and carbohydrate by methods 1) solid surfactants added to the bacterial cell pellet followed by the addition of water, 2) SDBS solution added to the bacterial cell pellet followed by the addition of a CTAT solution 3) CTAT solution added to bacterial cell pellet followed by the addition of solid SDBS 4) SDBS solution added to bacterial cell pellet followed by the addition of solid CTAT 5) bare vesicles added to the bacterial cell pellet. BCA assay indicated the presence of protein in the different extraction methods.

In order to visualize the cellular components incorporated into cationic vesicles, the various vesicle preparations were compared to the whole cell lysate and original cell pellet by gel electrophoresis followed by silver staining (Figure 4.1). The presence of LOS in vesicles was suggested by the presence of bands with electrophoretic mobility similar to that of purified F62 $\Delta$ lgtD LOS. We expected LOS to be readily incorporated into vesicles because the biophysical properties of Lipid A should be solubilized by the lipophilic bilayer. The distribution of proteins incorporated into the vesicles differed from the distribution of proteins obtained from whole cell lysates, suggesting that vesicles were only extracting a subset of bacterial proteins (Figure 4.1).

All fractions of Method 4 from SEC were analyzed by gel electrophoresis followed by silver staining in order to characterize the carbohydrates and proteins that were incorporated into the vesicles (Figure 4.2). These data indicated that numerous proteins eluted in the same fraction as intact vesicles, supporting the conclusion that the cellular components were incorporated into the vesicles.

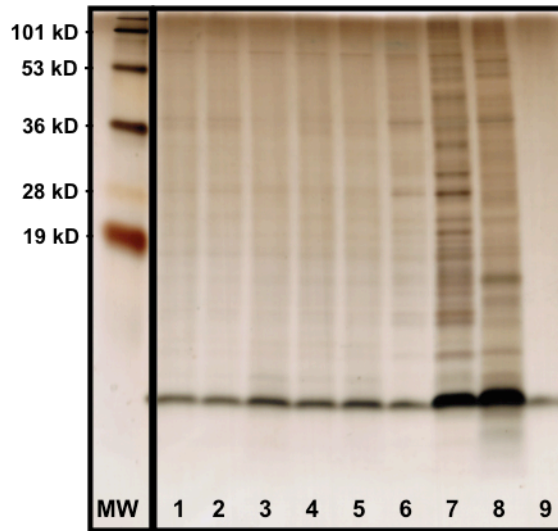


**Figure 4.1.** Vesicle-containing fractions purified by gel filtration followed by silver staining. Lanes 1-6 and 9 were loaded with 1  $\mu$ L, Lane 7 was loaded with 5  $\mu$ L, and Lane 8 was loaded with 167 nL of sample and analyzed by SDS-polyacrylamide Tris-tricine 16.5% v/v gels followed by silver staining. Lanes 1-6 corresponded to vesicle-containing fractions prepared from extraction methods 1-6, respectively, and showed similar protein patterns. Lane 7 showed the purified cell lysate disrupted by SDBS and purified by gel filtration. Lane 8 contained a very different protein pattern from resuspended GC cell pellet. Lane 9 contained purified LOS F62 $\Delta$ gtD as a standard.

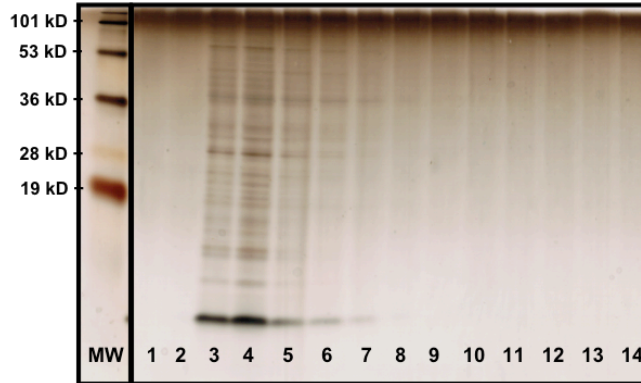


**Figure 4.2.** Vesicle extract fractions from gel filtration analyzed by silver staining. Lanes were loaded with 1  $\mu$ L of sample and analyzed by SDS-polyacrylamide Tris-tricine 16.5% v/v gels followed by silver staining. Lanes 1 and 2 represent the void volume and are free of protein and carbohydrate. Lanes 3 and 4 correspond to vesicle containing-fractions and indicate the presence of a range of proteins and a high concentration of the carbohydrate LOS F62 $\Delta$ lgtD with the darkest band at the bottom of the gel. Lanes 5-14 showed the diminishing presence of proteins and LOS.

Western blotting of the loaded materials from these surfactant vesicles showed the presence of LOS and the two predominant membrane proteins porin (36 kD) and Opa (25-30 kD) (Figure 4.3). Mass spectrometry analysis was performed by Dr. Catherine Fenselau's Group on vesicles containing gonococcal cell extracts and identified 157 gonococcal protein fragments. This analysis identified many of the known outer membrane proteins and membrane associated proteins found in the gonococcus. For example, mass spectrometry identified the major outer membrane protein porin P.IB, the outer membrane protein P.III, the major lipoprotein, components of the antibiotic resistance efflux pump, pilin and proteins associated with pilin assembly, numerous transport proteins, and putative two-component transport system proteins. This analysis also identified numerous ribosomal proteins and proteins involved in energy generation. These latter proteins, while not components of the outer membrane, represent major

proteins found in the bacterium, and would be expected to contaminate outer membrane fractions.

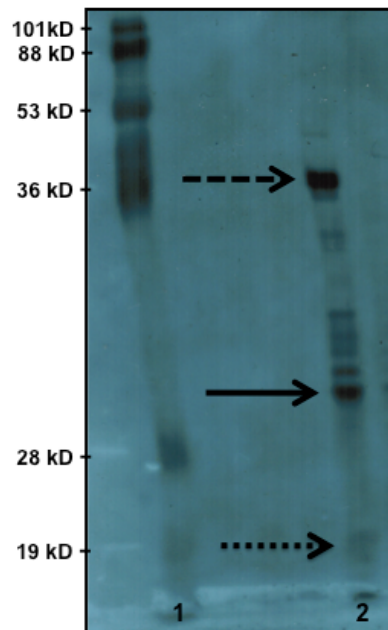


**Figure 4.3.** Western blotting of vesicle-containing fractions, lysate, and supernatant. The purified vesicle extract showed antibody binding to several proteins and LOS, specifically porin (36 kD) and OPA (25-30 kD). The lysate fraction did not show any antibody binding, indication that only vesicles contained surface antigens.

Proteinase K protection experiments were performed to determine if bacterial proteins were localized to the interior of the vesicles. Loaded vesicles were digested with proteinase K to determine if proteins associated with vesicles were protected from digestion. Both vesicle samples and the whole cell lysate showed complete digestion using this enzyme (Figure 4.4). Since proteinase K is a nonspecific digestion enzyme, these results demonstrated that any protein at the surface of vesicles was digested completely by the enzyme. This proteolytic enzyme does not digest the carbohydrate LOS, as seen by the band at the bottom of the gel (Figure 4.4).



**Figure 4.4.** Proteinase K digestion. Lanes 1 and 3 showed the protein pattern of the GC lysate and vesicle extract, respectively, after silver staining. Lanes 2 and 4 contained GC lysate and vesicle extract purified by gel filtration and show digestion of all protein bands and retention of LOS at the bottom of the gel.

Digestion of vesicles using trypsin gave a different pattern. Digested proteins in the form of peptide units were seen in great concentrations at the bottom of the gel (Figure 4.5). The vesicle samples showed protection for a few proteins, while the whole cell lysate fraction was completely cleaved by trypsin. This indicated that vesicles contained proteins embedded in the bilayer, where they are protected from cleavage from trypsin, but not proteinase K.

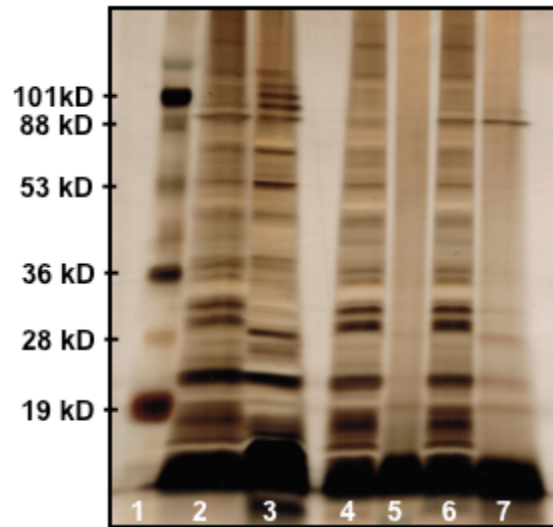


**Figure 4.5.** Protection from trypsin digestion. Lanes 2 and 3 showed the protein pattern of the whole cell lysate before and after digestion with trypsin, respectively. Lanes 4 and 6 contained GC lysate and vesicle extract purified by gel filtration, respectively. Lanes 5 and 7 showed the protein pattern of GC lysate and vesicle extract after digestion with trypsin, respectively. Digested vesicle extract showed the retention of a few proteins and LOS.

#### 4.3 Conclusions

This work offered a way to extract membrane components from pathogenic bacteria for potential vaccine formulation using cationic surfactant vesicles. Membrane components of a cell would be useful if they could be easily separated. The vesicle extraction procedure introduced here offers potential enrichment of LOS and other membrane components from *N. gonorrhoeae*. These cationic vesicles extracts are stable at room temperature for prolonged periods of time and offer an improvement over proteoliposomes. Furthermore, the structure of LOS involved in the meningococcal disease is identical to that expressed by the *N. gonorrhoeae* F62ΔlgtD used in vesicle extractions. Additional work will be devoted to generating a universal vaccine able to protect against all serotypes of *N. meningitidis*. The described vesicle extraction is

currently being studied for use with other pathogens, including *F. tularensis*, *P. aeruginosa*, and *E. coli*. Vesicle extracts from *E. coli* are currently being tested in cows for vaccination of dairy cow mastitis.

#### 4.4 *Experimental*

Animal studies were performed by under the direction of Dr. Daniel Stein in the Department of Cell Biology and Molecular Genetics at the University of Maryland covered by Environmental Safety Tracking Number 11-50 (E-946).

##### 4.4.1 *General Experimental*

All chemicals and solvents were purchased from commercial suppliers and were used as received unless otherwise noted. All aqueous vesicle solutions were prepared from a Millipore (18M $\Omega$ ) water purification system and all assays used water purified using an Elix 5 (Millipore) water purification system unless otherwise stated. An Ocean Optics USB 2000 Spectrometer was used to measure UV-VIS absorbance of samples.

##### 4.4.2 *Cell Cultures*

Cell cultures were grown by Lindsey Zimmerman. *N. gonorrhoeae* F62 $\Delta$ lgtD<sup>41</sup> cells were grown for 48 h to an OD of  $\sim$ 1.0 (650 nm) ( $10^9$  CFU). A 20 mL aliquot of bacterial cell culture was collected by centrifugation at 9,000 RPM for 30 min and the supernatant was decanted. Cell pellets were stored at -20°C until needed.

#### 4.4.3 Vesicle Preparation

Sodium dodecylbenzenesulfonate (SDBS) was purchased from TCI America and was utilized without further purification. Cetyltrimethylammonium tosylate (CTAT) was purchased from Sigma and was recrystallized from ethanol-acetone to give a white powder. The purified solid was stored at room temperature in a desiccator containing Drierite. Several vesicle preparation methods were tested to determine if the extraction varied between the order and type of addition of the surfactant components. Procedures for the other preparation methods can be found in the Experimental Section 2.4.2.

Method 4 vesicles were formed by adding 9.90 mL of an aqueous SDBS solution (0.0203 M) directly to the bacterial cell pellet and stirring for 1 h at room temperature. 30.0 mg of solid CTAT (0.0658 mmol) was added to the suspension and stirred for 1 h at room temperature.

Vesicles were centrifuged for 5 min at 5,000 RPM and the supernatant was decanted. The resulting colloidal supernatant, milky in appearance, was purified by SEC on Sephadex G-100 (Details in Chapter 2).

Fractions were characterized for the presence of carbohydrate and protein using a phenol-sulfuric colorimetric assay<sup>42</sup> and a modified procedure of the Pierce bicinchoninic acid (BCA) assay<sup>40</sup>, respectively (Details in Chapter 2).

#### 4.4.4 Gel Electrophoresis

Purified vesicle samples and a molecular weight standard were mixed with loading buffer (5x SDS-PAGE gel loading buffer, 0.25M Tris-HCl, pH 6.8, 15% SDS, 50% glycerol, 25%  $\beta$ -mercaptoethanol, and 0.01% bromophenol blue) and boiled for 10

min. Samples were loaded onto an SDS-polyacrylamide gel (Tris-tricine 16.5% v/v) using Tris-tricine 1X as the running buffer and run for 4.5 h at 100 V on ice (Bio-Rad Model 200/2.0 power supply).

#### 4.4.5 *Silver Staining*

After electrophoresis, the gels were incubated in a fixing solution (500 mL of 38% ethanol and 25 mL glacial acetic acid) overnight on a shaker at room temperature. Gels were silver stained according to a modified procedure.<sup>43</sup> The gel was transferred to 100 mL of aqueous periodic acid (0.036 M) and washed for 5 min and rinsed with water for 30 min on a shaker four times. The silver staining solution was prepared by adding 4.0 mL of diluted silver nitrate (4.7 mmol) dropwise to Solution 1 (1 pellet sodium hydroxide, 25 mL water, 1.40 mL of 30% ammonium hydroxide). If a brown color was present, additional ammonium hydroxide was added dropwise until the solution became clear and colorless. The silver staining solution was brought to a final volume of 100 mL with water and the gel was incubated for 15 min with the solution on a shaker at room temperature.

After staining, the gel was washed with water six times for 15 min each and incubated in a developing solution (95  $\mu$ L formaldehyde 37% solution, 1 mL citric acid 25 mg/mL, 500 mL water) until bands became visible. The gel was washed in water and then imaged.

#### 4.4.6 *Protection Experiments*

Vesicle-containing fractions were digested using 10  $\mu$ L proteinase K (25 mg/mL) for a 500  $\mu$ L sample incubated at 37°C. Aliquots were taken after 18 h, 23 h, and 46 h. A control of the cell pellet was prepared by suspending the pellet in 1.0 mL of water. Proteinase K was added to the cell pellet suspension and a sample of whole cell lysate and incubated at 37°C. Aliquots were taken after 18 h, 23 h, and 46 h and all samples were analyzed by electrophoresis and silver staining. The original samples from the proteinase K digestion were also digested with trypsin (0.25%, Corning cellgro), where 10  $\mu$ L was added to 500  $\mu$ L of sample and incubated at 37°C. Aliquots were taken after 18 h, 23 h, and 46 h and all samples were analyzed by electrophoresis and silver staining.

#### 4.4.7 *Western Blotting*

Western blotting was performed under standard conditions.<sup>44</sup> The nitrocellulose was rinsed with a PBS/Tween-20 solution 5 times for 15 min and then incubated with antigonococcal antisera (raised in a goat<sup>45</sup>) prepared in casein filler on a shaker for 2 h. The nitrocellulose was rinsed with a PBS 1X/Tween-20 solution five times for 15 min each and then incubated with donkey anti-goat HRP (Jackson ImmunoResearch laboratories Inc.) (1:100,000) secondary antibody solution prepared in casein filler on a shaker for 2 h. The nitrocellulose was rinsed with a PBS 1X/Tween-20 solution five times for 15 min each and then incubated with a standard Western blotting chemiluminescence solution (PerkinElmer, Waltham, MA) and analyzed using autoradiograph film.

#### 4.4.8 Proteomics Analysis

Vesicle extracts were prepared from cell pellets formed from 20 mL, 40 mL, or 60 mL of cells. The remaining proteomics analysis was performed by Avantika Dhabaria. Known amounts of protein were spotted from these preparations in each lane of a one-dimensional gel (Tris-HCl, 8-16% gradient). Whole cell lysate was spotted in a fourth lane. The gel was developed and stained with Coomassie blue stain (Sigma).

Fifteen slices were cut from each lane and subjected to overnight in-gel tryptic digestion (13 ng/ $\mu$ L) using a standard procedure.<sup>46</sup> The resulting peptides were extracted and injected into a capLC-MS/MS LTQ-orbitrap (ThermoFisher, San Jose, CA) as described elsewhere.<sup>47</sup> Peptide and protein candidates were analyzed using the search program MASCOT 2.3 (Matrix Science, London, UK), and protein identifications were based on the number of associated tryptic peptides and the reliability of the peptide identifications. Two protein databases were searched, one compiled of all *Neisseria* sequences from NCBI (www.ncbi.nlm.nih.gov) and one comprised from only the proteins in NCBI from the species *N. gonorrhoeae*. Coverage Table 1.7 was used to remove any proteins that shared the same peptides and to generate the percent of sequence coverage. Subcellular locations of the proteins were assigned using the Protein Information Resource.

## References

1. Scott, J. D.; Pawson, T., Cell signaling in space and time: where proteins come together and when they're apart. *Science* **2009**, *326* (5957), 1220-1224.
2. Boyle, E. C.; Finlay, B. B., Bacterial pathogenesis: exploiting cellular adherence. *Curr. Opin. Cell Biol.* **2003**, *15* (5), 633-639.
3. Lazar, V.; Chifiriuc, M. C., Architecture and physiology of microbial biofilms. *Roum. Arch. Microbiol. Immunol.* **2010**, *69* (2), 95-107.
4. Racker, E., Reconstitution of membrane processes. *Methods Enzymol.* **1979**, *55*, 699-711.
5. Racker, E., Reconstitutions: past, present and future. *Membr. Bioenerg., Int. Workshop* **1979**, 569-91.
6. Daghasanli Katia, R. P.; Ferreira Rinaldo, B.; Thedei, G., Jr.; Maggio, B.; Ciancaglini, P., Lipid composition-dependent incorporation of multiple membrane proteins into liposomes. *Colloids Surf. B Biointerfaces* **2004**, *36* (3-4), 127-37.
7. Girard, P.; Pecreaux, J.; Lenoir, G.; Falson, P.; Rigaud, J.-L.; Bassereau, P., A new method for the reconstitution of membrane proteins into giant unilamellar vesicles. *Biophys. J.* **2004**, *87* (1), 419-429.
8. Parmar, M. M.; Edwards, K.; Madden, T. D., Incorporation of bacterial membrane proteins into liposomes: factors influencing protein reconstitution. *Biochim. Biophys. Acta, Biomembr.* **1999**, *1421* (1), 77-90.

9. Macdonald, A. G.; Martinac, B.; Bartlett, D. H., Patch-clamp experiments with porins extracted from a marine bacterium (*Photobacterium profundum* strain SS9) and reconstituted in liposomes. *Cell Biochem. Biophys.* **2002**, *37* (3), 157-167.
10. Zollinger Wendell, D.; Babcock Janiine, G.; Moran Elizabeth, E.; Brandt Brenda, L.; Matyas Gary, R.; Wassef Nabila, M.; Alving Carl, R., Phase I study of a *Neisseria meningitidis* liposomal vaccine containing purified outer membrane proteins and detoxified lipooligosaccharide. *Vaccine* **2012**, *30* (4), 712-21.
11. Silvius, J. R., Solubilization and functional reconstitution of biomembrane components. *Annu. Rev. Biophys. Biomol. Struct.* **1992**, *21*, 323-48.
12. Rigaud, J. L., Membrane proteins: functional and structural studies using reconstituted proteoliposomes and 2-D crystals. *Braz. J. Med. Biol. Res.* **2002**, *35* (7), 753-766.
13. Rigaud, J.-L.; Pitard, B., Liposomes as tools for the reconstitution of biological systems. *Liposomes Tools Basic Res. Ind.* **1995**, 71-88.
14. Bouma, S. R.; Drislane, F. W.; Huestis, W. H., Selective extraction of membrane-bound proteins by phospholipid vesicles. *J. Biol. Chem.* **1977**, *252* (19), 6759-63.
15. Varnier, A.; Kermarrec, F.; Blesneac, I.; Moreau, C.; Liguori, L.; Lenormand, J. L.; Picollet-D'hahan, N., A simple method for the reconstitution of membrane proteins into giant unilamellar vesicles. *J. Membr. Biol.* **2010**, *233* (1-3), 85-92.
16. Sanchez, S.; Abel, A.; Marzoa, J.; Gorringer, A.; Criado, T.; Ferreira, C. M., Characterisation and immune responses to meningococcal recombinant porin complexes incorporated into liposomes. *Vaccine* **2009**, *27* (39), 5338-5343.

17. Humphries, H. E.; Williams, J. N.; Blackstone, R.; Jolley, K. A.; Yuen, H. M.; Christodoulides, M.; Heckels, J. E., Multivalent liposome-based vaccines containing different serosubtypes of PorA protein induce cross-protective bactericidal immune responses against *Neisseria meningitidis*. *Vaccine* **2006**, *24* (1), 36-44.
18. Augustyniak, D.; Mleczko, J.; Gutowicz, J., The immunogenicity of the liposome-associated outer membrane proteins (OMPs) of *Moraxella catarrhalis*. *Cell Mol. Biol. Lett.* **2010**, *15* (1), 70-89.
19. Wang, X.; Quinn, P. J., Endotoxins: lipopolysaccharides of gram-negative bacteria. *Subcell. Biochem.* **2010**, *53* (Endotoxins), 3-25.
20. Gupta, R. K.; Siber, G. R., Adjuvants for human vaccines - current status, problems and future prospects. *Vaccine* **1995**, *13* (14), 1263-76.
21. Zakirov, M. M.; Petrov, A. B.; Burkhanov, S. A.; Vartanian Iu, P.; Torchilin, V. P.; Trubetskoi, V. S.; Koshkina, N. V.; Dmitriev, B. A.; L'Vov V, L., The immunological activity of *Neisseria meningitidis* lipo-oligosaccharide incorporated into liposomes. *Zh. Mikrobiol. Epidemiol. Immunobiol.* **1995**, (1), 49-53.
22. Alving, C. R., Lipopolysaccharide, lipid A, and liposomes containing lipid A as immunologic adjuvants. *Immunobiology* **1993**, *187* (3-5), 430-46.
23. Alving, C. R.; Rao, M., Lipid A and liposomes containing lipid A as antigens and adjuvants. *Vaccine* **2008**, *26* (24), 3036-3045.
24. Ramsey, R. B.; Hamner, M. B.; Alving, B. M.; Finlayson, J. S.; Alving, C. R.; Evatt, B. L., Effects of lipid A and liposomes containing lipid A on platelet and fibrinogen production in rabbits. *Blood* **1980**, *56* (2), 307-10.

25. Richards, R. L.; Alving, C. R.; Wassef, N. M., Liposomal subunit vaccines: Effects of lipid A and aluminum hydroxide on immunogenicity. *J. Pharm. Sci.* **1996**, *85* (12), 1286-1289.
26. Richards, R. L.; Rao, M.; Wassef, N. M.; Glenn, G. M.; Rothwell, S. W.; Alving, C. R., Liposomes containing lipid A serve as an adjuvant for induction of antibody and cytotoxic T-cell responses against RTS,S malaria antigen. *Infect. Immun.* **1998**, *66* (6), 2859-2865.
27. Dijkstra, J.; Mellors, J. W.; Ryan, J. L., Altered in vivo activity of liposome-incorporated lipopolysaccharide and lipid A. *Infect. Immun.* **1989**, *57* (11), 3357-63.
28. Wassef, N. M.; Alving, C. R.; Richards, R. L., Liposomes as carriers for vaccines. *ImmunoMethods* **1994**, *4* (3), 217-22.
29. Richards, R. L.; Swartz, G. M., Jr.; Schultz, C.; Hayre, M. D.; Ward, G. S.; Ballou, W. R.; Chulay, J. D.; Hockmeyer, W. T.; Berman, S. L.; Alving, C. R., Immunogenicity of liposomal malaria sporozoite antigen in monkeys: adjuvant effects of aluminium hydroxide and non-pyrogenic liposomal lipid A. *Vaccine* **1989**, *7* (6), 506-12.
30. Stallforth, P.; Lepenies, B.; Adibekian, A.; Seeberger Peter, H., 2009, Carbohydrates: a frontier in medicinal chemistry. *J. Med. Chem.* **2009**, *52* (18), 5561-77.
31. Collins, B. S., Gram-negative outer membrane vesicles in vaccine development. *Discov. Med.* **2011**, *12* (62), 7-15.
32. Idanpaan-Heikkila, I.; Hoiby, E. A.; Chattopadhyay, P.; Airaksinen, U.; Michaelsen, T. M.; Wedege, E., Antibodies to meningococcal class 1 outer-membrane protein and its variable regions in patients with systemic meningococcal disease. *J. Med. Microbiol.* **1995**, *43* (5), 335-43.

33. Dull, P. M.; McIntosh, E. D., Meningococcal vaccine development--from glycoconjugates against MenACWY to proteins against MenB--potential for broad protection against meningococcal disease. *Vaccine* **2012**, *30 Suppl 2*, B18-25.
34. Cartwright, K.; Morris, R.; Rumke, H.; Fox, A.; Borrow, R.; Begg, N.; Richmond, P.; Poolman, J., Immunogenicity and reactogenicity in UK infants of a novel meningococcal vesicle vaccine containing multiple class 1 (PorA) outer membrane proteins. *Vaccine* **1999**, *17* (20-21), 2612-9.
35. Pace, D.; Cuschieri, P.; Galea Debono, A.; Attard-Montalto, S., Epidemiology of pathogenic *Neisseria meningitidis* serogroup B serosubtypes in Malta: Implications for introducing PorA based vaccines. *Vaccine* **2008**, *26* (47), 5952-5956.
36. Vermont, C. L.; van Dijken, H. H.; Kuipers, A. J.; van Limpt, C. J. P.; Keijzers, W. C. M.; van der Ende, A.; de Groot, R.; van Alphen, L.; van den Dobbelen, G. P. J. M., Cross-reactivity of antibodies against PorA after vaccination with a meningococcal B outer membrane vesicle vaccine. *Infect. Immun.* **2003**, *71* (4), 1650-1655.
37. Kaler, E. W.; Murthy, A. K.; Rodriguez, B. E.; Zasadzinski, J. A., Spontaneous vesicle formation in aqueous mixtures of single-tailed surfactants. *Science* **1989**, *245* (4924), 1371-4.
38. Kaler, E. W.; Murthy, A. K.; Rodriguez, B. E.; Zasadzinski, J. A., Spontaneous vesicle formation in aqueous mixtures of single-tailed surfactants. *Science* **1989**, *245* (4924), 1371-4.
39. Park, J.; Rader, L. H.; Thomas, G. B.; Danoff, E. J.; English, D. S.; DeShong, P., Carbohydrate-functionalized cationic surfactant vesicles: preparation and lectin-binding studies. *Soft Matter* **2008**, *4* (9), 1916-1921.

40. Smith, P. K.; Krohn, R. I.; Hermanson, G. T.; Mallia, A. K.; Gartner, F. H.; Provenzano, M. D.; Fujimoto, E. K.; Goeke, N. M.; Olson, B. J.; Klenk, D. C., Measurement of protein using bicinchoninic acid. *Anal. Biochem.* **1985**, *150* (1), 76-85.
41. Song, W.; Ma, L.; Chen, W.; Stein, D. C., Role of lipooligosaccharide in *opa*-independent invasion of *Neisseria gonorrhoeae* into human epithelial cells. *J. Exp. Med.* **2000**, *191* (6), 949-959.
42. Park, J.; Rader, L. H.; Thomas, G. B.; Danoff, E. J.; English, D. S.; DeShong, P., Carbohydrate-functionalized cationic surfactant vesicles: preparation and lectin-binding studies. *Soft Matter* **2008**, *4* (9), 1916-1921.
43. Chevallet, M.; Luche, S.; Rabilloud, T., Silver staining of proteins in polyacrylamide gels. *Nat. Protoc.* **2006**, *1* (4), 1852-1858.
44. Towbin, H.; Staehelin, T.; Gordon, J., Electrophoretic transfer of proteins from polyacrylamide gels to nitrocellulose sheets: procedure and some applications. *Proc. Natl. Acad. Sci.* **1979**, *76* (9), 4350-4.
45. LeVan, A.; Zimmerman, L. I.; Mahle, A. C.; Swanson, K. V.; DeShong, P.; Park, J.; Edwards, V. L.; Song, W.; Stein, D. C., Construction and characterization of a derivative of *Neisseria gonorrhoeae* strain MS11 devoid of all *opa* genes. *J. Bacteriol.* **2012**, *194* (23), 6468-6478.
46. Shevchenko, A.; Tomas, H.; Havlis, J.; Olsen, J. V.; Mann, M., In-gel digestion for mass spectrometric characterization of proteins and proteomes. *Nat. Protoc.* **2006**, *1* (6), 2856-2860.
47. Choksawangkarn, W.; Kim, S.-K.; Cannon Joe, R.; Edwards Nathan, J.; Lee Sang, B.; Fenselau, C., Enrichment of plasma membrane proteins using nanoparticle

pellicles: comparison between silica and higher density nanoparticles. *J. Proteom. Res.*  
**2013.**

## Chapter 5: Drug Delivery Applications for Catanionic Surfactant Vesicles

### *5.1 Introduction*

#### *5.1.1 Liposomes in Drug Formulation*

Liposomes were first loaded with biologically active substances in the early 1970's with the aim of using them as enzyme carriers in enzyme replacement therapy.<sup>1</sup> Since then, liposomal drugs have been approved by the Food and Drug Administration for clinical use, these approved drug products include Doxil and Myocet.<sup>2-6</sup> Both drugs are liposomal formulations of the drug doxorubicin HCl (Figure 5.1, A), where the drug is encapsulated inside of liposomes. In the case of Doxil, the surface of the liposome is coated with poly(ethylene glycol) (PEG), which acts as a protective coating to prevent clearance from the body (Figure 5.1, B). Daunorubicin (DaunoXome) is another example of a liposomal drug delivery system used in the treatment of breast cancer and lung cancer.<sup>4</sup>

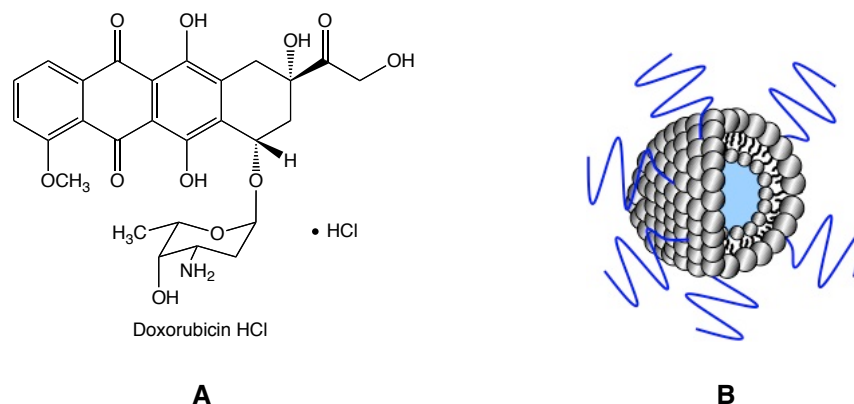


**Figure 5.1.** A) Chemical structure of doxorubicin. B) PEGylated liposomes provide a lipophilic barrier on the exterior of liposomes.

All of these liposomal formulations are used to increase drug solubility, circulation time in the body, and decrease toxicity. More importantly, drug efficacy is usually improved since a higher concentration of the drug can be loaded into liposomes, which will cause fewer side effects. For example, free doxorubicin drug causes cardiotoxicity in patients.<sup>7</sup> However, liposomal formulations containing doxorubicin penetrate malignant tissue better while decreasing cardiotoxicity due to the reducing cardiac exposure to doxorubicin.<sup>7</sup> Since the use of liposomes in drug delivery, additional liposomal formulations are being considered. Many of these liposomal formulations have already been approved for clinical use (Table 5.1).<sup>3, 4, 8</sup> Targeting agents have also been added to liposomes including carbohydrates, antibodies, folate, and peptides in order to direct the liposomal carrier to a specific tissue.<sup>8-11</sup>

<b>Drug Name</b>	<b>Formulation</b>	<b>Status</b>
<b>Doxil</b>	PEGylated liposomal doxorubicin	Approved
<b>DaunoXome</b>	Liposomal daunorubicin	Approved
<b>Myocet</b>	Liposomal doxorubicin	Approved
<b>MCC-465</b>	PEGylated liposomal doxorubicin containing antibody targeting agent	Phase 1
<b>Ambisome</b>	Liposomal amphotericin B	Approved
<b>DepoCyt</b>	Liposomal cytosine arabinoside	Approved
<b>Visudyne</b>	Liposomal verteporfin	Approved

**Table 5.1.** Liposomal formulations of drug delivery vehicles adapted from ref. 9, 12.

While liposomes are readily used in commercial drug applications, cationic surfactant vesicles have yet to be utilized in the clinic as drug carriers. In Chapters 3 and 4, we showed that cationic vesicles were loaded and characterized accordingly and could be used toward vaccine development. Furthermore, cationic vesicles were not toxic to animals when tested as vaccines by delivery vesicle intravenously or intraperitoneally. We are interested in extending the role of cationic vesicle systems for drug delivery applications in order to provide an alternative to their liposomal counterparts. As mentioned before, cationic vesicles can be easily prepared, are stable for years, and can be sterilized by autoclaving. Furthermore, cationic vesicles can be functionalized, allowing the ability for targeted drug delivery of a payload to specific

tissues. Toward this goal, we studied cationic vesicles loaded with the drug candidates doxorubicin, lutein, maytansine, and paclitaxel. As for targeted delivery applications, we studied the cytotoxicity of doxorubicin-loaded cationic vesicles functionalized with a targeting agent.

## 5.2 Results and Discussion

In order for cationic vesicles to be used in drug delivery, their loading efficiency and toxicity were studied. In addition, drug loaded cationic vesicles were functionalized with targeting agents toward cell lines that over express the receptor specific to the targeting agent. Cell toxicity was compared between targeted and untargeted cationic vesicles in order to determine if targeting increased drug uptake into cells (Figure 5.2).

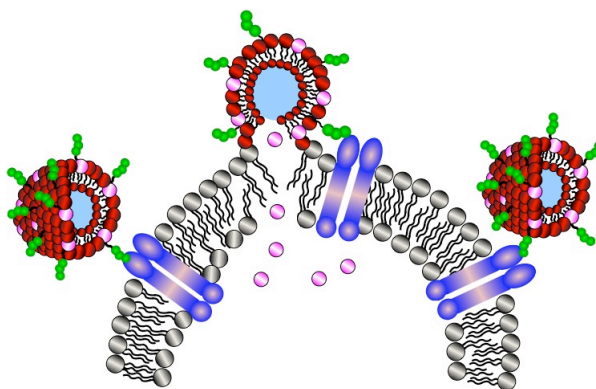


**Figure 5.2.** Targeting of cationic surfactant vesicles to cells.

### 5.2.1 Doxorubicin Loaded Cationic Surfactant Vesicles

Cationic surfactant vesicles were loaded with the drug doxorubicin in order to determine the retention of the drug over time. Vesicles were loaded with 19  $\mu\text{g/mL}$

doxorubicin (33  $\mu\text{M}$ ) and an aliquot of the vesicle stock suspension was purified by SEC each day over 15 days. Vesicles were  $140 \pm 10$  nm in diameter and their size did not change over the 15 day timeframe, as determined by DLS. These results indicated that cationic vesicles loaded with doxorubicin are larger in size when compared to unloaded vesicles ( $\sim 120$  nm) and remained stable over time.

Vesicle-containing fractions from each day were disrupted with ethanol and analyzed by UV/VIS. Cationic vesicle fractions purified on different days all showed complete retention of doxorubicin (Figure 5.3). These results indicated that doxorubicin was loaded into cationic vesicles and that these systems did not leak drug over time.

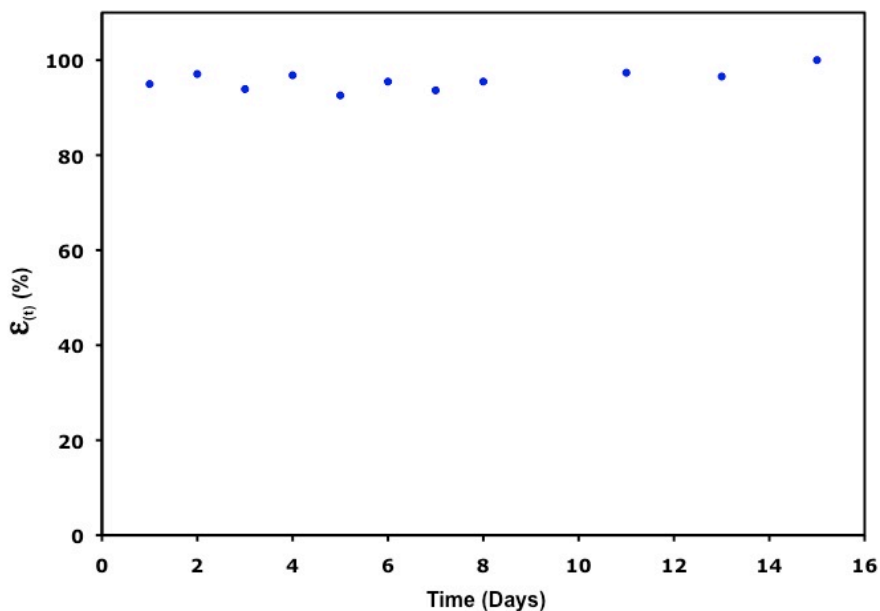


**Figure 5.3.** Retention of doxorubicin over fifteen days in cationic surfactant vesicles. Concentration of doxorubicin vesicle stock solution was 33  $\mu\text{M}$ . After purification by SEC, vesicle-containing fractions contained  $\sim 23$   $\mu\text{M}$  of the drug.

Since vesicles were proven to incorporate and retain doxorubicin at low concentrations, we wanted to determine the maximum loading of drug in vesicles.

Catanionic vesicle stock solutions were prepared containing 100 µg/mL (172 µM), 150 µg/mL (259 µM), 200 µg/mL (345 µM), and 300 µg/mL (517 µM) of doxorubicin. When using high concentration stock solutions of doxorubicin (200 µg/mL and 300 µg/mL), vesicles were formed but a red precipitate was observed. Catanionic vesicles containing these concentrations were centrifuged and the precipitate was removed. Suspensions were purified by SEC and vesicle containing fractions eventually formed a red precipitate. These result indicated that doxorubicin gradually leaked out of vesicles. If full retention of the drug is required, catanionic vesicles cannot be loaded with > 200 µg/mL (345 µM) of doxorubicin, where a typical clinical dose of doxorubicin is 40-60 mg/m<sup>2</sup>.

Vesicles prepared with 100 µg/mL and 150 µg/mL doxorubicin stock solutions were stable over an extended period and did not precipitate drug, even after purification by SEC (Table 5.2). These results showed that vesicles could be initially loaded with a maximum of 150 µg/mL of doxorubicin and after SEC contained 88 µg/mL of doxorubicin.

<b>Initial Concentration</b>	<b>Concentration after SEC</b>	
( $\mu\text{g/mL}$ )	( $\mu\text{g/mL}$ )	( $\mu\text{M}$ )
100	75	138
150	88	161
200	165	303
300	131	241

**Table 5.2.** Amount of doxorubicin in vesicles from increasing concentrations.

After determining the maximum loading of doxorubicin into cationic vesicles, we were interested in studying the toxicity of these drug formulations. As a benchmark for toxicity in humans, a typical dose of doxorubicin is 40-60 mg/m<sup>2</sup>. For a typical person, this amount equates to a total dose of ~150-200 mg of doxorubicin. The dose limiting toxicity (DLT) for doxorubicin is myelosuppression where nausea, vomiting, cardiotoxicity, and alopecia are other side effects. In order to determine toxicity of doxorubicin loaded cationic vesicles compared to the free drug, cationic vesicles were loaded with doxorubicin and exposed to several different human cancer cell lines. The WST-1 cell proliferation assay was used to measure the cytotoxic effects of cationic vesicles. All toxicity studies were performed by the Translational Laboratory Shared Service (TLSS) personnel under the direction of Dr. Rena Lapidus at the University of Maryland School of Medicine Greenebaum Cancer Center.

The cytotoxicity of cationic vesicles was initially studied in the human hepatocellular carcinoma cell line HepG2. These cells exhibit many of the characteristics

of normal liver cells. Since many drugs are toxic to the liver, these cell lines are used for screening the cytotoxicity of new drugs. HepG2 cells were used to study doxorubicin loaded cationic vesicles to determine if the toxicity of the drug in vesicles was less than free drug. The assay is based on the enzymatic cleavage of the tetrazolium salt of the WST-1 reagent to formazan by cellular mitochondrial dehydrogenases in living viable metabolically active cells. The formazan product absorbs at 450 nm in a spectrophotometer. In this assay, mitochondrial enzymes of living cells break down the WST-1 dye (formazan derivative) so that the break-down product absorbs at a wavelength of 450 nm. In other words, when cells are proliferating, formazan dye accumulates and the OD increases and when cells are not proliferating, the OD decreases..

Results of toxicity studies in HepG2 cells yielded an  $IC_{50}$  of 51  $\mu\text{g}/\text{mL}$  for DOX-loaded vesicles and an  $IC_{50}$  of 0.16  $\mu\text{g}/\text{mL}$  for free DOX (Figures 5.4 and 5.5). These results indicated a 300-fold reduction in doxorubicin's  $IC_{50}$  values compared to free drug. Therefore, the toxicity of doxorubicin is greatly reduced when loaded into cationic vesicles.

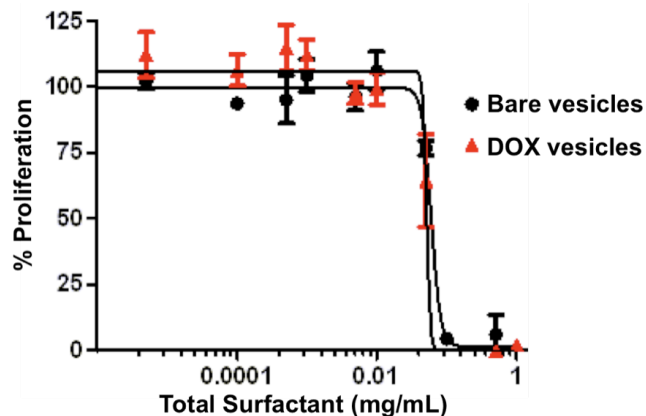


**Figure 5.4.** WST-1 cell proliferation assay on HepG2 cells treated with bare vesicles and doxorubicin loaded vesicles. Cells were treated for 72 h. Bare vesicles  $IC_{50} = 58 \mu\text{g/mL}$  and doxorubicin vesicles  $IC_{50} = 51 \mu\text{g/mL}$ . Studies were performed by TLSS at UMB.

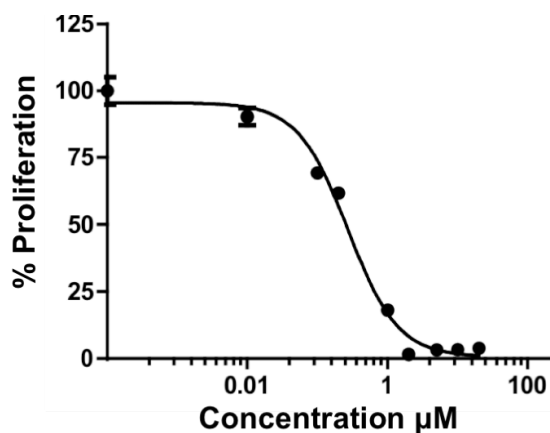


**Figure 5.5.** WST-1 cell proliferation assay on HepG2 cells treated with doxorubicin. Free drug was incubated with cells for 72 h.  $IC_{50} = 0.16 \mu\text{g/mL}$ . Toxicity studies performed by TLSS at UMB.

Next, we wanted to determine the toxicity of bare vesicles (unloaded vesicles) in HepG2 cells. The  $IC_{50}$  of bare cationic vesicles was  $58 \mu\text{g/mL}$  (Figure 5.4). This  $IC_{50}$  value indicated that bare and DOX-loaded cationic vesicles have the same cytotoxicity. Therefore, the toxicity of DOX-loaded vesicles resulted from the cationic vesicles themselves and not from DOX (Figure 5.6).

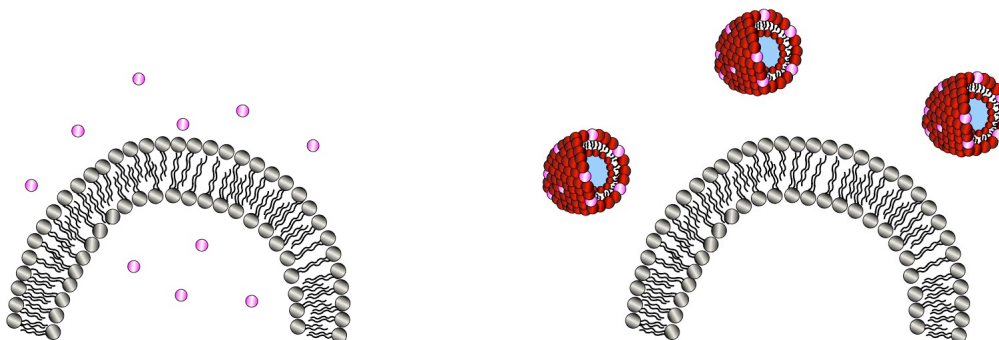


**Figure 5.6.** Free doxorubicin compared to doxorubicin loaded catanionic vesicles incubated with normal cells.

### 5.2.2 Targeted Doxorubicin Loaded Catanionic Surfactant Vesicles

Since DOX-loaded and unloaded catanionic vesicles have similar toxicity in the HepG2 cells, we wanted to study these systems with the addition of a targeting moiety. We studied targeted DOX-loaded catanionic vesicles to determine if toxicity increased as a result of uptake into cells via targeting agent-receptor binding (Figure 5.7).

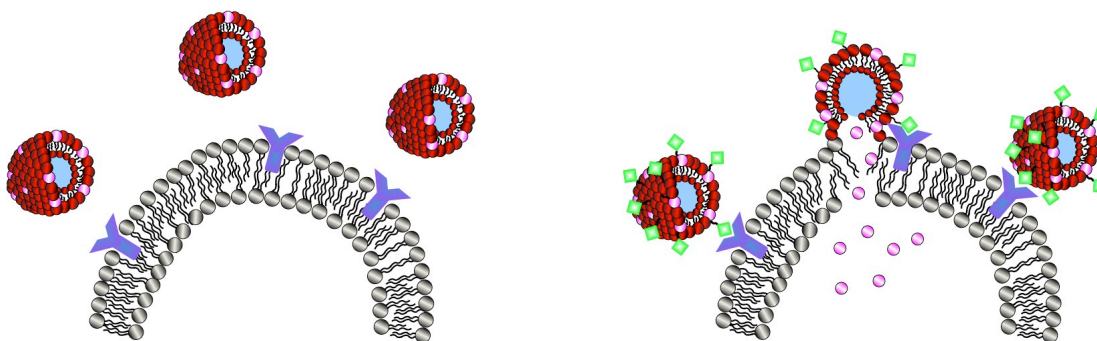


**Figure 5.7.** Doxorubicin loaded untargeted and targeted catanionic vesicles incubated with normal cells vs. cells that over express a receptor.

DOX-loaded catanionic vesicles were functionalized with C<sub>12</sub>-folate conjugate (Figure 5.8). Cytotoxicity of targeted DOX-loaded vesicles was determined in two different cell lines. Cells were grown in folate-depleted media so that the folate in the

media did not compete with the folate-targeting moiety on vesicles. A549 cells were chosen for initial studies because they have very low levels of the folate receptor. Cytotoxicity  $IC_{50}$  values of targeted unloaded vesicles and targeted-DOX vesicles in HepG2 cells were 7.2  $\mu\text{g/mL}$  and 5.6  $\mu\text{g/mL}$ , respectively (Figure 5.9). Therefore, both targeted-unloaded and targeted DOX-loaded vesicles had similar toxicities.

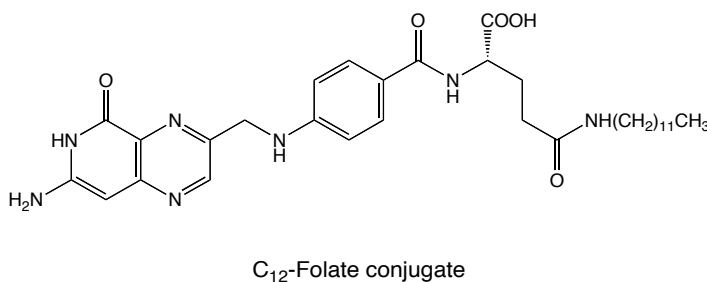


**Figure 5.8.** Chemical structure of  $C_{12}$ -folate conjugate.

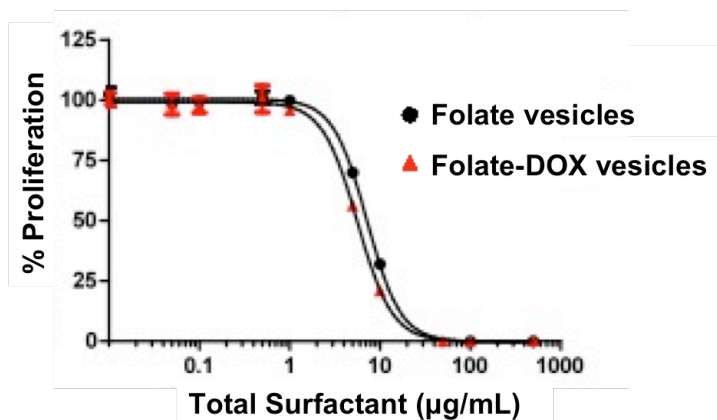


**Figure 5.9.** WST-1 cell proliferation assay on A549 cells treated with folate targeted cationic vesicles. Cells were treated for 72 h. Folate vesicles  $IC_{50} = 7.2 \mu\text{g/mL}$ , Folate-DOX vesicles  $IC_{50} = 5.6 \mu\text{g/mL}$ . Toxicity studies performed by TLSS at UMB.

Next, we wanted to determine the cytotoxicity of these systems when incubated in IGROV-1 cells. These cells were chosen because they highly express the folate receptor. Cytotoxicity  $IC_{50}$  values of targeted unloaded vesicles and targeted-DOX vesicles were

3.4  $\mu\text{g/mL}$  and 2.2  $\mu\text{g/mL}$ , respectively (Figure 5.10). These results indicated that targeted vesicles were not more toxic when incubated with cells that over express the specific receptor.

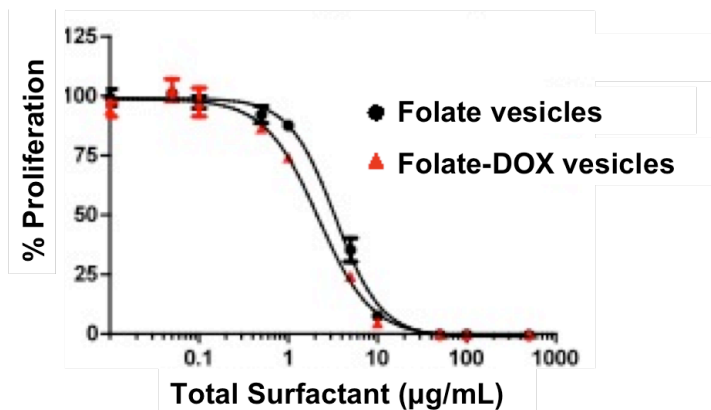


**Figure 5.10.** WST-1 cell proliferation assay on ovarian IGROV-1 cells, which over express folate, treated with folate targeted cationic vesicles. Cells were treated for 72 h. Folate vesicles  $\text{IC}_{50} = 3.4 \mu\text{g/mL}$ , Folate-DOX vesicles  $\text{IC}_{50} = 2.2 \mu\text{g/mL}$ . Toxicity studies performed by TLSS at UMB.

Results from toxicity studies with cationic vesicles did not show increased toxicity of targeted cationic vesicles. However, there could be several explanations as to why toxicity did not increase: 1) cationic vesicles were not loaded with enough targeting agent or 2) cationic vesicles were not taken up by cells. In order to study the latter possibility, future work will be devoted to determine whether cationic vesicles enter cells. Cationic vesicles will be loaded with a dye and functionalized with a targeting agent. Fluorescently labeled cationic vesicles will be incubated with cells and studied by microscopy to observe the rate at which cationic vesicles with and without a targeting agent are endocytosed by cells (Figure 5.11).

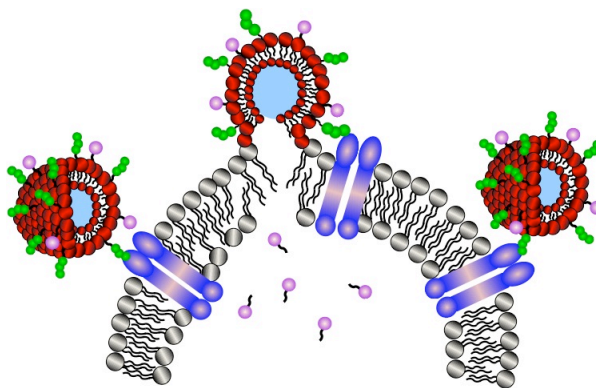


**Figure 5.11.** Fluorescently-labeled vesicles binding with cells.

### 5.2.3 *Lutein Loaded Catanionic Surfactant Vesicles*

Incorporation of the carotenoid lutein (Figure 5.12) into cationic surfactant vesicles was studied for potential use in vesicle-based eye drops for the treatment of eye diseases. The carotenoid lutein is believed to play a role in the prevention of age-related macular degeneration because of its presence in the neural retina of the human eye.<sup>41</sup> Unfortunately, lutein is very insoluble in aqueous solvents used in eye drops and is only soluble in organic solvents (i.e. methylene chloride). Due to the soft nature of cationic vesicles, these systems offer a convenient way to incorporate carotenoids into vesicles for eye drop technology. Lutein was expected to insert into the vesicle bilayer of cationic vesicles similar to their insertion into liposomes (Figure 5.14).<sup>42</sup> Delivery of lutein directly to the eye may aid in the prevention and treatment of macrodegenerative eye diseases.

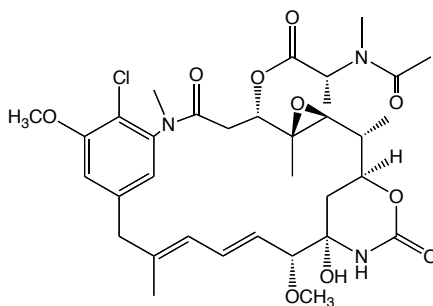


disrupted and released the lutein, which is sparingly soluble in ethanol and water. Therefore, the amount of lutein in cationic vesicles could not be quantitatively determined due to the insolubility of lutein after vesicle disruption. These studies will be continued with disruption of vesicles with other solvents that also solubilize lutein. For example, we have shown that cationic vesicles can be disrupted by THF and lutein is highly soluble in THF. Therefore, after disruption of vesicle-containing fractions with THF, the absorbance will be measured by UV/VIS to determine the amount of lutein incorporated into cationic vesicles.

#### *5.2.4 Maytansine Loaded Cationic Surfactant Vesicles*

Maytansine is an extremely toxic drug that is insoluble in water and most solvents (Figure 5.14). Cationic vesicles were loaded with the neutral hydrophobic drug maytansine in the hope that the drug could be solubilized and incorporated for drug delivery. Maytansine was solubilized in THF and then added during vesicle formation. This solubilization was required in order for maytansine to dissolve so that the drug could be incorporated into cationic vesicles. Vesicles had a hydrodynamic radius of  $126 \pm 3$  nm and were purified by SEC. All fractions were disrupted with ethanol and measured by UV/VIS. Unfortunately, maytansine does not contain a good chromophore (Figure 5.14). Maytansine has an absorbance at 290 nm, which is close to the absorbance of the surfactants used in our cationic vesicles. UV/VIS of the vesicle-containing fraction showed a peak at 290 nm and was compared to bare vesicle containing fractions (Figure 4.15). It was difficult to quantitatively determine incorporation of the drug since the absorbance of maytansine and the surfactants absorb light in the same region. For this

reason, a drug should be modified with a fluorescent tag so that incorporation into vesicles can be determined.



Maytansine

**Figure 5.14.** Chemical structure of maytansine.

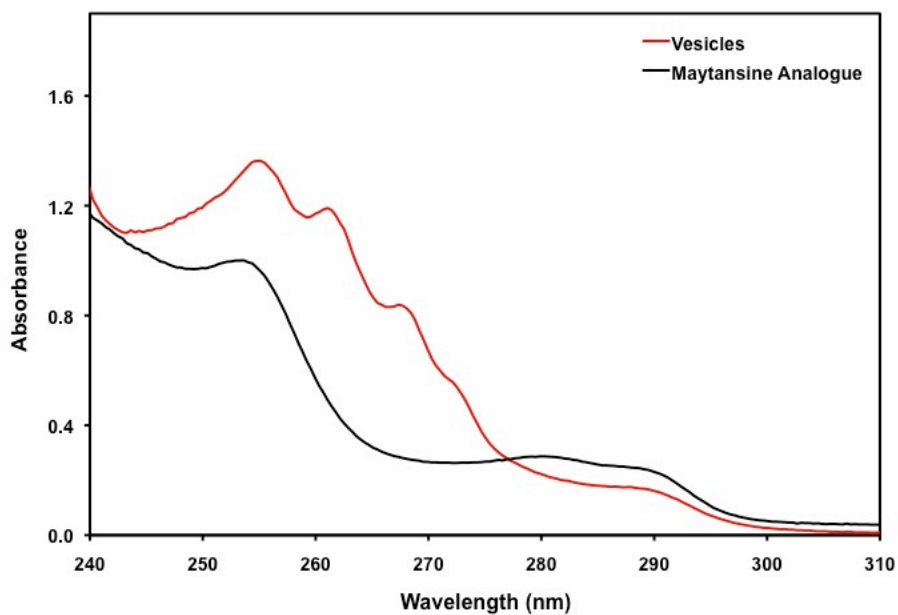
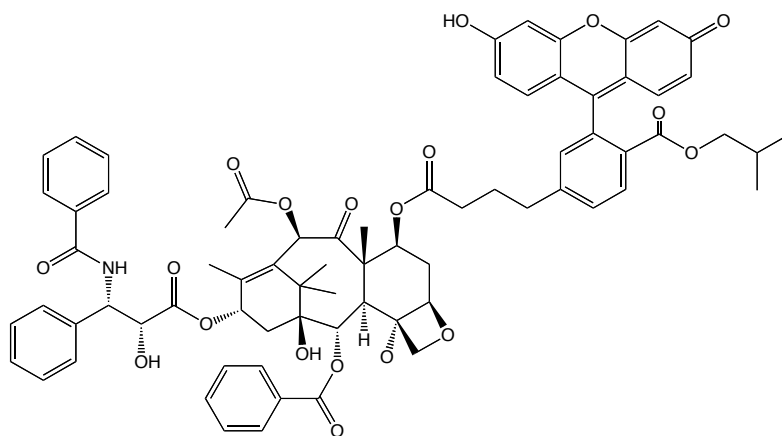


**Figure 5.15.** Absorbance of a maytansine analogue and maytansine loaded vesicle fraction from SEC. The maytansine analogue absorbs light at 290 nm.

### 5.2.5 Paclitaxel Loaded Catanionic Surfactant Vesicles

Since the lack of a chromophore made it difficult to characterize its loading in cationic vesicles, vesicles were loaded with a drug containing a fluorescent label. Paclitaxel fluorescein derivative (Figure 5.16) was added to vesicles prepared with dry surfactants and water. These vesicles formed but did not yield yellow suspensions. Due to the insolubility of paclitaxel, the drug was not incorporated during vesicle formation. Therefore, a solution of SDBS was used to solubilize paclitaxel by incorporating the drug into the hydrophobic region of micelles. Then, solid CTAT was added, and yellow cationic vesicles formed. After purification by SEC, vesicle-containing fractions remained yellow in color. These results indicated the presence of paclitaxel within cationic vesicles, likely by the initial incorporation of the drug into micelles followed by incorporation into the bilayer leaflet after the addition of the second surfactant. Fractions were disrupted with ethanol and their absorbance was measured at 445 nm. Results of UV/VIS show that paclitaxel conjugate was successfully incorporated in vesicles (Figure 5.17).



Paclitaxel fluorescein derivative

**Figure 5.16.** Chemical structure of paclitaxel fluorescein derivative.

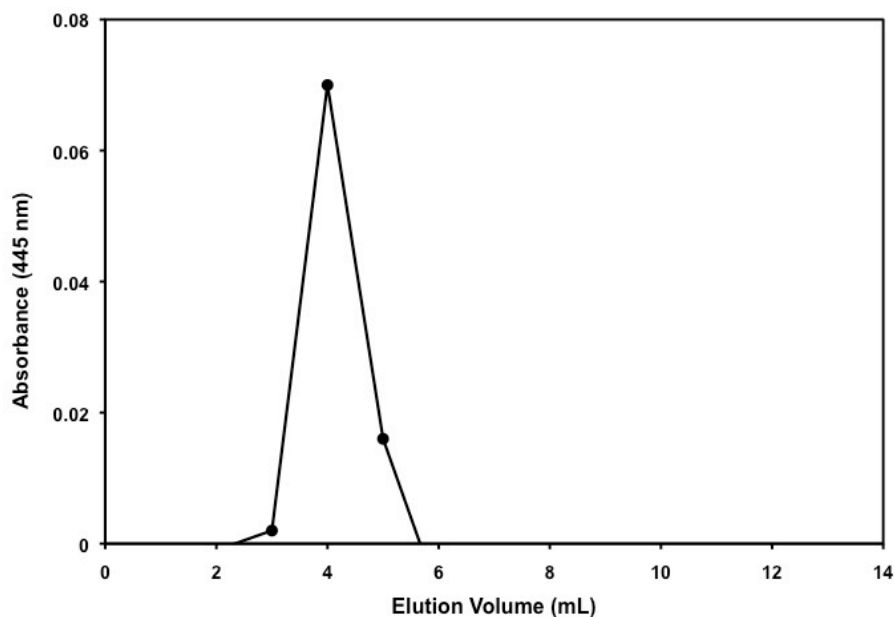


**Figure 5.17.** Absorbance of paclitaxel loaded vesicles at 445 nm. After purification by SEC, vesicle-containing fractions contained 0.9  $\mu\text{M}$  of drug.

### 5.3 Conclusions

Cationic vesicles can be loaded with drug molecules and functionalized with targeting agents. Cationic vesicles loaded with doxorubicin showed low toxicity in the presence of normal liver cells. Cationic vesicles could be used for drug delivery of doxorubicin similar to the liposomal formulation Doxil. Targeted cationic vesicles did not increase toxicity of drug-loaded vesicles, but further studies will be performed in order to increase the targeting agent and to determine whether cationic vesicles are incorporated into cells. We have also shown incorporation of other drugs into cationic vesicles. Fluorescently labeled drugs allow for better characterization in cationic vesicles.

## 5.4 *Experimental*

Cell studies and animal work were preformed by the Translational Laboratory Shared Service (TLSS) personnel under the direction of Dr. Rena Lapidus at the University of Maryland School of Medicine Greenebaum Cancer Center.

### 5.4.1 *Doxorubicin*

To prepare doxorubicin-loaded vesicles for release studies, an aqueous solution of 33  $\mu\text{M}$  doxorubicin (Figure 5.1, A) was prepared. To increase solubility of doxorubicin, the solution was sonicated in a water bath until full dissolution. Then, 70.0 mg of SDBS (0.200 mmol) and 30.0 mg of CTAT (0.0658 mmol) was weighed into the vial followed by the addition of 9.90 mL of the doxorubicin solution and stirring for 60 min. Vesicles were purified from free drug by SEC and analyzed by UV/VIS. A 0.5 mL portion of each vesicle fraction was transferred to an empty vial where 0.5 mL absolute ethanol was added to the sample to prevent light scattering during absorption measurements. The samples were vortexed and the absorbance was measured at 480 nm.

Doxorubicin-loaded vesicles for toxicity studies were carried out under sterile conditions using aseptic technique in a biosafety cabinet. All vials were autoclaved and all buffer solutions were initially sterile or were sterilized by filtration through a 0.2  $\mu\text{m}$  filter. Vesicle solutions were prepared using phosphate-buffered saline (PBS) 1X buffer. First, the PBS 1X was degassed *in vacuo* for 15-20 min. Then 172  $\mu\text{M}$ , 259  $\mu\text{M}$ , 345  $\mu\text{M}$ , and 517  $\mu\text{M}$  solutions of doxorubicin were prepared with the sterile degassed PBS 1X. Then, 70.0 mg of SDBS (0.200 mmol) and 30.0 mg of CTAT (0.0658 mmol) was weighed into a sterile vial followed by the addition of 9.90 mL of the doxorubicin

solution and stirring for 60 min. For doxorubicin-folate vesicles, 1 mg of C<sub>12</sub>-folate amide was prepared by Dr. Matthew Hurley and was added to the vesicle suspension and stirred overnight. Vesicles were purified from free drug by SEC using degassed PBS 1X as the elution buffer.

#### 5.4.2 *Lutein*

Lutein was recrystallized from dichloromethane/hexanes and was obtained from Dr. Frederick Khachik at the University of Maryland. The purity was checked by UV/VIS absorbance at 446 nm. Lutein was weighed directly into a vial containing SDBS and CTAT. During vesicle formation, the suspension was sonicated every 10 min for 30 s. The sample was purified by SEC. Vesicle-containing fractions were cloudy and appeared yellow in color.

#### 5.4.3 *Maytansine*

To prepare maytansine vesicles, maytansine was dissolved in THF (5.1 mg/ mL) and was obtained from ImmunoGen, Inc. A 196  $\mu$ L (1.00 mg) aliquot of the solution was added to a vial containing 70.0 mg of SDBS (0.200 mmol) and 30.0 mg of CTAT (0.0658 mmol). Then, 9.90 mL of water was added and stirred for 60 min. Vesicles were purified from free drug by SEC and analyzed by UV/VIS. A 0.5 mL portion of each vesicle fraction was transferred to an empty vial where 0.5 mL absolute ethanol was added to the sample to prevent light scattering during absorption measurements. The samples were vortexed and the absorbance was measured at 290 nm.

#### 5.4.4 *Paclitaxel*

To prepare paclitaxel vesicles, 0.5 mg of paclitaxel was dissolved in 9.90 mL (0.200 mmol) of an SDBS solution (7.07 mg/mL), which was obtained from Dr. Iwao Ojima at SUNY, Stony Brook. The solution was stirred for 60 min. Then 30.0 mg of CTAT (0.0658 mmol) was added and stirred for 60 min. Vesicles were purified from free drug by SEC and analyzed by UV/VIS. A 0.5 mL portion of each vesicle fraction was transferred to an empty vial where 0.5 mL absolute ethanol was added to the sample to prevent light scattering during absorption measurements. The samples were vortexed and the absorbance was measured at 445 nm.

#### 5.4.5 *Addendum*

Targeted vesicles were added to A549 and IGROV-1 cells and cell proliferation was followed over 102 h. Figure A.2.23 shows that folate overexpressed cells (IGROV-1) are much more sensitive to folate vesicles than A549 cells. The effect of folate-empty and folate –doxorubicin vesicles were equal in both cell lines. This data suggests that folate-targeting of vesicles is successful when incubated with cells that overexpress the corresponding receptor. Therefore, the previously reported  $IC_{50}$  values of folate-doxorubicin vesicles should be measured at different incubation times in order to determine a difference between targeted and untargeted vesicles.

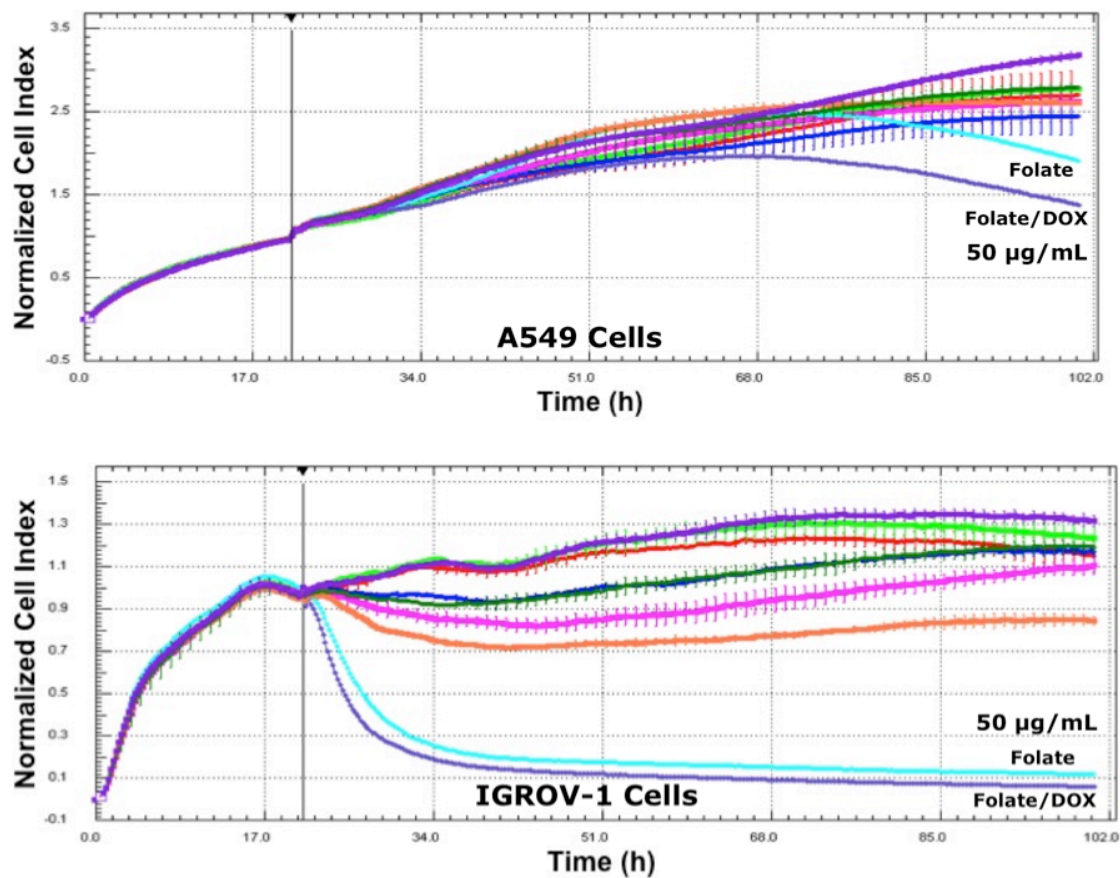


**Figure 5.18.** Time dependence of A549 and IGROV-1 cells in the presence of targeted cationic vesicles. When 50  $\mu\text{g/mL}$  of folate-targeted vesicles were added to A549 cells, the cells continued to proliferate. When 50  $\mu\text{g/mL}$  of DOX-folate-targeted vesicles were added to IGROV-1 cells, the cells no longer proliferated after 19 h.

## References

1. Gregoriadis, G.; Leathwood, P. D.; Ryman, B. E., Enzyme entrapment in liposomes. *FEBS Letters* **1971**, *14* (2), 95-9.
2. Barratt, G., Colloidal drug carriers: Achievements and perspectives. *Cell. Mol. Life Sci.* **2003**, *60* (1), 21-37.
3. Lasic, D. D., Novel applications of liposomes. *Trends Biotechnol.* **1998**, *16* (7), 307-321.
4. Samad, A.; Sultana, Y.; Aqil, M., Liposomal drug delivery systems: an update review. *Curr. Drug Deliv.* **2007**, *4* (4), 297-305.
5. Working, P. K.; Newman, M. S.; Huang, S. K.; Mayhew, E.; Vaage, J.; Lasic, D. D., Pharmacokinetics, biodistribution and therapeutic efficacy of doxorubicin encapsulated in Stealth liposomes (Doxil). *J. Liposome Res.* **1994**, 667-87.
6. Forssen, E. A.; Ross, M. E., Daunoxome treatment of solid tumors: Preclinical and clinical investigations. *J. Liposome Res.* **1994**, 481-512.
7. Kingsley Jeffrey, D.; Dou, H.; Morehead, J.; Rabinow, B.; Gendelman Howard, E.; Destache Christopher, J., Nanotechnology: a focus on nanoparticles as a drug delivery system. *J. Neuroimmune Pharmacol.* **2006**, *1* (3), 340-50.
8. Torchilin, V. P., Recent advances with liposomes as pharmaceutical carriers. *Nat. Rev. Drug Disc.* **2005**, *4* (2), 145-160.

9. Cheng, Z.; Al Zaki, A.; Hui, J. Z.; Muzykantov, V. R.; Tsourkas, A., Multifunctional nanoparticles: Cost versus benefit of adding targeting and imaging capabilities. *Science* **2012**, *338* (6109), 903-910.
10. Zhu, J.; Xue, J.; Guo, Z.; Zhang, L.; Marchant, R. E., Biomimetic glycoliposomes as nanocarriers for targeting P-selectin on activated platelets. *Bioconjugate Chem.* **2007**, *18* (5), 1366-1369.
11. Zhu, J.; Yan, F.; Guo, Z.; Marchant, R. E., Surface modification of liposomes by saccharides: Vesicle size and stability of lactosyl liposomes studied by photon correlation spectroscopy. *J. Colloid Interface Sci.* **2005**, *289* (2), 542-550.
12. Faraji, A. H.; Wipf, P., Nanoparticles in cellular drug delivery. *Bioorg. Med. Chem.* **2009**, *17* (8), 2950-2962.

# Appendix I: Chemistry Performed at the Surface of Cationic Surfactant Vesicles

## A.1 Introduction

Surfactants are often used as solubilizing agents for hydrophobic molecules by incorporation of molecules within the hydrophobic cavity of micelles.<sup>1</sup> Furthermore, surfactants have been utilized for chemical reactions between hydrophobic molecules in aqueous solvents. In such systems, reagents associate in the internal hydrophobic region of a micelle, causing close interactions between the reactive species. In addition, colloidal surfactant solutions are also used to increase the rate of these reactions by forcing molecules into close proximity.<sup>2</sup>

Others have proposed using surfactant molecules to perform “green chemistry” in which the solvent used is water. Such systems would replace the copious amounts of organic solvents used each year.<sup>3-7</sup> Well-known reactions, such as Suzuki–Miyaura coupling, ring closing metathesis, and Stille coupling have achieved success within micelles.<sup>4, 5, 7</sup>

Surfactants are also used as stabilizing agents in aqueous solvents for molecules that are reactive with water. For example, curcumin normally undergoes alkaline hydrolysis in water (Figure A.1, A). Wang *et al.* reported incorporation of curcumin into micelles, which stabilized curcumin enough to determine the  $pK_a$  of phenolic protons.<sup>8</sup> This indicated that the hydrophobic portion is associated with surfactant tails and the phenolic protons protrude from the micelle and are accessible for titration with base (Figure A.1, B).

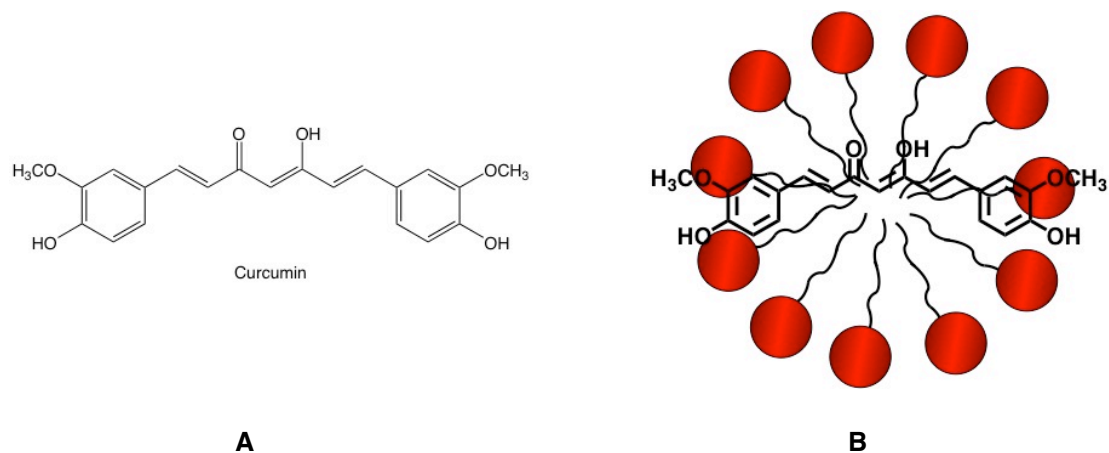
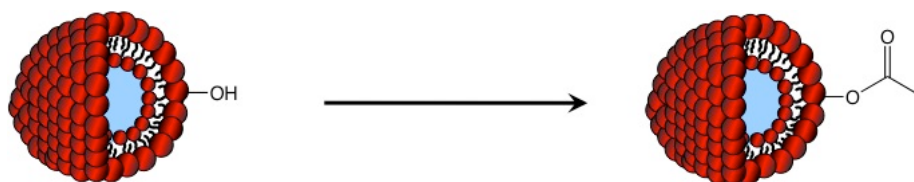


**Figure A.1.** Chemical structure of curcumin and orientation in micelles. The keto-enol form of curcumin is depicted above.

Based on the understanding of how micelles solubilize hydrophobic molecules, we anticipated that chemistry could be performed using cationic surfactant vesicles to selectively add or remove specific functional groups to molecules loaded in vesicles (Scheme A.1). Rather than chemistry occurring within the aqueous internal compartment of vesicles, molecules associated with the lipid bilayer would undergo chemistry on the portions protruding from the vesicle surface. The advantage of using cationic vesicle systems rather than micelle forming surfactant mixtures is their robust nature. Therefore, cationic vesicles provide another “green chemistry” alternative approach to synthetic routes. Furthermore, this work treats cationic surfactant vesicles as protecting groups, where reactions could only take place on the portion of the molecule sticking out of the vesicles, leaving embedded functional groups untouched (Figure A.2).



**Scheme A.1.** Chemistry at the surface of cationic surfactant vesicles.

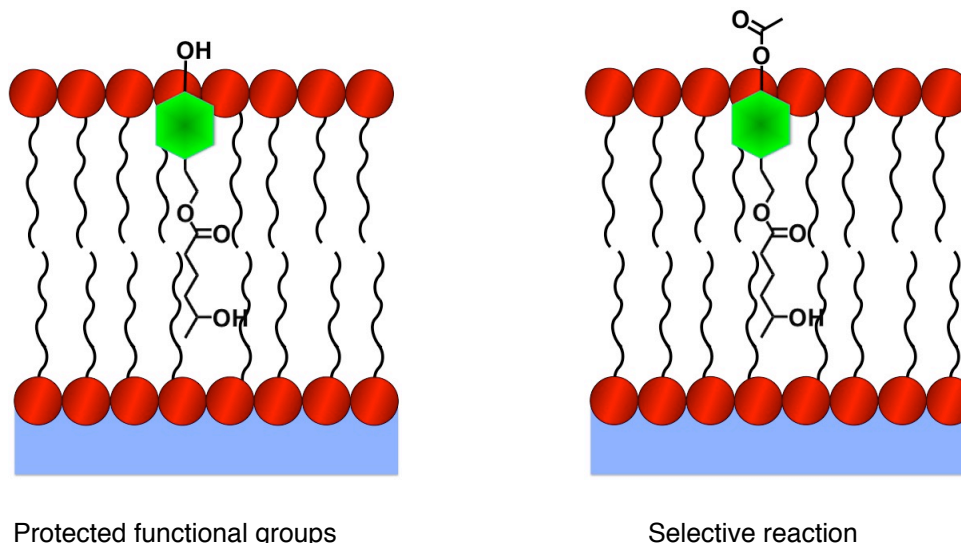


**Figure A.2.** Catanionic vesicles as protecting groups.

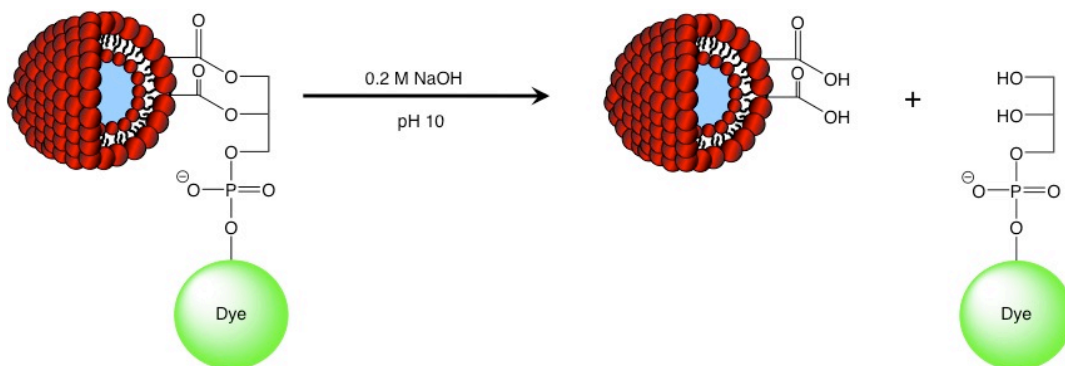
The purpose of this study was 1) to perform base hydrolysis on a lipid dye loaded in cationic surfactant vesicles and 2) to study acid-base equilibrium reactions with chemical indicators loaded in vesicles.

## *A.2 Results and Discussion*

### *A.2.1 Hydrolysis of Carboxyfluorescein-Lipid Dye from SDBS-rich Vesicles*

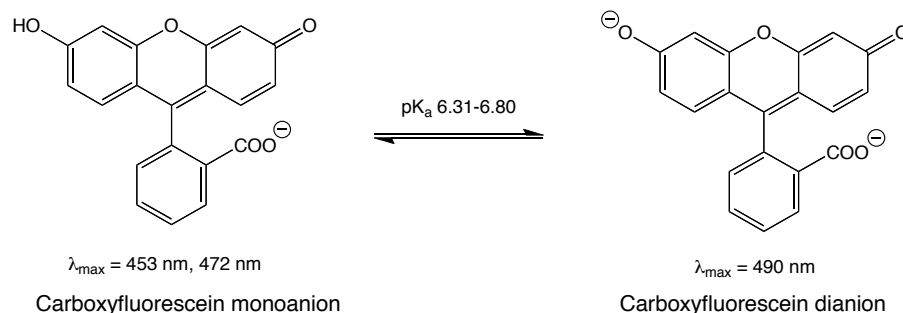
The cleavage of lipid-dye conjugates embedded in vesicles with NaOH was tested in order to show the promise of performing chemistry at the surface of intact cationic vesicles (Scheme A.2). SDBS-rich vesicles were loaded with the fluorescent dye carboxyfluorescein (CF) containing a phospholipid moiety. An anionic dye was specifically chosen for use in SDBS-rich vesicles to prevent electrostatic interactions

between the charged vesicle surface and free charged dye following phospholipid cleavage.



**Scheme A.2.** Hydrolysis reaction of CF-lipid in cationic vesicles via NaOH. Addition of NaOH cleaves the two phospholipid ester groups, freeing the chromophore from the lipid that remained associated with the vesicles.

After purification of CF-lipid vesicles by SEC, vesicle-containing fractions were separated into two aliquots: one serving as the control for unreacted dye and the second for monitoring the hydrolysis reaction. NaOH was added to the vesicle sample until the pH reached 10. Immediately after the addition of base, the vesicle solution turned pink in color, which is consistent with the dianion form of CF (Scheme A.3). After 24 h, vesicles were neutralized with HCl, where the colloidal solution returned yellow. This color change indicated the reversible deprotonation of the phenolic proton under basic conditions (Scheme A.3).



**Scheme A.3.** CF monoanion and dianion chemical structures. The neutral and monoanion are both yellow in color, while the dianion is pink. The absorbance of the monoanion is less intense and is blue-shifted relative to the dianion.

Both unreacted and reacted samples were purified a second time by SEC to separate any hydrolyzed dye from vesicles. The absorbance of all SEC fractions was measured by UV-VIS. For reacted vesicles, the chromophore was present in later fractions (Figure A.3). This result indicated that CF-lipid dye was cleaved from the surface of vesicles, as predicted (Scheme A.2). The same sample also showed the presence of chromophore in the vesicle-containing fractions. This result indicated that the vesicles retained a portion of the unreacted lipid-dye. Unreacted vesicles only showed absorbance in vesicle-containing fractions and no absorbance in later fractions. This result indicated that all CF-lipid was retained in untreated vesicles and the hydrolysis reaction did not occur.

Ideally, the absorbance of the vesicle-containing fractions would be far lower in absorbance than the unreacted samples. However, before purification, the reacted vesicle suspension was noticeably more intense in color, which indicated the presence of more dye. Therefore, since the two suspensions after purification were comparable in absorbance, the reacted sample did decrease in absorbance compared to the unreacted sample.

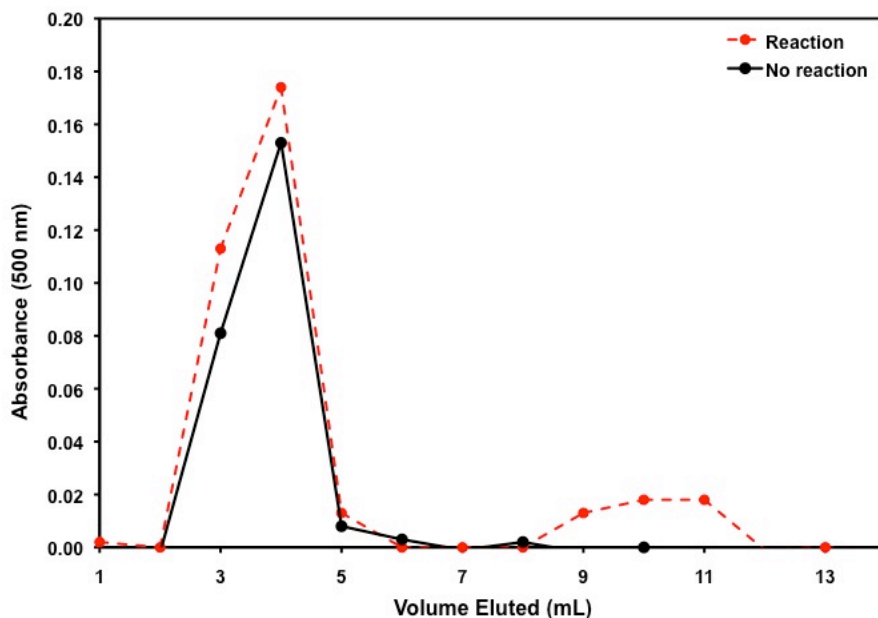
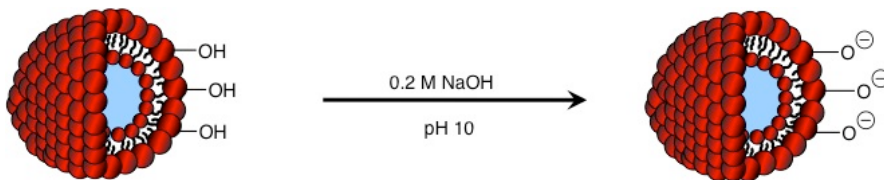


**Figure A.3.** Purification of CF-lipid vesicles reacted with NaOH and unreacted. Vesicles were purified by SEC and characterized by UV-VIS at 500 nm.

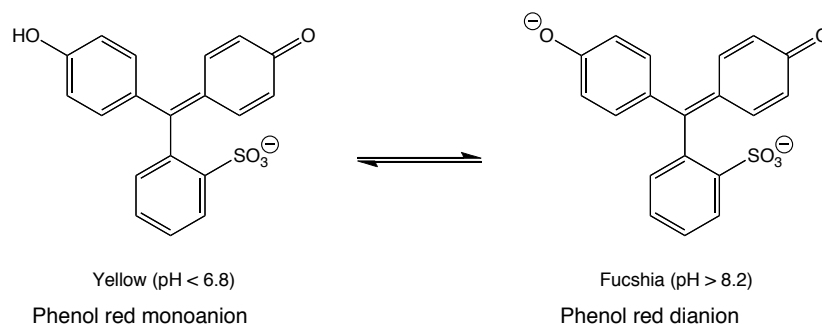
#### A.2.2 Surfactant Vesicles as Chemical Indicators

After observing a color change of CF-lipid dye loaded in vesicles following the addition of base, the loading of a chemical indicator without a lipid tail into vesicles was studied. We were interested in the ability to show that certain protons remain accessible at the surface of vesicles and can be deprotonated with base, even after their loading into vesicles. (Scheme A.4).

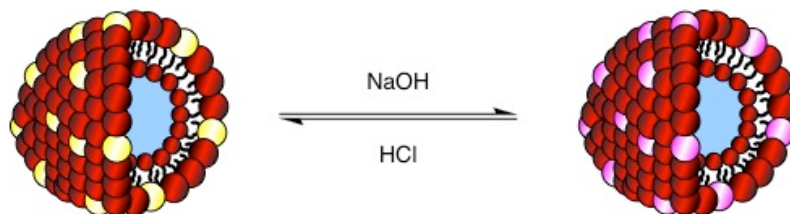


**Scheme A.4.** Deprotonation of protons at the surface of cationic surfactant vesicles.

To test our hypothesis, catanionic vesicles were loaded with phenol red, a dye that changes from yellow to fuchsia under neutral to basic conditions, respectively (Scheme A.5). By loading vesicles with phenol red and then adjusting the pH, one can determine if the phenolic proton is accessible by observing a color change of the vesicle suspension (Scheme A.6).



**Scheme A.5.** Phenol red monoanion and dianion chemical structures. The monoanion is yellow in color, while the dianion is fuchsia.



**Scheme A.6.** Phenol red loaded in CTAT-rich vesicles. Vesicles appear yellow in color under neutral conditions and fuchsia in color under basic conditions.

SDBS-rich and CTAT-rich vesicles were loaded with the chemical indicator phenol red. Only CTAT-rich vesicles (cationic) were yellow in color following purification by SEC. This result indicated that anionic dye had been retained within CTAT-rich vesicles, which contain a positive surface charge. SDBS-rich vesicles

(anionic) did not retain the dye because of the electrostatic repulsion between the anionic phenol red with the excess anionic surfactant.

For the CTAT-rich SEC fractions, NaOH was added and previously yellow fractions turned pink in color (Figure A.4), indicating that deprotonation occurred to form the dianion (Scheme A.5). After vesicles were reacidified with HCl, the color returned to yellow. This reaction indicated the reversibility of the acid-base reaction (Scheme A.5).



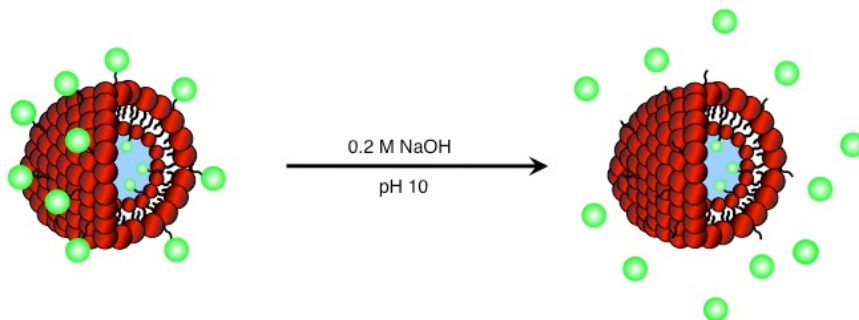
**Figure A.4.** CTAT-rich vesicles containing phenol red after SEC purification. A) All fractions are yellow in color from the monoanion at pH 7. B) After addition of NaOH, all fractions turned fuchsia in color, indicating the presence of the dianion in solution. Vesicle-containing fractions incorporated phenol red, leaving the acidic proton accessible for the acid-base reaction.

While phenol red is lipophilic, it is also charged and can therefore orient itself either completely within the bilayer or associate itself with the surfactant head groups. Since CTAT-rich vesicles loaded with phenol red changed color at pH 10, phenol red is not completely embedded within the bilayer, but the phenolic proton must be protruding for vesicles (Scheme A.4). The reversibility of the reaction within vesicles may be used for studying catanionic vesicles *in vivo*. For example, uptake of catanionic vesicles

loaded with various chemical indicators offers the visualization of these vesicle systems as they enter different pH environments.

### A.3 Conclusions

Cationic vesicles can be used to perform chemical reactions on molecules and also show potential toward protecting group chemistry. The ability to perform chemical reactions on only the outer leaflet of the vesicle provides the ability to determine how much material is incorporated within the inner leaflet of vesicles (Scheme A.7). Furthermore, this allows the possibility to use cationic vesicles as possible protecting groups where a reaction could be selective due to the orientation of the molecule inside of the vesicle bilayer (Figure A.5).



**Scheme A.7.** Determining the amount of dye incorporated within the internal region of vesicles.

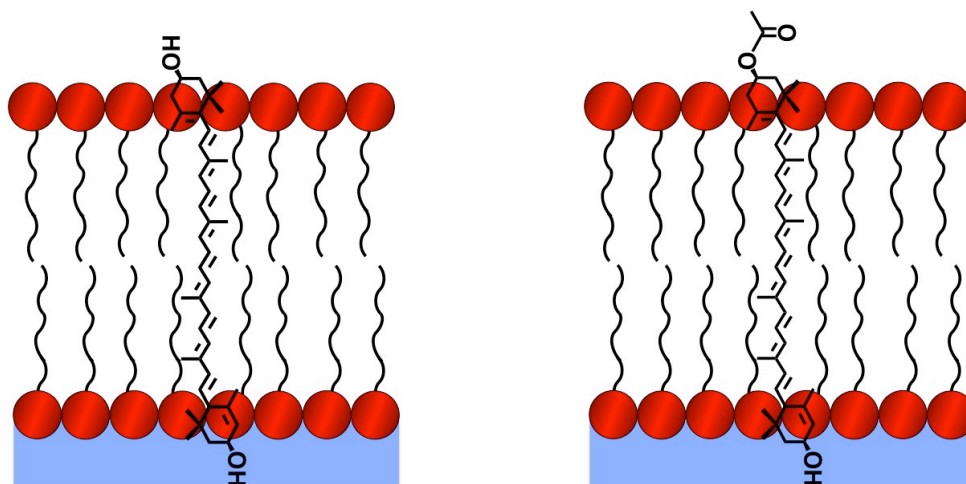


**Figure A.5.** Catanionic surfactant vesicles as protecting groups. For example, lutein spanning the bilayer of catanionic surfactant vesicles would undergo monoacetylation.

#### A.4 Experimental

The lipid dye 1,2-dioleoyl-*sn*-glycero-3-phosphoethanolamine-N-(carboxyfluorescein) (ammonium salt) (CF) was purchased from Avanti Polar Lipids, Inc. (Figure A.6). All other chemicals were purchased from commercial suppliers.

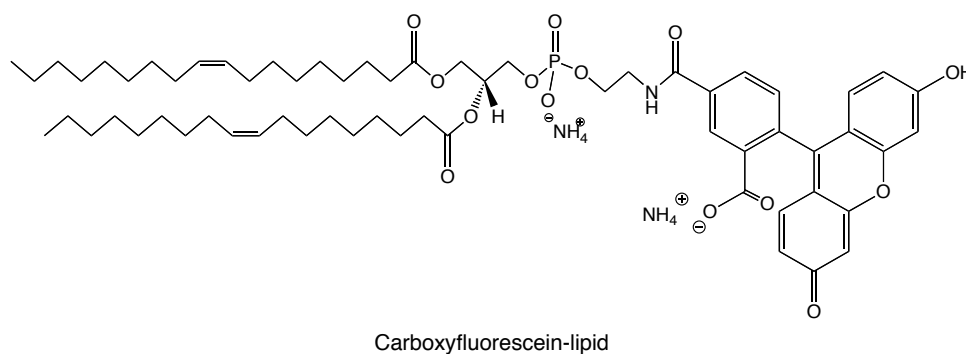


**Figure A.6.** Chemical structure of CF-lipid dye.

#### A.4.1 Hydrolysis of Dye from SDBS-rich Vesicles

An aliquot of CF-lipid was dried *in vacuo* and then dissolved in ethanol. To the sample, 0.2 M NaOH was added until the pH reached 11 and then was stirred at room temperature. The hydrolysis reaction was monitored by thin TLC using 65:30:5 CH<sub>3</sub>Cl:MeOH:H<sub>2</sub>O as the solvent to determine the progress of the reaction. Lipid components were detected by TLC using iodine.

SDBS-rich vesicles were prepared with CF-lipid (Figure 4). The dye was loaded into vesicles of opposite charge so that cleaved dye would not reassociate with the vesicle surface by electrostatic interactions. A 25  $\mu$ L aliquot (0.125 mg, 0.110  $\mu$ mol) of CF-lipid dye in chloroform was added to the solid surfactants, 70.0 mg (0.200 mmol) SDBS and 30.0 mg (0.0658 mmol) CTAT. The sample remained open until the solvent evaporated, followed by the addition of 9.9 mL of water and stirring for 1 h at room temperature. Based on earlier studies, vesicles prepared via this method have CF-lipid dye decorated within the outer and inner vesicle bilayer (Scheme A.1).

Vesicles were purified by SEC to remove any excess lipid dye prior to treatment with base. Unassociated lipid dye was retained on the column. Since the lipid dye is insoluble in water, the column was washed with a solution of SDBS (7.07 mg/mL) to remove the dye before further purifications. The pH of all SEC fractions was increased to a pH of 10 by the dropwise addition of 0.2 M NaOH. Vesicles were stirred at room temperature overnight. Vesicles were purified a second time by SEC to separate any cleaved dye from vesicles. Similarly, the control was purified a second time by SEC.

A 0.5 mL portion of ethanol was added to each 0.5 mL fraction from SEC to break up vesicles and prevent light scattering. The absorbance was monitored by UV/VIS at 500 nm for CF-lipid dye.

#### *A.4.2 Phenol Red Vesicles*

A 7.05  $\mu\text{M}$  (0.125 mg/mL) solution of phenol red was prepared in water and sonicated until all of the dye dissolved. Then, 9.9 mL (3.49  $\mu\text{mol}$ ) of the dye solution was added to 70.0 mg (0.200 mmol) SDBS and 30.0 mg (0.0658 mmol) to form SDBS-rich vesicles and 70.0 mg (0.154 mmol) CTAT and 30.0 mg (0.0861 mmol) to form CTAT-rich vesicles. The suspensions were stirred at room temperature for 1 h followed by purification by SEC. Since SDBS-rich vesicle-containing fractions did not contain phenol red, only CTAT-rich vesicles were used as follows.

Dropwise addition 0.2 M NaOH was added to each SEC fraction until the pH turned to 10, which was determined by pH paper. To determine the reversibility of the reaction, 1 N HCl was added dropwise until the pH returned to 7.

## References

1. Rangel-Yagui, C. O.; Pessoa, A., Jr.; Tavares, L. C., Micellar solubilization of drugs. *J. Pharm. Pharm. Sci.* **2005**, *8* (2), 147-163.
2. Rathman, J. F., Micellar catalysis. *Curr. Opin. Colloid Interface Sci.* **1996**, *1* (4), 514-518.
3. Abela, A. R.; Huang, S.; Moser, R.; Lipshutz, B. H., Sustainability: getting organic solvents out of organic reactions. *Chim. Oggi.* **2010**, *28* (5), 50-53.
4. Lipshutz, B. H.; Ghorai, S., Designer-surfactant-enabled cross-couplings in water at room temperature. *Aldrichimica Acta* **2012**, *45* (1), 3-16.
5. Lipshutz, B. H.; Ghorai, S.; Aguinaldo, G. T., Ring-closing metathesis at room temperature within nanometer micelles using water as the only solvent. *Adv. Synth. Catal.* **2008**, *350* (7), 953-956.
6. Lipshutz Bruce, H.; Taft Benjamin, R., Heck couplings at room temperature in nanometer aqueous micelles. *Org. Lett.* **2008**, *10* (7), 1329-32.
7. Lu, G.-p.; Cai, C.; Lipshutz, B. H., Stille couplings in water at room temperature. *Green Chem.* **2013**, *15* (1), 105-109.
8. Wang, Z.; Leung, M. H. M.; Kee, T. W.; English, D. S., The role of charge in the surfactant-assisted stabilization of the natural product curcumin. *Langmuir* **2010**, *26* (8), 5520-5526.